ROLE OF LIPID CATABOLISM IN THE PATHOGENICITY OF RICE-BLAST FUNGUS *Magnaporthe grisea*

MARILOU RAMOS-PAMPLONA

(M.Sc., University of the Philippines in Los Baños)

A THESIS SUBMITTED
FOR THE DEGREE OF DOCTOR OF PHILOSOPHY

TEMASEK LIFESCIENCES LABORATORY
and
DEPARTMENT OF BIOLOGICAL SCIENCES
NATIONAL UNIVERSITY OF SINGAPORE

2007

ACKNOWLEDGEMENTS

i

TABLE OF CONTENTS

SUMMARY

Biochemical genetics and extensive characterization of different metabolic mutants helped establish that lipid catabolism via peroxisomal and mitochondrial fatty acid beta-oxidation pathways is essential for the pathogenicity of *Magnaporthe grisea*. The isolation of nonpathogenic mutants harboring insertions in genes encoding peroxisome biogenesis proteins (*PEX6* and *PEX1*) provided the foundation for further investigation of the metabolic requirements during fungal pathogenesis. The *pex6Δ* strain was completely nonpathogenic due to nonfunctional appressoria, which were incapable of elaborating penetration pegs. An analysis of the ultrastructure of *pex6Δ* appressoria showed that the melanin layer, which functions in the maintenance of the high hydrostatic pressure required for appressorial function, was completely absent. These results indicate that peroxisome-associated metabolism is essential for biosynthesis of appressorial melanin. As melanin in *M. grisea* is synthesized through the polyketide pathway using acetyl-CoA as precursor molecules, the acetyl-CoA product of fatty acid oxidation within the peroxisomes must be utilized for synthesis of appressorial melanin. The movement of acetyl-CoA molecules across cellular compartments requires the transfer of the acetyl moiety to carnitine via a reaction catalyzed by carnitine acetyltransferases (CrAT). To confirm the role of peroxisome-derived acetyl-CoA in appressorial melanin synthesis, a targeted deletion of the two genes encoding putative *M. grisea* carnitine acetyltransferases (*PTH2* and *CrAT2*) was undertaken. Between the two CrATs, only Pth2 contributed the major cellular carnitine acetyltransferase activity and was required for fatty acid metabolism and pathogenicity. The appressoria of *pth2Δ* possessed a greatly reduced melanin layer and was incapable of host penetration. High concentrations of exogenous glucose could partially restore penetration peg formation in the *pth2Δ* appressoria, which

suggests that acetyl-CoA generated from peroxisomal metabolism is also utilized in gluconeogenic pathways. The products of gluconeogenesis may be used to synthesize cell wall components, which are required for elaboration of penetration pegs and development of infectious hyphae. As characterization of *pex6Δ* and *pth2Δ* mutants strongly indicated a role for lipid catabolism during *M. grisea* pathogenesis, creation and characterization of mutants harboring targeted deletions in genes encoding fatty acid beta-oxidation enzymes was done to specifically determine the contributions of this metabolic pathway to different stages of fungal pathogenesis and development. In addition to peroxisomes, fatty acid beta-oxidation is known to take place as well within the mitochondria. A concurrent characterization of two mutants in a peroxisome-specific (Fox2) and a mitochondria-specific (EchA) beta-oxidation enzyme demonstrated the presence of a mitochondrial beta-oxidation pathway in *M. grisea* and the requirement for both pathways during pathogenesis. The cooperative function of peroxisomal and mitochondrial beta-oxidation is necessary during growth on fatty acids and during the early stages of pathogenic development, particularly in the degradation of lipid bodies, appressorium morphogenesis and host penetration. The drastic reduction of the appressorial melanin layer only in the *fox2Δ* mutant confirmed that acetyl-CoA generated from peroxisomal fatty acid beta-oxidation serves as the preferred pool of precursors for melanin biosynthesis. Mitochondrial beta-oxidation, on the other hand, is required for optimum vegetative growth, maintenance of mitochondrial morphology and proliferation of the infectious hyphae within the host tissue.

LIST OF TABLES

LIST OF FIGURES

LIST OF ABBREVIATIONS

AAA-ATPase	ATPase associated with diverse cellular activities
AOX	Acyl-CoA oxidase
BFP	Bifunctional protein
cAMP	Cyclic adenosine monophosphate
CoA	Coenzyme A
CrAT	Carnitine acetyltransferase
DHN	Dihydroxynapthalene
ECH	2-enoyl-CoA hydratase
GFP	Green fluorescent protein
HADH	3-Hydroxyacyl-CoA dehydrogenase
ICL1	Isocitrate lyase 1
MFP	Multifunctional protein
MLS1	Malate synthase
MTS	Mitochondrial targeting signal
ORE	Oleate response element
ORF	Open reading frame
PEX	Peroxin
PTS1	Peroxisome targeting signal type 1
PTS2	Peroxisome targeting signal type 2
RFP	Red fluorescent protein
TAG	Triacylglycerol
TGL	Triacylglycerol lipase
TCA	Tricarboxylic acid cycle
UAS	Upstream activating sequence
WB	Woronin bodies

Publications

First author publication

Ramos-Pamplona, M. and Naqvi, N.I. 2006. **Host invasion during rice blast disease requires carnitine-dependent transport of peroxisomal acetyl-CoA.** Molecular Microbiology 61(1):61-75.

Co-author publication

Soundararajan, S., Jedd, G., Li, XL., Ramos-Pamplona, M., Chua, N.H., Naqvi, N. 2004. **Woronin body function in *Magnaporthe grisea* is essential for efficient pathogenesis and for survival during nitrogen starvation stress.** Plant Cell 16(6):1564-74.

CHAPTER I INTRODUCTION

1.1   *Magnaporthe grisea*, the rice blast pathogen

The filamentous fungus *M. grisea* is the causal pathogen of the agriculturally important blast disease, which affects cereal crops and other grass species (Ou, 1985). During field trials of upland cultivars in South America from 1995-97, rice blast disease was found to cause grain yield losses of up to 18-44% (Prabhu et al., 2003). Present day rice blast disease management strategies, which consist of deployment of blast-resistant varieties and fungicide applications, have proven inadequate for long term disease control. Breakdown of resistant varieties occurs after one or two seasons of planting owing to the limited disease resistance incorporated and to the continuous evolution of new pathogen populations. Fungicides have demonstrated some effectiveness in controlling blast/leaf spot disease during initial applications; however resistant isolates of *M. grisea* have promptly emerged (Avila-Adame and Koller, 2003; Sawada et al., 2004).

The infection cycle of *M. grisea* is comprised of distinct developmental and morphogenetic events during the host pre-penetration and the *in planta* proliferation stages (Tenjo and Hamer, 2002) (Figure 1). The disease is initiated by asexual spores or conidia, which in nature are dispersed mainly by water splashes and moist air. Upon landing and subsequent hydration on the leaf surface, the conidium germinates and forms a short germ tube (Howard et al., 1991a). The tip of the germ tube differentiates into a dome-shaped infection structure known as appressorium. The development of a mature and functional appressorium involves the synthesis of molar concentrations of glycerol within the appressorial cell (De Jong et al., 1997) and the deposition of a melanin layer between the cell wall and the plasma membrane

1

(Chumley and Valent, 1990). The influx of water from the environment in response to the high internal glycerol concentration generates an enormous hydrostatic pressure within the appressorium. The melanin layer deposited at the periphery of the cell maintains the turgor pressure by effectively decreasing the membrane pore size to prevent the efflux of glycerol (Howard and Ferrari, 1989). The mature appressorium utilizes this massive hydrostatic pressure as a mechanical force to push a thin penetration peg through the host cuticle (Howard et al., 1991b). Once inside the host, the penetration peg develops into an infectious hypha, which ramifies and colonizes adjacent plant cells (Hamer and Talbot, 1998). At later stages of infection, the invading hyphae develop aerial mycelia, which in turn produce spores that serve as inoculum for successive rounds of the disease cycle.

In addition to being an agriculturally and economically important pathogen, *M. grisea* serves as a good model system to study fungal pathogenesis. *M. grisea* can easily be propagated and maintained under laboratory conditions (Tenjo and Hamer, 2002). Its pathogenicity phenotype can be readily assessed under greenhouse conditions or under laboratory conditions using simple detached leaf assays. It is possible to cytologically and biochemically monitor and assess distinct events of its pathogenesis cycle in the laboratory using either artificial membranes or leaf surfaces. The appealing characteristic of *M. grisea* as being genetically tractable and amenable to molecular manipulations has been amply demonstrated through extensive research carried out in order to identify pathogenicity genes using different approaches (Sweigard et al., 1998; Balhadere et al., 1999; Ebbole et al., 2004).
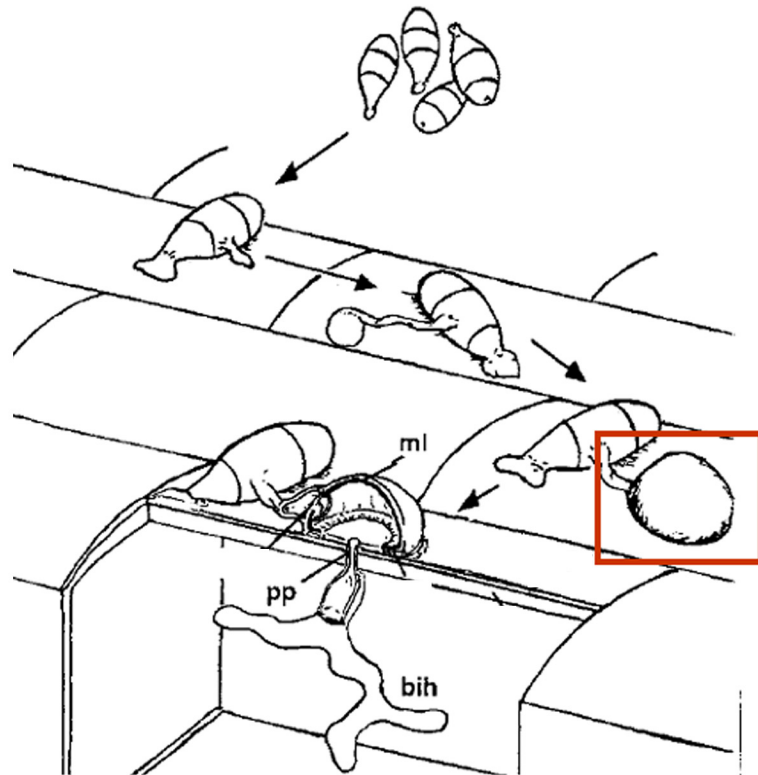
Figure 1. General schematic representation of *M. grisea* infection cycle.
This diagrammatic sketch of the *M. grisea* infection cycle is adapted from Clergeot et al. (2001). The tricellular asexual spores/conidia germinate and form a small germ tube upon landing on the plant surface. The tip of the germ tube develops into the dome-shaped appressorium (marked by red box). During development, a melanin layer (ml) is deposited around the periphery of the appressoria. Upon maturation, the appressoria uses mechanical pressure to force a penetration peg (pp) through the host epidermis. The penetration peg eventually develops into a branching infectious hypha (bih) which colonizes neighboring plant cells.

1.2 Genetic and biochemical regulation of *M. grisea* pathogenesis

The comprehensive study of *M. grisea* pathogenesis has resulted in the discovery of key components involved during the infection cycle. One of the most critical aspects of pathogenic development is the formation of a functional appressorium, which is required by the fungus to breach the host epidermis. Signaling pathways mediated by cyclic adenosine monophosphate (cAMP) and mitogen activated protein (MAP) kinases play a role in the developmental decision for appressorium formation (Lengeler et al., 2000). The capability of exogenous cAMP to induce appressorium formation from germinating conidia or vegetative hyphae on noninductive surfaces first suggested a central role for this signaling molecule during appressorium {Lee, 1993 #32}. Strains harboring mutations in *MAC1*, which encodes a membrane-bound adenylate cyclase that catalyzes the production of cAMP from ATP, exhibit pleiotropic vegetative and pathogenic defects (Choi and Dean, 1997). Vegetative growth defects include poor mycelial growth, decreased conidiation and inability to form sexual perithecia. The pathogenic defects include inability to form appressoria,which can be rescued by exogenous cAMP (Choi and Dean, 1997). The function of cAMP during appressorium formation is likely mediated via the cAMP-dependent protein kinase A (PKA) (Mitchell and Dean, 1995). However, mutants in the catalytic subunit of PKA, *cpkA*Δ, are not blocked in appressorium formation (Adachi and Hamer, 1998). The various pleiotropic defects of the *mac1*Δ strain can be suppressed by a mutation, which alters the cAMP-binding domain of the regulatory subunit of PKA (*SUM1*). The *mac1*Δ *sum1-99* strain exhibits wild-type vegetative growth and appressorium formation on hydrophilic surfaces and in the presence of 2% yeast extract, which are conditions that are inhibitory to wild-type appressorium formation (Adachi and Hamer, 1998). As protein kinase activity in the fungus can be

solely attributed to CpkA, it is hypothesized that other downstream effectors may be required to mediate cAMP signaling during pathogenesis (Adachi and Hamer, 1998).

The ability of cAMP supplementation to partially restore appressorium formation in the MAP kinase 1 mutant *pmk1Δ* indicated that there is a crosstalk between cAMP and MAP kinase signaling pathways (Xu and Hamer, 1996). In the presence of exogenous cAMP, the tips of the germ tubes of *pmk1Δ* could be induced to undergo swelling and hooking and form incipient appressoria (Xu and Hamer, 1996). Site-specific mutation experiments of *PMK1*, which encodes a homolog of *S. cerevisiae* pheromone response MAP kinase Fus3, have demonstrated that the kinase activity and the phosphorylation sites of Pmk1 are required for its role during pathogenesis (Bruno et al., 2004).

The signaling pathways mediated by cAMP and MAP kinases have been shown to directly regulate the metabolic processes, which take place during the development of the appressorium (Lengeler et al., 2000). As the major storage products in the conidia consist of lipids and glycogen, the energy source and the secondary metabolites required for pathogenicity are derived primarily from the metabolism of carbohydrates and fatty acids (Wang et al., 2005). The mass transfer of glycogen and lipid bodies from the germinating conidium into the germ tube tip takes place during the early stage of appressorium (Thines et al., 2000). Once compartmentalized within the incipient appressorium, the glycogen and lipid stores are broken down rapidly. The complete degradation of the storage products coincides with the breaching of the host cuticle with a penetration peg by the mature appressorium. Mutants in *PMK1* and *CPKA* exhibit a block and retardation, respectively, in the mobilization of lipid bodies

from the germinated conidium into the incipient appressorium. And a mutation in the regulatory subunit of *PKA* (*mac1Δsum1-99*) results in the accelerated, untimely degradation of lipid bodies within the appressoria. The regulated mobilization and catabolism of storage reserves, which is required for the development of a functional appressorium, is under the genetic control of the cAMP and *PMK1* MAP kinase pathways (Thines et al., 2000).

Catabolism of lipid reserves is of primary importance during appressorium morphogenesis. Lipid bodies are autophagocytosed and rapidly degraded within the vacuoles of the developing appressorium (Weber et al., 2001). The synthesis of glycerol, which is the central osmolyte for the generation of turgor pressure within the appressorial cell, is achieved via the catabolism of lipids by triacylglycerol lipases (TGL) (Thines et al., 2000). TGL enzyme activity exhibits a progressive increase concurrent with the period of appressorium maturation. In contrast, the enzyme activity of glycerol-3-phosphate dehydrogenases, which are involved in glycerol production from carbohydrate sources, remains at a similar level during appressorium development. The contribution of lipid metabolism for fungal pathogenesis is likely to extend further than glycerol synthesis, as can be inferred from the work on another *M. grisea* metabolic mutant. The deletion of the gene encoding the glyoxylate cycle enzyme Isocitrate lyase 1 (*ICL1*) resulted in the delay and impairment of virulence-associated functions such as conidial germination, appressorium formation and host cuticle penetration (Wang et al., 2003). The glyoxylate cycle serves as an auxiliary pathway of lipid metabolism wherein the C2 product (acetyl-CoA) of fatty acid oxidation can be utilized to generate C4 carbon compounds for gluconeogenesis.

In addition to lipid and glycogen catabolism, there are most likely other metabolic pathways which function during the different stages of pathogenesis. The opposite pathways of biosynthesis and breakdown of the storage carbohydrate trehalose participate in two independent infection-related events during pathogenesis (Foster et al., 2003). The initial stages of appressorium morphogenesis and host penetration require trehalose biosynthesis. Disruption of *TPS1,* which encodes trehalose-6-phosphate synthase, results in impairment of turgor generation and penetration peg formation. However, once the fungus is inside the host, the breakdown of trehalose is required for its efficient *in planta* proliferation. Mutation of the gene encoding neutral trehalase 1 (*NTH1*) results in compromised pathogenicity due to inefficient colonization of host tissue after ingress (Foster et al., 2003). The significance of other metabolic pathways and their secondary metabolite is suggested by studies on an *M. grisea* mutant lacking the polyketide synthase/peptide synthase Ace1 (Bohnert et al., 2004). The product of Ace1 biosynthetic activity acts as an avirulence protein, which enables the host plant to detect the invading pathogen and consequently mount a defense response. However, the exact identity of the secondary metabolites produced by Ace1 activity remains to be ascertained.

Due to the extensive research effort of many labs, a basic understanding of the signal transduction and metabolic pathways involved in *M. grisea* pathogenesis has been obtained. There is also a continuous accumulation of knowledge regarding other pathogenesis-related aspects such as surface sensing and the role of "novel" pathogenesis genes. More effort is clearly needed for a better understanding of the known mechanisms in fungal pathogenesis, and to gain new insights into yet-to-be discovered aspects of pathogenesis.

7

1.3   Overview of lipid catabolism

1.3.1.   General pathway of cellular lipid catabolism

The basic mechanism of lipid catabolism within the cell is through the beta-oxidation of fatty acids. Cellular lipid stores are composed of triacylglycerols, which are acted upon by different lipases to release free fatty acids (Wagner and Daum, 2005). Based on the length of the carbon chain fatty acids are classified as being short-chain (from C4 to C6), medium-chain (from C8-C12), long-chain (from C14-C18) or very long-chain (greater than C22). The starting molecule of the beta-oxidation pathway is a fatty acid, which could be of any chain length, esterified to Coenzyme A (CoA) (Hiltunen and Qin, 2000). The activation of a fatty acid to its acyl-CoA derivative is catalyzed by fatty acyl-CoA synthetases, which exhibit chain length-based specificities (Osmundsen et al., 1994).

The fatty acid beta-oxidation pathway is a cycle of four consecutive enzymatic reactions, which at every turn shortens the starting fatty acyl-CoA molecule by two carbons which are released as one acetyl-CoA (Kunau et al., 1995). Thus, lipid oxidation is achieved by the repetitive chain shortening of a fatty acid coupled with the production of acetyl-CoA. Following are the four enzymatic reactions of a typical beta-oxidation cycle: (1) dehydrogenation of the beta-carbon of the fatty acyl-CoA which results in desaturation in the 2,3-position (enoyl-CoA intermediate); (2) hydration of the enoyl-CoA intermediate which results in hydroxylation at the 3-position; (3) dehydrogenation of the hydroxyacyl-CoA intermediate which results in the oxidation of the hydroxyl group to a carbonyl group; and (4) thiolytic cleavage at the 3-position by CoA thereby generating the two-carbon acetyl-CoA molecule. The enzymes which catalyze these reactions are as follows: (1) acyl-CoA oxidase (AOX)

or acyl-CoA dehydrogenase (ADH); (2) 2-enoyl-CoA hydratase (ECH); (3) 3-hydroxyacyl-CoA dehydrogenase (HADH); and (4) 3-ketoacyl-Co thiolase. The oxidation of fatty acids involves the transfer of electrons to either molecular oxygen (O_2) or nicotine adenine dinucleotide (NAD) or flavin adenine dinucleotide (FADH) coenzymes. Therefore, the byproducts of fatty acid beta-oxidation include hydrogen peroxide or reduced derivatives of NAD (NADH) or FAD (FADH2) (Hiltunen et al., 2003).

Essentially, fatty acid beta-oxidation occurs via the successive dehydrogenation-hydration-dehydrogenation-thiolysis reactions, which are catalyzed by corresponding enzymes (Hashimoto, 2000). However, a level of complexity exists due to the presence of various types of fatty acid substrates, which are processed via beta-oxidation. Besides saturated fatty acids of varying chain length, beta-oxidation substrates include unsaturated, methyl-branched and dicarboxylic fatty acids. Thus, multiple isoforms of the beta-oxidation enzymes with different yet overlapping specificities are present in the cell to accommodate these various fatty acid substrates (Kunau et al., 1988). These multiple beta-oxidation isozymes are distinct not only for their substrate specificities but also for their cellular compartmentalization, their capacity to catalyze single or multiple reactions, their ability to form monofunctional units or enzymatic complexes and the alternative stereochemistry of the intermediates (Hiltunen and Qin, 2000).

1.3.2. Genetic regulation of lipid catabolism

Fatty acids have been shown to be capable to inducing the expression and activity of enzymes involved in their metabolism. A similar phenomenon of massive

9

proliferation of peroxisomes and significant induction of the activity of beta-oxidation enzymes have been observed in the budding yeast *S. cerevisiae* and the filamentous fungi *Aspergillus nidulans* after glucose-grown cells were transferred to oleic acid medium (Veenhuis et al., 1987; Valenciano et al., 1996). In *S. cerevisiae*, the most characterized regulatory elements involved in oleic acid induction are Pip2p and Oaf1p (Rottensteiner et al., 1996) (Luo et al., 1996). The strong oleic acid induction of beta-oxidation genes is mediated by a heterodimer of Oaf1p and Pip2p, which binds to upstream activating sequences (UAS) called oleate response elements (ORE) (Rottensteiner et al., 1997). A UAS, which was subject to oleate induction and glucose repression, was first characterized in the gene encoding peroxisomal acyl-CoA oxidase POX1 (Wang et al., 1994). Presently, the ORE consensus consists of palindromic CGG triplets spaced by 14 to 18 intervening nucleotides (Hiltunen et al., 2003). However, a survey of Oaf1p-Pip2p binding sites revealed that a defined consensus is not always requisite for regulation of some ORE-responsive genes (Karpichev and Small, 1998). Recently, in *A. nidulans*, two genes regulating the transcriptional induction of lipid catabolic genes by short- and long-chain fatty acids were identified (Hynes et al., 2006). *farA* and *farB* encode Zn_2-Cys_6 binuclear proteins and operate through a 6-basepair binding site, which has been found to be conserved in the 5' region of genes involved in fatty acid beta-oxidation, peroxisome biogenesis and the glyoxylate cycle (Hynes et al., 2006).

1.4   Cellular compartmentalization of fatty acid beta-oxidation

Two parallel pathways of cellular fatty acid beta-oxidation have been identified. These two pathways consist essentially of the same four consecutive enzymatic reactions, but are located in two different organelles, the peroxisome and the

mitochondrion. However, not all organisms have been shown to possess two separate beta-oxidation pathways. The earliest studies of beta-oxidation in animals indicated that fatty acid catabolism is the exclusive function of the mitochondria (Schulz, 1991). However, observations that hypolipidemic drugs, which reduce serum lipid levels, also induced a proliferation of peroxisomes, hinted at a possible role for peroxisomes in lipid catabolism. Different structurally unrelated types of hypolipidemic drugs were all similarly capable of inducing an increase in peroxisome number (Reddy and Krishnakantha, 1975). A fatty acyl-CoA oxidizing system, which was also induced by hypolipidemic drugs was then detected in the peroxisomal fraction of treated mice liver (Lazarow and De Duve, 1976). This peroxisomal beta-oxidation pathway utilized the same mitochondrial beta-oxidation enzymatic reactions of hydration-dehydrogenation-thiolysis and also produced acetyl-CoA (Lazarow, 1978).

In plants, investigations on lipid catabolism focused on the germinating seeds which depended on lipid catabolic products for energy and macromolecular synthesis. Here, fatty acid beta-oxidation takes place in specialized organelles called glyoxysomes, which house fatty acid catabolic machinery and an auxiliary pathway called the glyoxylate cycle (Cooper and Beevers, 1969). The glyoxylate cycle allows the utilization of beta-oxidation products for biosynthesis reactions. Recently, however, beta-oxidation enzymes have been detected in mitochondrial fractions (Bode et al., 1999), suggesting the existence of fatty acid breakdown machinery within the mitochondria.

In yeasts, which have been extensively used to study fatty acid catabolism, beta-oxidation is thought to be exclusively located in the peroxisome organelle (Kunau et

al., 1988). Yeasts are useful in studying beta-oxidation as they exhibit peroxisome proliferation and induction of beta-oxidation enzymes during growth on fatty acids. In *Candida lipolytica*, a fatty acid-inducible acyl-CoA oxidizing system was detected only in the peroxisomes (Mishina et al., 1978). Recently, however, the activity of mitochondrial beta-oxidation enzymes has been demonstrated in the yeast-like fungus *Sporidiobolus* (Feron et al., 2005). In the filamentous fungus *Neurospora crassa*, the beta-oxidation pathway is housed in specialized microbodies, which also contain the glyoxylate cycle enzymes (Kionka and Kunau, 1985). However, *Aspergillus nidulans* contains the mitochondrial as well as the peroxisomal beta-oxidation machineries (Maggio-Hall and Keller, 2004).

The dual compartmentalization of the beta-oxidation pathway is found in many, but not all, organisms. As the two pathways utilize the same enzymatic mechanisms, multiple isoforms of the beta-oxidation enzymes exist and are differentially targeted to the peroxisomes or the mitochondria. The peroxisomal and mitochondrial isozymes exhibit extensive similarity which suggests that they are derived from a common ancestor and had probably acquired targeting information during evolution (Arakawa et al., 1987). The prevalence of two distinct lipid catabolic pathways within the cell suggests different physiological roles for each of them. The numerous and extensive studies on dual pathways of fatty acid oxidation have led to the identification of certain features which are characteristic to either peroxisomal or mitochondrial fatty acid oxidation.

1.5　Peroxisomal beta-oxidation

1.5.1　The peroxisomes

1.5.1.1 Types of peroxisomes and cellular functions

The peroxisome is a single-membrane bound organelle, which belongs to the microbody family (Latruffe et al., 2003). These organelles were first observed as the cellular compartments of catalase and peroxidase enzymes. Over the years, diverse metabolic functions have been attributed to peroxisomes in different organisms and have resulted in the identification of different types of peroxisomes (Titorenko and Rachubinski, 2004). Moreover, some peroxisome types lack the characteristic peroxidase and catalase content (Thieringer and Kunau, 1991a) (Jedd and Chua, 2000). In animals, peroxisome function is required for fatty acid beta-oxidation as well as for cholesterol and bile synthesis (Wanders, 2000). The critical requirement for peroxisomal metabolic function in normal physiology is exemplified by the numerous genetic disorders, which are attributed to a lack of either all or a subset or peroxisomal functions (Gould and Valle, 2000). In plants, peroxisomes undergo several morphological and metabolic transformations during development (Hayashi et al., 2000). In germinating seeds, peroxisomes house both enzymes of the beta-oxidation pathway and the glyoxylate pathway and are thus referred to as glyoxysomes {Cooper, 1969 #244). When the plant is capable of photosynthesis, the peroxisomes mostly house the photorespiration enzymes. During senescence, glyoxysomes constitute a majority of the peroxisome population (Nishimura et al., 1993). In filamentous fungi, besides the typical peroxisomes for beta-oxidation, a specialized class of peroxisomal vesicles called Woronin bodies is found which functions in septal pore sealing (Jedd and Chua, 2000; Soundararajan et al., 2004).

1.5.1.2 Peroxisome biogenesis

Two major hypotheses have been put forth regarding the biogenesis of the peroxisome organelle. The first hypothesis suggests that peroxisomes originate only from pre-existing peroxisomes (Lazarow and Fujiki, 1985). The other hypothesis, for which there is recent favorable evidence, suggests that peroxisomes are derived from the endoplasmic reticulum {Hoepfner, 2005 #200}. In either hypothesis, a group of proteins known as Peroxins encoded by peroxisome biogenesis genes (PEX) have been implicated as key players during peroxisome biogenesis (Subramani et al., 2000). About 32 peroxins have been identified to date and most of them have homologs across different organisms (Purdue and Lazarow, 2001). These include peroxisomal membrane proteins (Schliebs and Kunau, 2004), peroxisomal import receptors (Pex5 and Pex7) (Rehling et al., 1996; Elgersma et al., 1998; Kragler et al., 1998), peroxisome proliferation regulators (Pex11) (van Roermund et al., 2000; Li and Gould, 2002; Thoms and Erdmann, 2005) and ATPases Associated with diverse cellular Activities (AAA ATPases) (Pex1 and Pex6) (Portsteffen et al., 1997) (Kiel et al., 1999).

The proper targeting of peroxisomal membrane proteins requires Pex3 and Pex19. In the absence of Pex3 and Pex19, peroxisomal matrix proteins accumulate and are rapidly degraded in the cytosol. (Hettema et al., 2000). During the early stage of peroxisome biogenesis from the endoplasmic reticulum, the integral membrane protein Pex3 was shown to aggregate in distinct foci on the membrane. Subsequently, the farnesylated cytosolic protein Pex19 is enriched at the Pex3-containing foci and is thought to regulate the budding of immature peroxisomes (Hoepfner et al., 2005). Vps1 is a dynamin-like protein, which has been shown to regulate peroxisome

numbers. The protein may be involved in the membrane fission events of peroxisome biogenesis (Hoepfner et al., 2001).

1.5.1.3 Peroxisomal protein import machinery

There are at least two known mechanisms by which peroxisomes import proteins. Both of these involve conserved peroxisome targeting sequences (PTS) and receptor proteins. The conserved PTSs are either the highly conserved PTS1 class present as A/S-K/R-L tripeptide at the carboxy terminus of the imported peroxisomal proteins (Gould et al., 1989; Keller et al., 1991) or the less conserved PTS2 type nonapeptide at the amino terminus (Flynn et al., 1998; Petriv et al., 2004). The receptor proteins are Pex5 for PTS1 (Klein et al., 2001) and Pex7 for PTS2 (Rehling et al., 1996). The receptor proteins through binding to the PTS1 or PTS2 of the peroxisomal protein deliver the proteins to the peroxisomal membrane (van der Klei and Veenhuis, 2002). After which, the proteins are translocated across the peroxisomal membrane while the receptors are recycled back to the cytoplasm. The peroxisomal matrix protein import machinery consists of Pex13 and Pex14, which serve as docking sites for the Pex5 and Pex7 receptors (Schell-Steven et al., 2005). In addition to PEX5- and PEX7-mediated peroxisomal import pathways, some peroxisomal matrix proteins are thought to "piggy-back" with other targeted/imported peroxisomal proteins (Holroyd and Erdmann, 2001). Fatty acid beta-oxidation enzymes utilize either a Pex5 or Pex7 import mechanism. A conserved PTS1 has been identified in AOX (Koller et al., 1999). Peroxisomal import of thiolase is mediated by a PTS2 signal (Johnson and Olsen, 2003).

1.5.1.4 Peroxin 6

The Pex1 and Pex6 peroxins are members of the family of AAA (ATPase associated with diverse cellular activities) proteins. Pex6 and Pex1 have been shown to interact in an ATP-dependent manner (Faber et al., 1998). The physical association/interaction of Pex6 and Pex1 *in vivo* requires their first AAA cassette (D1) as well as ATP binding to the 2nd AAA cassette (D2) of Pex1 (Birschmann et al., 2005). The heterodimeric Pex6-Pex1 complex is associated with membranous vesicles that are important for peroxisome biogenesis (Faber et al., 1998). Pex1-Pex6 interaction requires ATP binding to both D1 and D2 but not ATP hydrolysis in D2 of both proteins. Pex1 forms cytoplasmic homo-oligomers which are disrupted by its interaction with Pex6 (Tamura et al., 2006). Pex1 and Pex6 initially interact in the cytosol and then associate with the peroxisomal membranes through the membrane anchor Pex15. The dissociation of the AAA-complex from the peroxisomal membrane requires Pex4 (Rosenkranz et al., 2006). The biogenesis of mature peroxisomes is hypothesized to proceed through a multistep pathway involving the formation and fusion of various peroxisomal vesicular intermediates (Titorenko et al., 2000). The two AAA family ATPases have been shown to be required during the membrane fusion step of the peroxisomal intermediates (Titorenko and Rachubinski, 2000). The recruitment of Pex6 to peroxisomal membranes is through an interaction with an integral membrane protein that requires ATP binding and hydrolysis at its AAA cassettes (Birschmann et al., 2003; Tamura et al., 2006). In *S. cerevisiae*, Pex15, a phosphorylated integral peroxisomal membrane protein, functions as the recruiting partner of Pex6 (Elgersma et al., 1997; Birschmann et al., 2003). In mammalian cells, Pex26 serves as the membrane receptor for Pex6 (Matsumoto et al., 2003; Tamura et al., 2006).

The loss of Pex6 function in Chinese hamster ovary cells results in the formation of peroxisomal membrane structures devoid of protein content, which are known as peroxisomal ghosts (Hashiguchi et al., 2002). This then suggests a possible role for Pex6 in peroxisomal matrix protein import. In *Pichia pastoris*, *PEX6* and *PEX1* mutants likewise possess only vesicular remnants of the peroxisomes (with some residual matrix proteins) with the bulk of peroxisomal proteins mislocalized to the cytosol (Faber et al., 1998). Based on epistatic interactions among different *pex* mutants in *P. pastoris*, Pex1 and Pex6 are predicted to act late in peroxisomal matrix protein import, and after the matrix protein translocation step (Collins et al., 2000). During peroxisomal protein import, Pex6, and Pex1 play a role in the recyling of the Pex5 receptor (Platta et al., 2005). The dislocation of the Pex5 receptor from peroxisomal membranes after delivery of peroxisomal proteins requires ATP binding and hydrolysis by the second conserved AAA domain (Platta et al., 2005).

1.5.2 Peroxisomal beta-oxidation machinery

1.5.2.1 Substrate specificity and import

The substrates of peroxisomal beta-oxidation comprise a broad range of fatty acids, which include saturated, unsaturated, methyl-branched and dicarboxylic fatty acids of various chain lengths (Schulz, 1991). Peroxisomal beta-oxidation is capable of oxidizing very long chain fatty acids but is incapable of catabolizing fatty acids shorter than eight carbons (Schulz, 1991). Depending on the chain length of the fatty acid substrate, two pathways may be utilized for fatty acid uptake into the peroxisomes (Hettema and Tabak, 2000). Medium chain length fatty acids enter the peroxisomes as free fatty acids and are then activated to their acyl-CoA form by the

peroxisomal acyl-CoA synthetase (FAA2) (Johnson et al., 1994). The peroxin Pex11 is hypothesized to play a role during the import of medium chain fatty acids across the peroxisomal membrane (van Roermund et al., 2000). However, work by another group suggests that Pex11 has a direct role in peroxisome division with only a consequent indirect effect on peroxisome metabolism (Li and Gould, 2002). Even in the absence of peroxisomal metabolic activity, overexpression of Pex11 has been shown to promote peroxisomal division. Long chain fatty acids, on the other hand, are esterified to coenzymeA in the cytosol and then transported into the peroxisome by ATP Binding Cassette (ABC) transporters located in the peroxisomal membranes (Hettema et al., 1996).

1.5.2.2 Enzymology

The first enzyme of the conventional peroxisomal beta-oxidation pathway is an acyl-CoA oxidase (AOX), which transfers electrons from the fatty acyl-CoA substrate to molecular oxygen thereby generating hydrogen peroxide (Okazaki et al., 1986). The hydrogen peroxide thus generated is degraded by the peroxisomal catalases. The constant association between catalase and peroxisomal lipid catabolism is a consequence of the perceived requirement for catalase activity to detoxify hydrogen peroxide. Catalase A and acyl-CoA oxidase have been demonstrated to be coinduced in cells cultivated in fatty acids (Skoneczny et al., 1988). Multiple isoforms of AOX which exhibit different substrate specificities are present in the peroxisomes and thus impart the capability to metabolize a broad range of substrates including straight-chain and branched-chain fatty acids (Van Veldhoven et al., 1992; Vanhove et al., 1993).

However, in *N. crassa*, the fatty acid-inducible beta-oxidation system does not involve the AOX enzyme but rather an acyl-CoA dehydrogenase activity ADH (Kionka and Kunau, 1985). This is perhaps consistent with the characteristic of the atypical *N. crassa* beta-oxidation pathway, which is located in specialized peroxisomes that are devoid of catalases (Thieringer and Kunau, 1991a). Interestingly, sequences coding for AOXs are not present in the genome of *Magnaporthe grisea*, though multiple ADH-encoding sequences are have been identified (Dean et al., 2005).

The second and third steps of peroxisomal beta-oxidation are catalyzed by a multifunctional protein (MFP) or bifunctional protein (BFP), which has both 2-enoyl-CoA hydratase (ECH) and 3-hydroxyacyl-CoA dehydrogenase (HADH) activities. In rat, exon I-V codes for the enoyl-CoA hydratase activity whereas exon VII has 3-hydroxyl-CoA-dehydrogenase activity (Ishii et al., 1987; Minami-Ishii et al., 1989). The N-terminal part of rat MFEII is responsible for the 3-hydroxyacyl-CoA dehydrogenase activity (Qin et al., 1997). There are two distinct isoforms of this protein, which reflects the two possible stereoisomers through which the reaction may proceed (Furuta et al., 1980; Adamski et al., 1992). The 3-hydroxyacyl-CoA intermediate can be either in D-isomer or in the L-isomer depending on the MFP enzyme, i.e. either D-BP or L-BP (Jiang et al., 1996). In mammals, the L-BP and the D-BP isoforms have both been identified (Osumi and Hashimoto, 1979){Qin, 1997 #90. The D-BP exhibits activity towards both straight and branched-chain substrates. It is also thought that only the D-BP is required for oxidation of methyl-branched fatty acids (Jiang et al., 1997) and bile acids (Dieuaide-Noubhani et al., 1996). Only a D-isoform of the MFP known as FOX2 exists in the yeast *Saccharomyces cerevisiae*

(Hiltunen et al., 1992). The FOX2 protein of *N. crassa*, however, is the L-isoform (Thieringer and Kunau, 1991b). The physiological significance of this alternative stereochemistry is uncertain as rat peroxisomal MFE which is L-intermediate isomer specific is capable of complementing the loss of the D-specific MFP of yeast (Filppula et al., 1995). The different MFP isoforms may indicate some underlying evolutionary relationships across different organisms. For example, only the human D-BP exhibits homology to the yeast multifunctional proteins (Wanders et al., 2000).

In addition to the ECH and HADH activities, some multifunctional proteins also possess other enzyme functions. For instance, an additional isomerase activity was detected in the rat BP, which potentially enables it to metabolize polyunsaturated fatty acids (Palosaari and Hiltunen, 1990). The MFP in *Candida tropicalis* and in *N.crassa* possesses an additional epimerase domain (Moreno de la Garza et al., 1985; Thieringer and Kunau, 1991b). These additional enzymatic functions complement the hydratase-dehydrogenase activities and perhaps enable the organism to metabolize a broader range of substrates. Alternatively, different isomers of the intermediates of the beta-oxidation pathway may allow these molecules to be redirected to other pathways, such as the polyhydroxyalkanoate synthesis in bacteria (Park and Lee, 2003).

Peroxisomal multifunctional enzymes are targeted to the peroxisome via a conserved PTS1 at the carboxy terminus. Rat MFEII possesses a C-terminal AKL (Qin et al., 1997). The MFPs of *Glomus mossease* (Requena et al., 1999), *Dictyostelium* (Matsuoka et al., 2003) and *S. cerevisiae* (Hiltunen et al., 1992) all possess a C-terminal SKL.

The peroxisomal 3-ketoacyl-CoA thiolase enzyme which catalayzes the last step of the beta-oxidation cycle also exists in multiple isoforms. The isoforms differ in the transcriptional profiles, one being expressed at a low constitutive level and the other significantly induced with clofibrate treatment (Hijikata et al., 1990), as well as their substrate specificities with only one of the two exhibiting activity towards methyl-branched fatty acids (Antonenkov et al., 1997).

1.6   Mitochondrial beta-oxidation

1.6.1   The mitochondria

1.6.1.1 Functions and origin

Mitochondria are organelles surrounded by double membranes of which the inner one is organized into cristae-like structures. The mitochondria contribute diverse cellular roles which include aerobic respiration to generate ATP, regulation of apoptosis and fatty acid synthesis. Mitochondria are capable of generating and conveying calcium signals primarily emitted from the endoplasmic reticulum (Ichas et al., 1997). The most favored model for the origin of the mitochondria is the serial endosymbiosis theory (Gray, 1989). This model suggests that a bacterial endosymbiont which became established in a nucleus-containing but amitochondriate host is the ancestor of the mitochondria (Dyall et al., 2004). However, recent discoveries which are mostly attributed to the comparative analyses of diverse mitochondrial genomes (Lang et al., 1999) have led to the hypothesis that the mitochondria may have originated at the same time as the nucleus rather than at a later event (Gray et al., 1999).

1.6.1.2 Morphological architecture

The name mitochondrion is derived from the Greek term meaning "thread-grain" which corresponds to the two distinct architectures of these organelles (Skulachev, 2001). These two structures consist of an extended filamentous network (thread) and isolated spherical bodies (grain) which are interchangeable. The mitochondrial filaments are thought to represent an electrical continuum which facilitates the distribution of energy to remote parts of the cell (Amchenkova et al., 1988). Extended mitochondrial networks form when cells experience a high energy demand. On the other hand, the isolated mitochondria represent the "transportable form" of these organelles. During the initiation of programmed cell death (PCD), the clustering of spherical mitochondria around the nucleus is thought to facilitate the delivery of mitochondrial pro-apoptotic proteins to the nucleus (De Vos et al., 1998; Susin et al., 1999). In addition, isolated forms of the mitochondria are important for proper segregation of these organelles during cell division. Recently, fatty acid synthesis has been shown to be required for the maintenance of mitochondrial morphology and function. The disruption of a mitochondrial 3-hydroxyacyl-ACP dehydratase, which is one of the enzymes of FA synthesis, in *S cerevisiae* results in abnormal mitochondrial morphology and respiratory defects (Kastaniotis et al., 2004).

1.6.1.3 Protein import

The mitochondrial organelle synthesizes a minimal component of its protein content. The majority of mitochondrial proteins is encoded by nuclear genes and synthesized in the cytosol. Thus a specific need for a mitochondrial protein import machinery for the sorting and delivery of mitochondria-specific proteins. Mitochondria-specific proteins are synthesized as preproteins which possess an N-terminal presequence responsible for its recognition by the mitochondrial import machinery. The 20-50

residue long presequences of different mitochondrial proteins do not share amino acid similarity but have conserved characteristics such as being enriched in positively-charged, hydroxylated and hydrophobic residues (Roise and Schatz, 1988). The presequences enable the recognition and interaction of the mitochondrial preproteins with mitochondrial outer and inner membrane translocases which guide such proteins into the matrix. Once inside the matrix, the presequences are cleaved by peptidases and the mature proteins folds into their functional conformation (Pfanner, 2000).

1.6.2   Mitochondrial beta-oxidation machinery

1.6.2.1 Substrate specificity and import

Mitochondrial beta-oxidation accepts long-, medium- and short-chain fatty acids as substrates (Kerner and Hoppel, 2000). The uptake of long chain (C16) fatty acids across the mitochondrial membrane involves the formation of import-competent carnitine intermediates (McGarry and Brown, 1997). The fatty acyl molecule is transferred from coenzyme A to carnitine, by carnitine palmitoyltransferase I (CPTI) which is an integral membrane protein of the mitochondrial outer membrane (Prip-Buus et al., 1998). The transport of the fatty acyl-carnitine derivative across the inner mitochondrial membrane is facilitated by a specific mitochondrial membrane translocase, carnitine/acylcarnitine translocase (CACT) (Idell-Wenger, 1981). Once inside the inner mitochondrial lumen, the fatty acyl-carnitine is reactivated to its CoA derivative by carnitine palmitoyl transferase II (CPTII), which catalyzes the exchange of the carnitine moiety with Coenzyme A (Woeltje et al., 1990).

1.6.2.2 Enzymology

The enzyme activities utilized during mitochondrial beta-oxidation are essentially similar to those in peroxisomal beta-oxidation. These common enzymatic reactions are catalyzed by multiple enzyme isoforms, which are as monofunctional units or incorporated into multi-enzyme complexes. The monofunctional units consist of: (1) short, medium and long-chain acyl-CoA dehydrogenase, (2) short chain enoyl-CoA hydratase, (3) short-chain 3-hydroxyacyl-CoA dehydrogenase and (4) 3-ketoacyl-CoA thiolase. The multienzyme complex is comprised of long chain enoyl-CoA hydratase/long chain 3-hydroxyacyl-CoA dehydrogenase (alpha subunit) and long chain 3-ketoacyl-CoA thiolase (beta-subunit) (Kamijo et al., 1993). These two distinct enzyme organizations utilize the same pathway, which proceeds via the sequential dehydrogenation-hydration-dehydrogenation-thiolysis reaction.

The first dehydrogenation step of mitochondrial beta-oxidation is catalyzed by acyl-CoA dehydrogenases (ADH), which transfer the electrons from fatty acyl-CoA to a flavoprotein coenzyme electron acceptor (FAD) (Wanders et al., 1999). The byproduct of this first step is a reduced electron acceptor (FADH2), which can immediately participate in the electron transport chain. The mitochondrial ADHs are classified into four types based on their substrate specificity: short chain ADH (SCAD) for C4, medium chain ADH (MCAD) for C6-C10, long chain ADH (LCAD) for C14-C22 and very long chain (ACAD) (Ikeda et al., 1985; Izai et al., 1992).

The second step of mitochondrial beta-oxidation involves the hydration of trans-delta 2,3-enoyl-CoA intermediates and is catalyzed by enoyl-CoA hydratases (ECH). There are two known isoforms of ECH enzymes (Fong and Schulz, 1977). ECH1 or crotonase shows maximal activity towards C4 enoyl-CoA intermediates and its

24

activity decreases progressively as the substrate chain length increases. ECH2 or long chain enoyl-CoA hydratase, on the other hand, exhibits maximal activity towards C8 intermediates, has greater activity than crotonase for substrates up to C16 carbons and has very low activity for C4 substrates (Schulz, 1974) ECH1 and ECH2 work in a complimentary manner to ensure that all the unsaturated intermediates of the fatty acid beta-oxidation pathway are hydrated (Fong and Schulz, 1977). In addition, ECH1 and ECH2 are proposed to work together to catalyze an epimerization reaction based on a dehydration-hydration reaction (Hiltunen et al., 1989).

The enoyl-CoA hydratases belong to a family of hydratase/isomerases, thus some members exhibit both hydratase and isomerase activities. Two conserved glutamic acid (Glu) residues have been shown to be critical for hydratase and/or isomerase catalytic activities. Glutamic acid at position 144 is conserved in ECHs possessing only the hydratase activity (Wu et al., 1997). On the other hand, glutamic acid at position 164 is conserved in ECH-proteins capable of catalyzing hydration and isomerization reactions (Muller-Newen et al., 1995). Multifunctional enzymes capable of hydratase activities also maintain the conserved Glu164 residue. The Glu164 residue does not play a role in substrate binding but rather in the protonation and deprotonation reactions (Muller-Newen et al., 1995). Replacement of the conserved Glu residues with alanine results in a protein still capable of proper folding and assembly but with greatly reduced hydratase activity (Kiema et al., 1999). Mitochondrial ECH1 possesses the conserved Glu164 residue and also has isomerase catalytic properties (Kiema et al., 1999).

Resolved crystal structures of the ECH enzyme have provided insights into the protein's capability to bind different substrates and the stereochemistry of the hydratase reaction. The ability of ECH to bind fatty acids of different chain lengths is accomplished by the movement of the B-factor loop in the fatty acid binding pocket (Engel et al., 1998). ECH forms an extended conformation to accommodate the tail of longer chain fatty acids. Two geometric isomers, (S) or (R) 3-hydroxyacyl-CoA are possible with ECH hydration reaction. The higher preference for the (S) isomer is due to the selective activation of this bound substrate form (Bell et al., 2002). In bacterial fatty acid beta-oxidation, the (R) 3-hydroxyacyl-CoA product, which is formed by a specialized ECH, is re-directed to the polyhydroxyalkanoate pathway (Park and Lee, 2003). Quite intriguingly, *N. crassa* cells grown in sucrose exhibit a relatively high basal level of mitochondria-associated enoyl-CoA hydratase activity (Kionka and Kunau, 1985). The failure to detect other mitochondria-associated beta-oxidation enzymatic activities suggests that this mitochondrial ECH activity is involved in pathways other than fatty acid catabolism.

The third step of mitochondrial beta-oxidation is the dehydrogenation of the 3-hydroxyacyl-CoA intermediate and involves a 3-hydroxyacyl-CoA dehydrogenase. The terminal step of thiolytic cleavage is catalyzed by 3-ketoacyl-CoA thiolase. Alternatively, the 2nd, 3rd and 4th steps of mitochondrial beta-oxidation can be catalyzed by a trifunctional protein, which contains the hydratase-dehydrogenase activities in its alpha-subunit and the thiolase activity in the beta-subunit (Uchida et al., 1992).

1.7 Auxiliary pathways of lipid catabolism

1.7.1 Carnitine-mediated pathways

The acetyl-CoA generated from fatty acid beta-oxidation in the peroxisomes needs to be transported to either the cytosol for macromolecular biosynthesis or the mitochondria for energy production and complete oxidation via the tricarboxylic acid cycle. Acetyl-CoA in itself is membrane impermeable. The transport of acetyl-CoA across membranes requires the transfer of the acetyl unit from coenzyme A (CoA) to carnitine. Carnitine is a methylated derivative of the amino acid lysine and is essential for metabolic processes. Higher eukaryotes are capable of synthesizing carnitine endogenously. Yeasts, however, are unable to synthesize carnitine but rely on its uptake up from the extracellular environment (Swiegers et al., 2001).

The formation of acetyl-carnitine intermediates is catalyzed by the enzyme carnitine acetyltransferase (CRAT). This enzyme belongs to a family of carnitine acyltransferases, which catalyze the reversible exchange of acyl groups between coenzyme A and carnitine (Ramsay et al., 2001). In addition to CRAT which is specific for the acetyl moiety and short chain fatty acids, this family includes carnitine palmitoyltransferase I and II (CPT I/II) and carnitine octanoyltransferase (COT) which have substrate preferences for long chain and medium chain fatty acids, respectively (Kerner and Hoppel, 2000). CPT I/II participates in the transport of long-chain fatty acids destined for beta-oxidation across the mitochondrial inner membrane. COT is involved in the transfer of shortened medium chain fatty acid products of peroxisomal beta-oxidation to the mitochondria for complete oxidation. Based on the structural analysis of CRAT, the family of carnitine acyltransferases is inferred to be capable of catalyzing the hydrolysis of both acyl-CoA and acylcarnitine

without the formation of an acyl-enzyme intermediate (Jogl and Tong, 2003; Wu et al., 2003).

In *S. cerevisiae*, acetyl-CoA is generated from peroxisomal fatty acid beta-oxidation and cytosolic metabolism of acetate and ethanol. The catabolism of ethanol and acetate involves the enzymes of the mitochondrial tricarboxylic acid cycle and the glyoxylate and gluconeogenic pathways (McCammon, 1996). The complete oxidation of the cytosolic acetyl-CoA by the tricarboxylic acid cycle requires its transport to the mitochondria. Three different genes encoding CRAT have been identified in budding yeast (Kispal et al., 1991; Schmalix and Bandlow, 1993). And the CRAT activities found to be induced by fatty acids and other nonfermentable carbon sources such as acetate, glycerol and ethanol.

The major carnitine acetyltransferases activity in budding yeast is due to the YCat/Cat enzyme (Kispal et al., 1991), which is localized predominantly in the mitochondria. Its primary function is thought to be in the delivery cytosol-activated acetyl units from acetate into the mitochondrial matrix (Kispal et al., 1993). A canonical type 1 peroxisome targeting sequence, however, is present at its C-terminus, which indicates a possible peroxisomal localization (Schmalix and Bandlow, 1993). Through the mechanism of alternative splicing Ycat gets dually localized in the mitochondria and/or peroxisomes (Elgersma et al., 1995). Yat1, which localizes to the mitochondrial outer membrane, contributes <1% of total mitochondrial CRAT activity (Schmalix and Bandlow, 1993). Yat2, which is localized to the cytosol, contributes major CRAT activity during growth on ethanol (Swiegers et al., 2001).

Though carnitine-dependent metabolism is essential for utilization of fatty acids and other non-fermentable carbon sources, a bypass pathway involving the glyoxylate cycle has been identified in budding yeast. The viable phenotype of any of the single CRAT gene deletion mutants on fatty acid and/or acetate medium indicate the presence of another pathway which enables the transport of acetyl/acyl activated molecules without the requirement for carnitine. This bypass pathway is thought to be through the citrate and succinate products of the glyoxylate shunt (van Roermund et al., 1995).

In *Aspergillus nidulans*, two different carnitine acetyltransferases, AcuJ and FacC, are essential for the metabolism of fatty acids and for acetate, respectively (Stemple et al., 1998). AcuJ CRAT activity represents the major cellular CRAT and is induced by both acetate and Tween80 (Midgley, 1993). AcuJ is required for growth on both acetate and fatty acids and suggests that it may also be dually localized to the peroxisome and the mitochondria. FacC, on the other hand is required for growth on acetate, and its cytosolic CRAT activity is induced solely by acetate (Stemple et al., 1998). The glyoxylate bypass mechanism which complements the yeast carnitine mutants does not seem to function similarly in *A. nidulans*.

The transport of acetylcarnitine molecules from the mitochondrial matrix to the cytosol involves a carnitine/acylcarnitine transporter. In *A. nidulans*, AcuH encodes one such enzyme.. AcuH, which is required for growth on acetate and long-chain fatty acids, contains a hydrophobic domain which is highly conserved among diverse members of the mitochondrial carnitine carrier family (De Lucas et al., 1999). Crc1, the orthologous protein in *S. cerevisiae*, has been shown to function in the transport of

acetylcarnitine molecules from the peroxisome to the mitochondria (van Roermund et al., 1999).

1.7.2   Glyoxylate pathway

The glyoxylate cycle is a modified version of the tricarboxylic acid cycle (TCA), which bypasses two decarboxylation steps thereby allowing the net synthesis of C4 intermediates for gluconeogenesis (Eastmond and Graham, 2001). The following enzymes are common between the glyoxylate cycle and the TCA: citrate synthase, aconitase and malate dehydrogenase. Isocitrate lyase (ICL) and malate synthase (MLS) are unique to the glyoxylate pathway. Through the activity of ICL, citrate (product of acetyl-CoA and oxaloacetate) is cleaved to form glyoxylate and succinate. Succinate then serves as the key C4 intermediate for the synthesis of sucrose. There is a strong correlation between the expression of ICL and MLS and lipid catabolism during postgerminative growth (Kornberg and Krebs, 1957). Through the glyoxylate pathway, acetyl-CoA derived from fatty acid beta-oxidation is utilized for biosynthesis of sugars. The inhibition of fatty acid breakdown in germinating seedlings of *Arabidopsis icl* mutants indicates that there is coordinated regulation between lipid catabolism and the glyoxylate cycle (Eastmond et al., 2000). Though the glyoxylate cycle is not essential during postgerminative growth under optimum conditions, it was found to be required for seedling establishment during suboptimum light conditions. Experiments, which utilize radioactively-labelled molecules, have shown that the incorporation of acetate moieties into sugars is accomplished primarily through the glyoxylate pathway. Exogenous sucrose is capable of rescuing the phenotypic defects associated with the loss of ICL function. The glyoxylate cycle also

functions to replenish TCA cycle intermediates during growth on fatty acid substrates (Eastmond and Graham, 2001).

1.7.3 Polyketide synthesis

The polyketide pathway is long recognized as an important pathway for the synthesis of diverse secondary metabolites such an antibiotics (Hutchinson and Fujii, 1995). One of the well-studied products of the polyketide pathway is fungal melanin, which serves as critical virulence/pathogenicity factors for plant and animal pathogens (Bell and Wheeler, 1986). The melanin of *M. grisea* consists of polymers of dihydroxynapthalene (DHN) (Langfelder et al., 2003) and is likely synthesized through the polyketide pathway utilizing acetyl-CoA as precursor(Chumley and Valent, 1990). In the related pathogenic fungus *Colletotrichum lagenarium*, malonyl-CoA, which is a carboxylated derivated of acetyl-CoA has been shown to be utilized during the pentaketide synthesis of melanin (Fujii et al., 2000). The sequential steps of the polyketide pathway that leads to the synthesis of melanin is as follows: transformation of malonyl-CoA to 1,3,6,8 tetrahydroxynapthalene (1,3,6,8 THN) by PKS1 (polyketide synthase 1), reduction of 1,3,6,8 THN to scytalone, dehydration of scytalone to 1,3,8 trihydroxynapthalene which is afterwards reduced to vermelone, and final dehydration of vermelone to 1,8 dihydroxynapthalene (DHN) (Langfelder et al., 2003). DHN then dimerizes and polymerizes to form melanin.

1.8   Physiological roles of lipid catabolism

1.8.1   Requirement for lipid catabolism during pathogenesis

The importance of lipid catabolism for pathogenicity is strongly indicated by the upregulation of lipid metabolic genes during pathogenesis and the isolation of

nonpathogenic strains, which harbor mutations in genes encoding components of lipid metabolic pathways. Transcriptional profiling of the human opportunistic pathogen *Candida albicans* showed that beta-oxidation and glyoxylate cycle genes are upregulated during the macrophage sequestration stage of its infection cycle (Prigneau et al., 2003). Three of these upregulated genes were found to encode carnitine acetyltransferases, *CTN1, CTN2* and *CTN3*. Based on primary sequence data, the subcellular localization of these proteins is predicted to be: cytosolic for Ctn1, peroxisomal and mitochondrial for Ctn2 and peroxisomal for Ctn3 (Prigneau et al., 2003). A *ctn3Δ* exhibits reduced viability within macrophages and has a defect in forming filamentous hyphae both within macrophages and on solid media (Prigneau et al., 2004). Genes coding for the isocitrate lyase 1 (*ICL1*) and malate synthase 1 (*MLS1*) enzymes of the glyoxylate cycle were also found to be upregulated during macrophage phagocytosis (Lorenz and Fink, 2001). The *icl1Δ* exhibits decreased virulence in a mouse model. Survival within the macrophage most likely requires a metabolic re-programming that involves a switch to lipid catabolism. In addition, *C. albicans* grown on lipids and serum and *C. albicans* recovered from in vivo incubation in mice both exhibited an increase in peroxisome number and formation of fibrillar extensions from the cell (Sheridan and Ratledge, 1996).

Icl1 function is required for the successful colonization and pathogenicity of *Leptosphaeria maculans* on oilseed rape (Idnurm and Howlett, 2002). Development of wild-type lesion size in the *icl1Δ* can be restored by exogenous supplementation with 2.5% glucose. Overexpression of peroxisomal 3-ketoacyl-CoA thiolase results in reduced pathogenicity of *L. maculans* attributed to a defect in invasive growth (Elliott and Howlett, 2006). The overexpressing strain exhibit decreased pycnidiospore

germination away from inoculation site and sparse hyphal growth at inoculation site. Exogenous supplementation with either 25mM Tween80 or 25mM glucose did not rescue pathogenicity defect and resulted only in increased pycnidiospore germination at the surface and hyphal proliferation at inoculation site but not into plant tissue (Elliott and Howlett, 2006).

1.8.2 Lipid catabolism during development

1.8.2.1 Lipid catabolism during plant development

Lipid catabolism is of primary importance as a source of energy and carbohydrates for macromolecular synthesis during the process of seed germination (Penfield et al., 2005). Fatty acid beta-oxidation interconnects with the glyoxylate cycle, through which acetyl-CoA is converted to succinate, which in turn is converted into glucose or other metabolic intermediates. The transfer of metabolites between the fatty acid beta-oxidation and glyoxylate cycle is facilitated by the colocalization of the components of both pathways within glyoxysomes (Cooper and Beevers, 1969). Upon development of photosynthetic capabilities, which generate glucose, glyoxysomes are replaced by peroxisomes which are devoid of isocitrate lyase and malate synthase activities (Baker et al., 2006). Seedling establishment requires the function of the peroxisomal multifunctional beta-oxidation enzyme MFP2 (Rylott et al., 2006). During seed germination, acetyl-CoA from fatty acid beta-oxidation is transported out of the peroxisome as citrate. Disruption in genes encoding peroxisomal citrate synthases CSY1 and CSY2 impairs seed germination and blocks triacylglycerol metabolism (Pracharoenwattana et al., 2005). The utilization of endospermic lipid reserves requires gluconeogenesis and transport of sugars to the germinating embryo (Penfield et al., 2005). The energy requirements and the production of specialized

signaling and structural metabolites during reproductive development is also dependent on fatty acid beta-oxidation (Richmond and Bleecker, 1999). A mutation of AIM1, which is a homolog of MFP2, results in plants with normal vegetative growth but exhibits abnormal meristem development. Inflorescence development was found to be delayed and to consist of abnormal patterning.

1.8.2.2 Lipid catabolism during animal development

In animal models, peroxisomal lipid catabolism has been shown to be essential during neurological development. Peroxisomes were found to be abundant in mice glial cells thereby indicating a requirement for peroxisomal function during neuronal cell development (Nagase et al., 2004). Mice harboring a mutation in the peroxisomal multifunctional protein MFP2 exhibit a neurological phenotype characterized by astroglial damage (Huyghe et al., 2006b). An impairment of mitochondrial fatty acid beta-oxidation in *Drosophila* has been found to result in severe developmental defects. The *scully* gene, which encodes a mitochondrial beta-oxidation enzyme with hydroxylacyl-CoA dehydrogenase activity, is essential for reproductive development (Torroja et al., 1998). Mutant *scully* males exhibit reduced testes, which accumulate lipids in the cytoplasm, whereas mutant *scully* females are blocked in oogenesis. There is presumably a high reliance on mitochondrial beta-oxidation for the provision of energy generation during reproductive development. The formation of rhabdomere structures within the eye organ is also abolished in *scully* mutants. Mitochondrial beta-oxidation is also hypothesized to provide intermediates for lipid synthesis during rhabdomere formation (Torroja et al., 1998). A disruption in the Enigma locus, which encodes the first enzyme in the mitochondrial beta-oxidation cycle results in a

developmental delay characterized by a prolonged larval and pupal stage (Mourikis et

al., 2006).

CHAPTER II MATERIALS AND METHODS

2.1   Molecular methods

2.1.1 Creation of plasmid vectors for targeted deletion and genetic complementation

Gene-deletion mutants were generated using the standard one-step gene replacement strategy in *M. grisea*. For each locus, about 1 kb regions immediately upstream and downstream of the ORF were PCR amplified and ligated sequentially into either pFGL44/59 or pFGL97 to flank the selectable marker cassette (hygromycin phosphotransferase gene (*HPH1*) or bialaphos resistance gene (*BAR*), respectively, under the control of the TrpC promoter). The PCR-amplified fragments were cloned into either the right border side of the construct (*Pst*I/*HinD*III sites) or the left border side of the construct (combination between *Xho*I, *EcoR*I, *Sac*I, *Kpn*I, *Sma*I and *BamH*I sites). For this study, the targeted deletion of the following genes was performed: *PEX6* (MG00529.4), *CRAT1*/*PTH*2 (MG01721.4), *CRAT2* (MG06981.4), *FOX2* (MG06148.4) and *ECHA* (MG06272.4). The primers used for the amplification of the 5' and 3' fragments are given in Table 1. The deletion constructs were confirmed by DNA sequencing prior to their introduction into the wild-type *M. grisea* strain.

For genetic complementation of *pex6Δ*, the rescuing construct consisted of a 7.25 kb *Kpn*I fragment from BAC clone 2A14 which contained the entire *PEX6* ORF and about 800 bp of 5'UTR cloned into pFGL97. For genetic complementation of the *fox2Δ* and *echAΔ* strains, the genomic fragment carrying the full-length locus with at least 1 kb of upstream and downstream sequences were PCR amplified and cloned

into pFGL97 or pFGL44, respectively. The primers used for the amplification of the complementing genomic fragments are given in Table 1.

2.1.2   Creation of plasmid vectors for RFP and GFP tagging

For expression of GFP-PTS1, a fragment encoding GFP-SRL was cloned under the control of the *MPG1* promoter and TrpC terminator from plasmid pFC2-ORF-GFP (a kind gift from Heidi Bohnert and Marc-Henri Lebrun). This construct was transformed into the wild type and the *pex6Δ* strains. For subcellular localization of Pth2 protein, an RFP-SKL tag was introduced at the C-terminus immediately before the SKL coding region of the genomic copy of *PTH2*. The fusion construct pFGL421 was created by cloning 1 kb of the *PTH2* 3'UTR into the *Pst*I/*Hin*DIII sites of pFGL347. The gene encoding Red Fluorescent Protein (RFP) was amplified from the plasmid pDsRed-Monomer-N1 (Clontech, CA, USA) with a reverse primer that incorporated the tripeptide SKL before the stop codon. The RFP-SKL was cloned in frame with the last 377 bp of the *PTH2* C-terminus (just proximal to the codons encoding SKL, which were excluded) in the *Xho*I/*BamH*I sites of pFGL421. The fusion construct was verified by nucleotide sequencing and transformed into a *Magnaporthe* strain expressing GFP-PTS1. For subcellular localization of Fox2 and EchA, about 1 kb of genomic sequence immediately before the stop codon was PCR-amplified and translationally fused to RFP or GFP.

2.1.3   Bacterial transformations and plasmid preparations

Plasmid DNA was transformed into chemical competent *E. coli* strain XL1-Blue or MC1061 by heat shock treatment. XL1-Blue and MC1061 were made chemically competent by the calcium chloride method (Sambrook, 1989) and stored in 200 μl

aliquots at -70^0C until use. For transformation, the cells were thawed on ice for 10 minutes, mixed with about 50 ng DNA, incubated at 42^0C for 100 seconds, immediately transferred to ice and supplemented with 800 µl cold Luria-Bertani (LB, per L: 10 g of tryptone, 5 g of yeast extract and 10 g of NaCl) medium. After 1 hour incubation at 37^0C, the cells were plated on LB plates containing 100 µg/ml kanamycin. After overnight incubation at 37^0C, isolated colonies were inoculated in 2.5 ml of LB + kanamycin. The liquid cultures were incubated at 37^0C with 200 rpm shaking for 10-16 hours. Two ml of the grown cultures were used for plasmid extraction. Plasmid extractions were carried out using the Qiaprep Spin miniprep kit according to manufacturer's instructions (Qiagen Inc, Valencia, CA, USA).

2.1.4 *Agrobacterium*-mediated transformation of *M. grisea*

The constructs were electroporated in *Agrobacterium tumefaciens* strain AGL1. The transformed Agrobacterium strain was activated in liquid induction medium (IM, per liter: K salts 10 mL, M salts 20 mL, NH_4NO_3 (20%) 2.5 mL, $CaCl_2$ (1%) 1 mL Glucose 5 mM, MES 40 mM, Glycerol 0.5% w/v; K salts: K_2HPO_4, 20.5, KH_2PO_4 14.5%; M salts: $MgSO_4-7H_2O$ 3%, NaCl 1.5%, $(NH_4)_2SO_4$ 2.5%) with acetosyringone (ACS). To introduce the constructs into *M. grisea*, transformed *Agrobacterium* was cocultivated with *M. grisea* conidia in minimal medium containing acetosyringone according to previously described methodology {de Groot, 1998 #131}. The minimal medium is composed of, per liter: K salts 10 mL, M salts 20 mL, Z salts 5 mL, NH_4NO_3 (20%) 2.5 mL, $CaCl_2$ (1%) 1 mL, Glucose 5 mM, MES 40 mM, Glycerol 0.5% w/v, $FeSO_4$ (0.01%) 10 mL, Agar 20 g; Z salts: $ZnSO_4-7H_2O$, $CuSO_4-5H_2O$, $MnSO4-H_2O$, H_3BO_3, $Na_2MbO_4-2H_2O$, each at 0.01%. After 48-96 hour incubation at 28^0C, the *Agrobacterium* was selectively killed with 200 µM cefotaxine and *M. grisea*

38

transformants were selected either on CM containing 250 μg/ml hygromycin or defined complex medium (DCM; 0.16% yeast nitrogen base without amino acids, 0.2% asparagine, 0.1% ammonium nitrate and 1% glucose, pH 6.0 with Na_2HPO_4) containing 40 ug/ml ammonium glufosinate (Cluzeau Info Labo, France). Correct gene replacement events were confirmed by PCR and DNA gel blot analyses.

2.1.5 DNA extraction and Southern blot analysis

The potassium acetate method was used for extraction of fungal DNA (Naqvi et al., 1995). Mycelia harvested from a 3-5 day liquid culture was pressed dry on paper towels and ground into a fine powder in liquid nitrogen. The ground mycelium was resuspended in 850 μl of extraction buffer (100mM Tris-Cl, pH8.0, 100mM EDTA, 250mM NaCl) and 85 μl 10%SDS, thoroughly mixed and incubated at 65^0C for 30 minutes. The mixture was then acidified with 350 μl of 5M Potassium acetate and stored on ice for 15 minutes after mixing. The mixture was centrifuged at 14000 rpm for 10 minutes to precipitate cellular debris. The supernatant was transferred to a fresh 2ml tube and extracted with an equal volume of chloroform:isoamyl alcohol solution (24:1). After centrifugation (14000 rpm, 5 minutes), the top layer was transferred to a fresh tube and precipitated with 2/3 volume isopropanol. The DNA pellet was recovered by centrifugation at 14000 rpm for 10 minutes and washed with 2 X 1ml 70% ethanol. After air-drying, the pellet was resuspended in minimal volume of sterile distilled water (~100 μl). DNA gel blot analysis was performed using standard protocols (Sambrook, 1989). Probe-labeling and DNA blot detections were done using the ECL direct nucleic acid labeling and detection system (Amersham Biosciences, UK).

2.1.6 RNA extraction and RT-PCR

For Reverse Transcriptase PCR (RT-PCR) analyses, total RNA was extracted from cultures grown 24 h in glucose minimal medium and then transferred to the medium containing either glucose, olive oil or acetate for 8 h. RNA was extracted using sodium acetate buffer (50mM sodium acetate, 10mM EDTA, 1%SDS) and acidic phenol and precipitated with isopropanol. AMV reverse transcriptase (Roche Diagnostics, Penzberg, Germany) was used to synthesize cDNA from 2 μg of total RNA. RT-PCR products were amplified using primers designed (Table 1) for the following *M. grisea* genes: *PTH2* (MG01721.4), *CRAT2* (MG06981.4), MG00803.4 (β-tubulin) and *MPG1* (MG10315.4). To assess the specificity and to serve as a negative control, the RNA sample in each instance was also processed without a reverse transcriptase step prior to the PCR amplification.

Table 1. List of oligonucleotide primers used in this study. Restriction enzyme sites introduced for cloning purposes are written in lower case in the primer sequences.

Gene (Locus)	Description	Selection marker	Enzyme site	Primer sequence
PEX6 (MG00529.4)	Deletion construct	Hygromycin		
CRAT1/PTH2 (MG01721.4)	Deletion construct	Hygromycin	*Kpn*I *Bam*HI *Pst*I *Hin*DIII	GAGAGTGAAggtaccCTAGGATTGTTTGGGTAT GAGAGTGAggatccACAGCAGCAGCAGCACAG GAGAGTGTTctgcagACGGGTGGGAGTCAGGTCA GAGAGTGTTaagcttTGAGAAGGGTGGCAGGCT
	RT-PCR	-	-	ATGGCTTCTGGAAGCAAAAG ACATCCACTTGTAGCTGTCC
	C-terminal tagging with RFP	Hygromycin	*Eco*RV *Nde*I	GAGAGTGgatatcGAGGAGCGTGCGCACGCCTAC GAGAGTGcatatgCTTGGGAGCCTCAATGGTG

Gene (Locus)	Description	Selection marker	Enzyme site	Primer sequence
CRAT2 (MG06981.4)	KO construct	Bialaphos	*Sma*I *Bam*HI *Pst*I HindIII	GAGAGTGAcccgggAACCACCACCACGATAGA GAGAGTGAggatccGATTGTCGTCTGTCGTCA GAGAGTGTTctgcagAGGAATTGGATGCCGGTC GAGAGTGTTaagcttAAATTTTCTTCTGCTTGA
	RT-PCR	-	-	ATGCCCAGCCAAGTTCGCAT GAACAAACTCGAGTGCTGAT
FOX2 (MG06148.4)	Deletion construct	Hygromycin	*Eco*RI *Bam*HI *Pst*I *Hin*DIII	GAGAGTGAgaattcGTAAGCGACACCTTGGTATC GAGAGTGAggatccGGTATGTGATAGAGTAGAGG GAGAGTGTTctgcagGTGATCAGATGGGGGAAAGT GAGAGTGTTaagcttAACAAGCTCACGTGTCCATG
	Genetic complementation	Bialaphos	*Eco*RI *Bam*HI	GAGAGTGAgaattcGCTTCAATGACGGTGGTTTG GAGAGTGAggatccAACAAGCTCACGTGTCCATG
	RT-PCR			GACTTCCAGGTCTTGCCAAC GAGATGCCAAAGAAGCAGAG
	C-terminus tagging with RFP	Hygromycin	*Eco*RI *Nde*I	GAGAGTGAgaattcCTTAAGTCGTACGGCAAG GAGAGTGTTcatatgGTACAGCTCCGCCGCGGC

Gene (Locus)	Description	Selection marker	Enzyme site	Primer sequence
ECHA (MG06272.4)	KO construct	Bialaphos	*Kpn*I *Bam*HI *Pst*I *Hin*DIII	GAGAGTGAAggtaccACGAACTCTCGATAATCTG GAGAGTGAggatccGATGATCGATTTGTTCACAG GAGAGTGTTctgcagCTTGTTGCCAGAAGTATGCA GAGAGTGTTaagcttGAAAGCACAGAGGACAGCAG
	Genetic complementation	Hygromycin	*Kpn*I *Bam*HI	GAGAGTGAAggtaccGAATTATGCTGTCAGGTCCG GAGAGTGAggatccCTCATGCACCCCAACATCAC
	RT-PCR			ATGAACGCCTTCAGAGCTCT CCAAAGTTGGCCGATTCGGT
	C-terminus tagging with GFP	Hygromycin	*Kpn*I *Nde*I	GAGAGTGAggtaccGACCTGACCACTCAGGTC GAGAGTGAcatatgCTGATGAGTCCATTCGGG
MPG1 (MG10315.4)	RT-PCR control	-	-	ATCATCCCAAATGCTCACCA TGATCGCATGCATCCCTGAT

2.2 Carnitine acetyltransferase assays

M. grisea strains were grown for 3 days (28^0C, 120 rpm) in Minimal Medium (MM; per liter: 0.5 g of KCl, 0.5 g of $MgSO_4$, 1.5 g of KH_2PO4, 6 g of NaNO3 and 10 g of glucose) after which they were transferred to MM containing either 1% glucose or 1% olive oil or 50 mM sodium acetate and incubated for another 4 hours. Protein extracts were prepared by grinding filtered mycelia in liquid nitrogen and resuspending in extraction buffer (50mM Tris-Cl pH 7.5, 50mM NaCl, 0.2% Triton X-100, proteinase inhibitors). Cell debris was removed by centrifugation and total protein concentrations were determined using the Bio-Rad protein assay reagent (Bio-Rad Laboratories, Hercules, CA, USA). Equal protein concentrations were used for the assays. CrAT assays and quantifications of the specific activity therein, were performed as described (Stemple et al., 1998). The reaction mixture contained 40 mM KH_2PO_4 (pH8.0), 0.05 mM acetyl-CoA, 0.12 mM 5,5'-dithiobis-(2-nitrobenzoic acid) (DTNB) and crude protein extract. The reaction was initiated by addition of 2.2 mM DL-carnitine. Reaction mixture without carnitine was used as a negative control.

2.3 Fungal strains and culture conditions

The *Magnaporthe grisea* wild-type strain B157 was obtained from the Directorate of Rice Research (Hyderabad, India). Prune agar medium (PA; per liter: 40 mL of prune juice, 5 g of lactose, 1 g of yeast extract and 20 g of agar, pH 6.0) was used for standard culture maintenance and conidiation. PA plates inoculated with mycelial plugs were incubated in the dark in a 28^0C incubator for five days. To induce conidiation, plates were then exposed to continuous light at room temperature for another five days. For harvesting conidia, ten ml of antibiotic water (sterilized

distilled water containing 100 ug/ml carbenicillin and 100 ug/ml streptomycin sulfate) was added to the light-exposed plates and the mycelial surface was gently scraped with an inoculating loop. The suspension was filtered through two layers of miracloth to remove mycelial debris and then briefly centrifuged. A minimal volume of antibiotic water was used to resuspend the conidial pellet. Conidial suspensions were adjusted to the required concentrations after counting with a hemacytometer.

For preservation of fungal cultures, sterilized 5 mm^2 filter papers were placed on top of mycelial growth from five-day old plates. The plates were incubated for another 3-5 days in the 28^{0}C incubator to allow fungus to grow on the filter papers. Fungal-colonized filter papers were removed aseptically and placed in sterile coin envelopes which were dried using dehydrated silica gel. Dried samples were stored at -20^0 C.

For the assessment of carbon source utilization on plates, the basal medium consisted of 0.67% yeast nitrogen base without amino acids, 0.1% yeast extract, adjusted to pH 6.0 with Na_2HPO_4 with 2% agar. The carbon sources tested were 1% glucose, 1% olive oil/0.05% Tween20 (as emulsifier), 50 mM sodium acetate, 4.9 mM erucic acid, 6 mM oleic acid, 8.5 mM myristic acid, 10 mM lauric acid, 12 mM decanoic acid, 15 mM octanoic acid and 20 mM hexanoic acid. Colony growth was evaluated on plates inoculated with mycelial plugs of wild-type and test strains after incubation at 28^{0}C for 7-10 days.

For assessment of sensitivity to cell wall destabilizing chemicals, PA plates containing 100 μg/ml calcofluor or congo red were inoculated with serial dilutions of

conidial suspensions from the wild-type and test strains. Growth was evaluated after incubation at 28^0C for 3-5 days.

For extraction of genomic DNA, total RNA, and total protein, mycelial cultures were grown in liquid medium, either complete medium (CM; per liter: 10 g sucrose, 6 g casein hydrolysate, 6 g yeast extract) or minimal medium (MM), for 3-5 days at 28^0C with 120 rpm shaking.

2.4   Evaluation of pathogenicity and pathogenicity-related traits

The detached barley leaf assay, adapted from Dr Marc-Henri Lebrun's laboratory, was used to assess pathogenicity in the laboratory. Three to five cm-long pieces of barley leaves from 14-day old seedlings were washed for 2 minutes in 40% ethanol and several rinses of sterile distilled water. Washed leaves were briefly dried on paper towels and then mounted on kinetin agar plates (2 mg/ml kinetin, 1% agar). Conidial suspensions were inoculated as 10-15 ul water droplets with increasing conidial concentrations (500-2000 conidia/droplet). The plates were incubated in a 22^0C humidified chamber with a 16-hour light/8-hour dark cycle. Disease symptoms were assessed 7-10 days post-inoculation. For chemical supplementation experiments, the conidial droplet contained 0.1% or 2.5% glucose, 1% sodium citrate, 1% sodium malate or 1% succinate.

For assessment of pathogenicity on rice plants, 14-day old seedlings of cultivar CO39 were spray-inoculated with 10^4-10^5 conidia/ml suspension containing 0.01% Tween20. To maintain a high humidity, the inoculated seedlings were kept covered with a plastic bag sprayed with water and incubated for 24 hours in a humidity

chamber before being transferred to a growth chamber. Disease symptoms were assessed 5-7 days after inoculation.

Quantitative assessment of appressorial function was performed on detached barley leaf assays. Inoculated barley leaves were harvested at different timepoints (24-, 48-, 72- and 96-hours post-inoculation) and cleared overnight with 100% methanol. Cleared leaves were stained with aniline blue (0.1% aniline blue/67 mM K_2HPO_4, pH 9.0) to visualize host leaf papillary callose formation. Callose formation underneath the appressoria was taken as a measure of penetration peg formation. In addition, the number of infectious hyphae was counted under a bright field microscope.

Appressorium formation was assessed on the hydrophobic surface of artificial polyester membranes (Gelbond^{TM}, Biowhittaker Molecular Applications, Rockland, ME, USA) as well as on detached barley leaves. The total number of appressoria formed was quantified after an incubation period of 24 hours.

2.5   Microscopy

2.5.1   Fluorescence microscopy

GFP epifluorescence was observed using a Zeiss LSM510 inverted confocal microscope (Carl Zeiss Inc., Thornwood, N.Y., USA) equipped with a 30 mW argon laser. The objectives used were either a 63X Plan-Apochromat (numerical aperture, 1.4) or a 100X Achromat (n.a. 1.25) oil immersion lens. EGFP was imaged with 488 nm wavelength laser excitation, using a 505-530 nm band pass emission filter, while RFP imaging used 543 nm laser and a 560 nm long-pass emission filter.

2.5.2   Staining with fluorescent dyes

To visualize lipid bodies, fungal samples were incubated in a 2.5 μg/ml Nile Red (Sigma-Aldrich, USA) solution in 50 mM Tris-maleate buffer, pH 7.5 with 20 mg/ml polyvinylpyrrolidone (Thines et al., 2000). The following settings were used for visualization: excitation at 450 to 490 nm, 505 nm dichroic mirror and 520 nm barrier filter. To visualize mitochondria, fungal samples were incubated for 15 minutes in a 100 nm Mitofluor594 (Molecular Probes, Invitrogen, Madison, WI, USA) solution in 1X phosphate buffered saline.

2.6   Phylogenetic analysis

For phylogenetic analysis, amino acid sequences of the requisite proteins were submitted to the Internet Web Gene Bee services of the Belozersky Institute of Moscow State University ([www.genebee.msu.su)](www.genebee.msu.su). The phylogenetic trees were generated using the ClustalW algorithm of the Tree Top phylogenetic tree prediction software with bootstrap analysis of 100 iterations.

CHAPTER III PEROXISOME-ASSOCIATED METABOLISM DURING

Magnaporthe **PATHOGENESIS**

3.1   Introduction

Peroxisomes are ubiquitous single membrane-bound organelles which are capable of diverse cellular functions (Purdue and Lazarow, 2001). Lipid metabolism with the ensuing production of acetyl-CoA for energy production and breakdown of hydrogen peroxide constitute the long established peroxisomal processes. Recently though, novel peroxisomal functions in a wider range of cellular processes have begun to emerge (Titorenko and Rachubinski, 2004). In humans, peroxisomal disorders constitute an important class of genetic disorders attributed to either the loss of a single peroxisomal enzyme function or the loss of the entire peroxisomal organelle (Gould and Valle, 2000).

In plants, the most well-characterized peroxisomal function is lipid metabolism in specialized peroxisomes known as glyoxysomes (Cooper and Beevers, 1969). The metabolism of lipid stores is necessary to provide an energy source for the developing embryo. Fatty acid beta-oxidation consists of a cycle of four enzymatic reactions which progressively reduce fatty acids by two carbon units which are then liberated as an acetyl-CoA moiety (Wanders et al., 2000). Acetyl-CoA is then made available to other cellular compartments for energy production and biosynthesis reactions via carnitine intermediates. The peroxisome-based fatty acid beta-oxidation pathway then interconnects with other metabolic pathways through the provision of acetyl-CoA (Eastmond and Graham, 2001). A number of *Arabidopsis* peroxisome mutants are developmental mutants whose embryonic lethal phenotype can be rescued by exogenous sucrose (Schumann et al., 2003; Zolman and Bartel, 2004). Recently, it has

been shown that peroxisome-derived reactive oxygen species, such as hydrogen peroxide and nitric oxide, are important signaling ligands for the photomorphogenesis in plants (Hu et al., 2002).

In filamentous fungi, a role for peroxisomes has been demonstrated in pathogenesis, mating and stress response to hyphal lysis. The loss of pathogenicity in the *pex6Δ* mutant of *Colletotrichum lagenarium* is attributed to the loss of the appressorial melanin layer, which is essential for appressorium-mediated host penetration (Kimura et al., 2001). The *Podospora anserina pex2Δ* mutant is impaired in the nuclear fusion stage of sexual development (Boisnard et al., 2003). This *pex2Δ* phenotypic defect is likely related to the defect in peroxisomal fatty acid uptake and to the accumulation of toxic substances since it is partially rescued by the overexpression of the *ABC1* (ATP Binding Cassette) transporter, which potentially serves both functions (Boisnard et al., 2003). Woronin Bodies which are peroxisome-derived vesicles have been shown to function in septal pore plugging during hyphal lysis in *Neurospora crassa* (Jedd and Chua, 2000) and to be required for full pathogenicity of *M. grisea* (Soundararajan et al., 2004).

To identify genes required for pathogenicity in *M. grisea*, a collection of insertional mutants was generated by *Agrobacterium* Transferred-DNA (T-DNA) mediated insertional mutagenesis and screened for pathogenicity defects. A number of insertions were identified in genes required for the biogenesis of functional peroxisomes. The first of these insertions was in *Peroxin 6* (PEX6). To investigate the requirement for peroxisomal metabolic function during pathogenesis, I created and extensively characterized a *pex6Δ* mutant. The loss of the melanin layer in the

pex6Δ appressoria strongly indicated the importance of peroxisomal acetyl-CoA for melanin biosynthesis. As an extension of the study of peroxisomal metabolism and pathogenicity, deletion mutants for genes encoding enzymes, which catalyze the export of peroxisome generated acetyl-CoA, were also created and characterized.

3.2   Results

3.2.1   Screening for nonpathogenic mutants using *Agrobacterium*-mediated T-DNA insertions

An insertional mutagenesis screen was carried out to identify novel genes required during *M. grisea* pathogenesis. Germinating conidia of *M. grisea* from wild-type backgrounds B157 and Guy11 were transformed with plasmid pFGL59, which contained a hygromycin resistance gene (*HPH1*) under the *TRPC* promoter cloned in a T-DNA vector. Transformants which harbored random insertions of Pr*TRPC*-*HPH1* were selected on hygromycin-containing medium. As part of the general laboratory effort, about 3,000 insertion mutants were isolated and characterized over a period of three years. Conidia harvested from isolated transformants were used to assess appressorium formation and pathogenicity in detached barley leaf assays.

One of the transformants which exhibited a total loss of pathogenicity was TMP6-2. TMP6-2 contained a single insertion of the hygromycin resistance cassette (*HPH1*) containing T-DNA and disrupted a region on Contig 2.95 (*Magnaporthe* Genome Database, Broad Institute, USA). A 7.25 kb *Kpn*I fragment was identified that corresponded to this region and further annotation of this genomic fragment revealed that the disruption was in the second exon of an open reading frame (ORF) predicted to encode Peroxin6 (hereafter Pex6), a peroxisome biogenesis protein found in several

eukaryotes (Figure 2A). This gene was designated as *MgPEX6* (hereafter simply referred to as *PEX6*) and further *in silico* analyses of the deduced nucleotide sequence of the gene and the coding sequence suggested that the ORF spans 4.309 kb and is interrupted by two short introns (Figure 2A). *PEX6* was predicted to encode a protein of 1375 amino acid and showed a domain organization reminiscent of the members of the AAA-ATPase family.
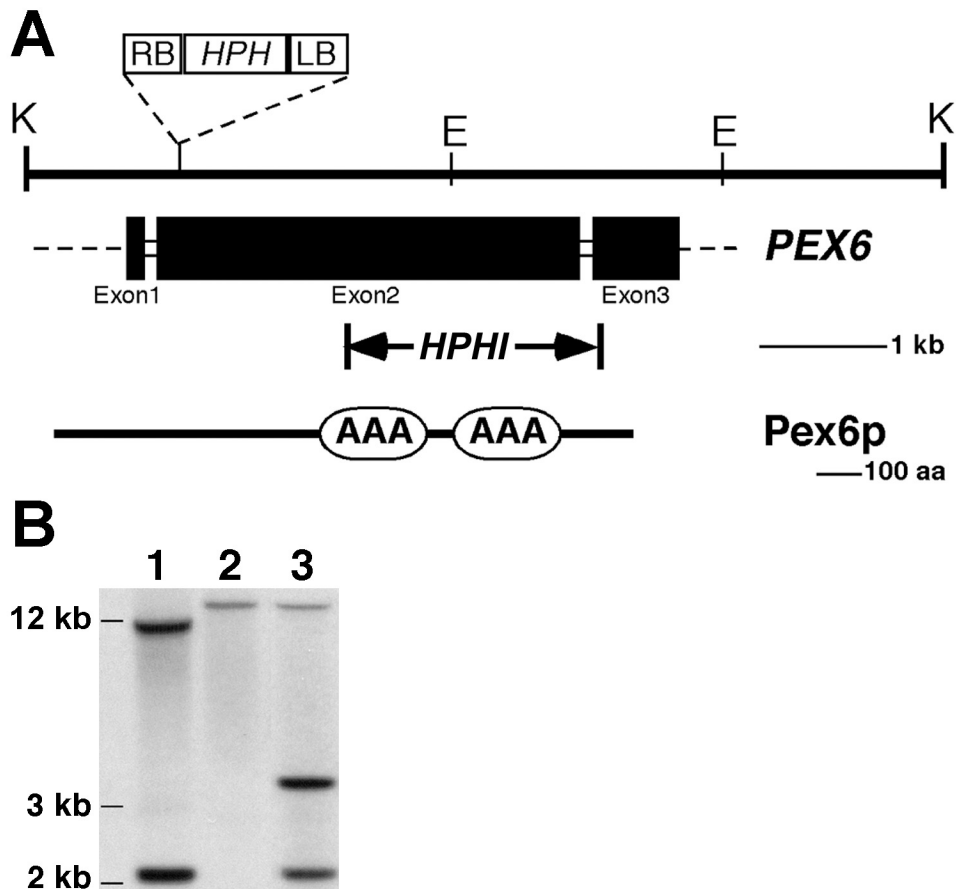
Figure 2. Identification and characterization of a *pex6Δ* mutant in *M. grisea*.
(A) Annotation and schematic representation of the *M. grisea PEX6* locus spanning a *Kpn*I (denoted as K; E refers to EcoRI sites) fragment on BAC clone 2A14 from *M. grisea*. Solid bars and short open boxes indicate the coding regions and the introns, respectively, and are drawn to scale. RB and LB represent the right and left border sequences of T-DNA (open box) integrated in the TMP6-2 mutant strain. Opposing arrows demarcate the genomic region deleted to create the *pex6Δ* strain using the *HPH1* cassette. The *PEX6* region spanning one kb either side of the first *Eco*RI site was used as the probe for the Southern blot analysis shown in (B). Scale bar denotes 1 kb or 100 amino acids as shown.

(B) DNA gel blot analysis of *PEX6* deletion and rescued strains. Genomic DNA from B157 wild-type (1), *pex6Δ* (2) and a *pex6* rescued strain (lane 3; carrying an ectopic single copy integration of the *Kpn*I fragment described above) was digested with *Eco*RI, and processed for DNA gel blot analysis. The appearance of the 12.5-kb band in the pex6̦ strain, with the concomitant loss of the wild-type 11.2-kb and 2.1-kb band, was diagnostic of the correct gene replacement event. Ectopic integration of the complementation construct in the rescued strain resulted in the retention of the 12.5 kb band and the restoration of the wild-type 2.1 kb band. The appearance of a 3.5 kb band in the complemented strain is due to an internal *Eco*RI site in the rescue construct.

In addition to TMP-6-2, a nonpathogenic transformant, TMT2298, was separately identified which contained an insertion in the gene (*PEX1*) for a related peroxisome biogenesis protein Peroxin1.

As both insertions occurred in genes related to peroxisome biogenesis, assessment of fatty acid utilization, a known peroxisome-localized metabolic pathway, was done for both mutants. Both TMP6-2 and TMT2298 were totally incapable of growing on medium containing 1% olive oil or oleic acid as sole carbon source though they grew to wild-type levels on glucose-containing medium. Taken together, these data indicated that the insertions in *PEX6* and *PEX1* resulted in loss of functional peroxisomes and likely led to the disruption of the fatty acid beta-oxidation pathway.

The functions of Pex6 and Pex1 during peroxisome biogenesis in yeast have been well studied (Portsteffen et al., 1997; Kiel et al., 1999). Both peroxins belong to the AAA-ATPase family and are known to interact with each other. They are essential for the formation of functional peroxisomes through either the fusion of preperoxisomal vesicles or the recycling of receptors which facilitate the import of peroxisomal matrix proteins. Given that both Pex6 and Pex1 are known from other systems to act in the same pathway and that both insertion mutants (TMP6-2 and TMT2298) displayed similar phenotypic defects, further work was carried out on the *PEX6* locus.

3.2.2   Creation of *PEX6* deletion and complemented strains

The loss-of-function mutants (*pex6::HPH;* hereafter *pex6Δ*) in the *M. grisea PEX6* was created by replacing about 44% of the coding sequence, in particular the region encoding the two catalytic AAA ATPase domains, with the *HPH1* cassette, using

homology-assisted recombination. This exercise was carried out in the wild-type strain B157 and the resultant gene replacement events confirmed by DNA gel blot analysis (Figure 2B).

The *Kpn*I fragment containing the full-length genomic copy of *PEX6* was introduced into the deletion strains to test for complementation of the defects associated with the loss of *PEX6* function. An RFLP associated with the complementing allele was identified between the wild-type (lane 1) and the complemented strain (lane 3). Genomic DNA digested with *EcoR*I was probed with the *PEX6* specific probe (Figure 2A). The WT showed a 2.1 kb and a 11.2 kb fragment, whereas the *pex6Δ* (lane 2) showed the loss of the 2.1 kb band and the appearance of the 12.5 kb fragment. The complemented strain regained the 2.1 kb specific fragment and in addition showed the presence of the 3.5 kb fragment. At least two independent strains in each instance (deletion and complemented) were used for confirmation and further investigations.

3.2.3   Peroxisomal defects of *pex6Δ* mutant

In yeasts, metabolism of medium (8-10 Carbon) and long chain (12-18 Carbon) fatty acids occurs through the process of beta-oxidation which takes place in the peroxisomes (Kunau et al., 1995). To evaluate peroxisomal function in the *pex6Δ* strain, growth utilizing either glucose or olive oil as the sole carbon source was assessed. On basal medium with glucose as the carbon source, the *pex6Δ* mutant showed slightly reduced growth compared to the wild-type (Figure 3). On olive oil containing medium, the wild-type grew normally, whereas growth of the *pex6Δ* strain was completely abolished (Figure 3).
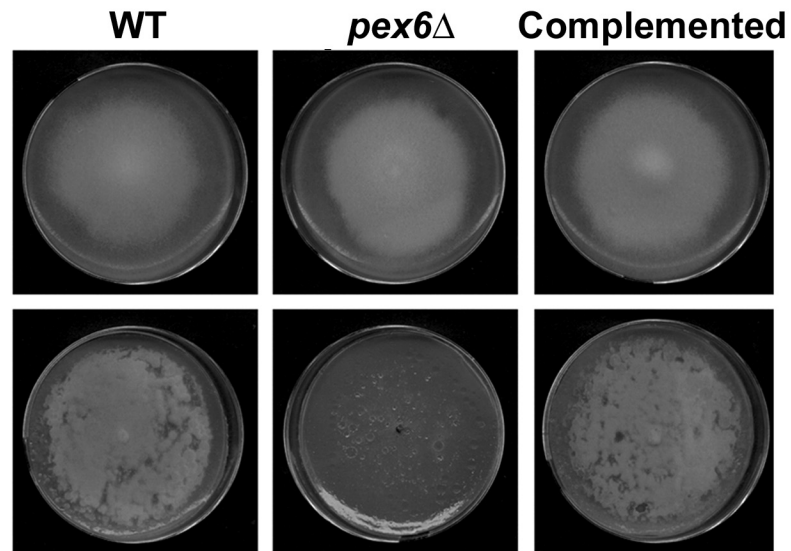
Figure 3. Loss of fatty acid metabolism in the *pex6Δ* strain.
The wild-type, *pex6Δ* or the *pex6Δ*-complemented strains were grown on basal medium supplemented with either 1% glucose (upper panel) or 1% olive oil (lower panel) for ten days.

To evaluate the functional integrity of peroxisomes, peroxisomal matrix protein import was assessed in the *pex6Δ* strain. Towards this end, GFP fused to a C-terminal PTS1 (S-R-L, amino acid serine-arginine-leucine (Miura et al., 1992)) was introduced into both the wild-type and the *pex6Δ* strains. Subcellular localization of GFP-SRL epifluorescence was then investigated during the vegetative (mycelia) and the pathogenic (conidia, germ tubes and appressoria) growth phases of the *GFP-SRL* strains. In the *GFP-SRL* strain, punctate GFP fluorescence, indicative of intact peroxisomes, was observed during all the growth stages (Figure 4). In contrast, only a diffused cytoplasmic fluorescence was detected in the different growth stages of the *pex6Δ/GFP-SRL* strain. Taken together, these results indicated that the *pex6Δ* mutant lacks functional peroxisomes and as a consequence is defective in β-oxidation of long-chain fatty acids and in the import and transport of peroxisomal matrix proteins.

Wildtype/GFP-SRL
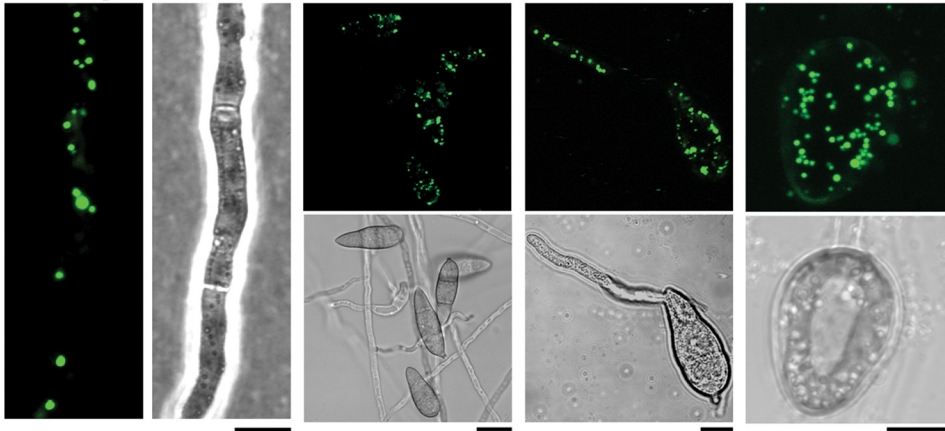
pex6Δ/GFP-SRL
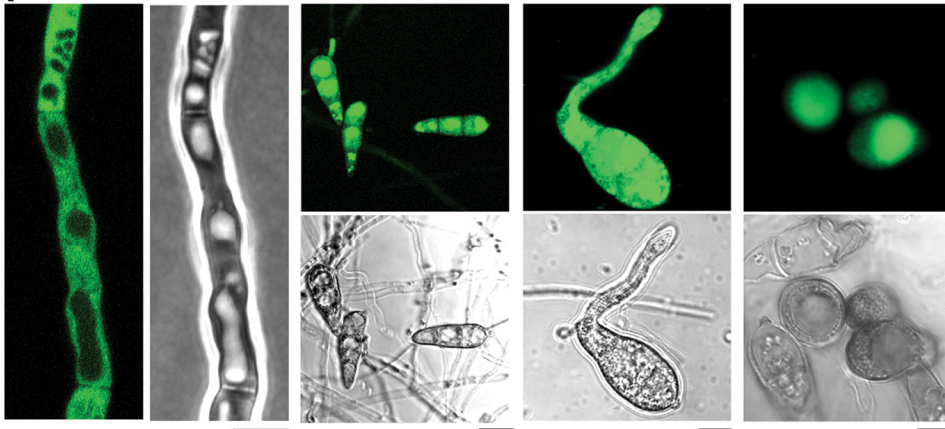
Figure 4. Peroxisomal defects of the *pex6*Δ strain.
Impairment of peroxisomal matrix protein import in the ***pex6*Δ** strain. The wild-type and the *pex6*Δ strains were transformed with a GFP-PTS1 construct and observed using epifluorescence microscopy during the different stages of vegetative and pathogenic development. In the wild-type strain, the GFP-PTS1 fusion protein was observed as punctate fluorescence, whereas in the *pex6*Δ strain, the GFP epifluorescence was predominantly cytoplasmic. Scale bars for panels showing the mycelia, germinating spores or the appressoria = 5 μm. Scale bars sizing conidia represent 10 μm.

3.2.4 Loss of pathogenicity and pathogenicity-related defects of *pex6Δ*

Since *M. grisea* infects several monocot species, the pathogenicity of *pex6Δ* mutant was tested on two different hosts, barley and rice. In a barley detached leaf assay, inoculation with wild-type conidia resulted in the formation of visible blast lesions, which started at four days post-inoculation and which continued to coalesce and spread over the leaf surface (Figure 5, upper panels). However, the *pex6Δ* mutant did not elicit any disease symptoms even when inoculated with a four-fold higher conidial load. The *pex6Δ* was likewise completely nonpathogenic on rice cultivar CO39 (Figure 5, lower panels). Spray inoculations with even a two-fold higher conidial load than the wild-type did not enable the *pex6Δ* to cause blast disease on rice seedlings.
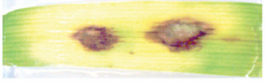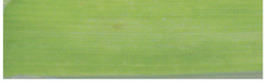
Figure 5. ***pex6Δ* infection assays on barley and rice.**
Conidia from the wild-type, *pex6Δ* and complemented strains were used to inoculate leaf explants of barley (upper panel) and seedlings of rice cultivar CO39 (lower panel). The number of conidia inoculated on the detached barley leaf is indicated. Disease symptoms for both experiments were assessed 7 days post-inoculation.

Detailed microscopic observations of the infection process were undertaken to determine which stage of pathogenesis was affected in the *pex6Δ* mutant. The ability to form appressoria (upon conidial germination) was greatly reduced in the *pex6Δ* mutant. Quantitative appressorium formation assays conducted on artificial membranes (Gelbond^TM, Biowhittaker Molecular Applications, Rockland, ME USA) and on leaf surfaces demonstrated that the capability to form appressoria in the *pex6Δ* was reduced to ~50% of that observed in the wild-type strain (Figure 6A). Moreover, appressoria formed by *pex6Δ* were completely nonfunctional and unable to elaborate penetration pegs as judged by papillary callose deposition assays using aniline blue (Figure 6A, appressorium function). The penetration pegs and infection hyphae were never elaborated by *pex6Δ* appressoria during leaf infection assays even after 96 hours post inoculation (Figure 6B). In wild-type inoculations, ramifying and invasive infectious hyphae, which originate from the appressoria, were clearly seen 48 hours after inoculation. These results suggest that the nonpathogenicity defect of *pex6Δ* could be attributed directly to a defect in appressorium-mediated host penetration.
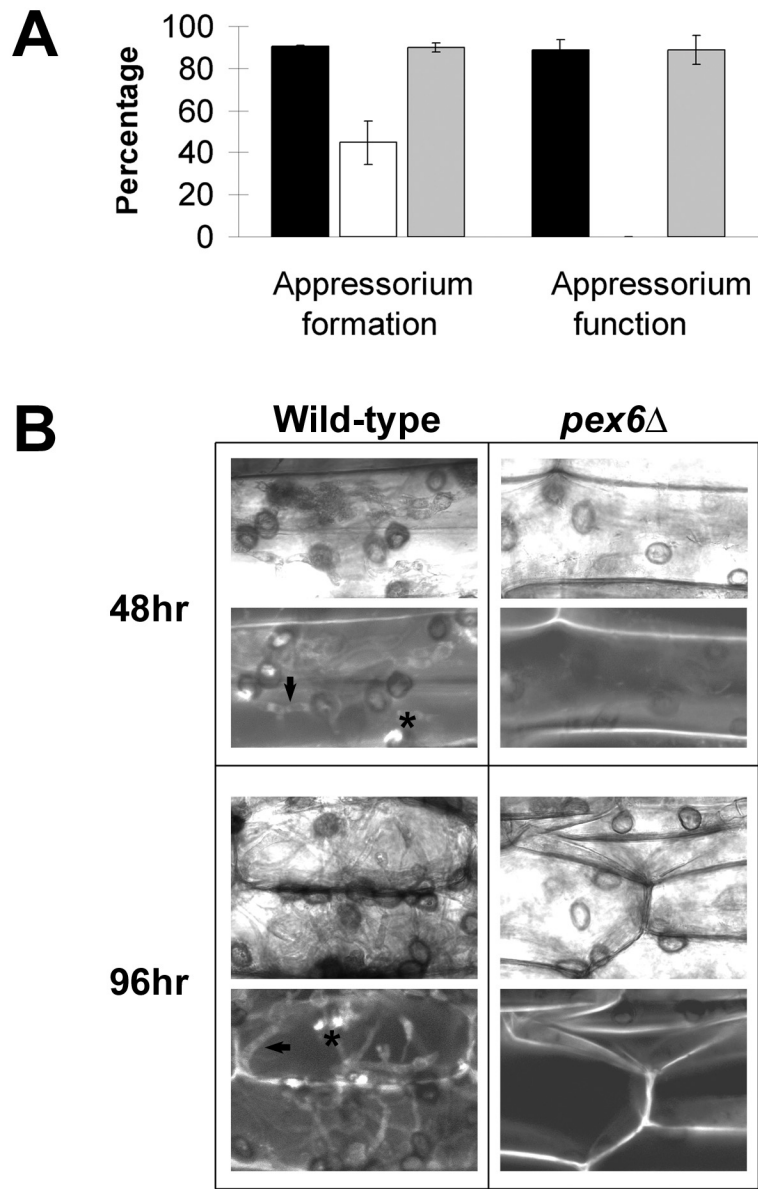
Figure 6. Pathogenicity-related defects of the *pex6*Δ strain.
(**A**) Equal number of conidia of the wild-type (black bar), *pex6*Δ (open bar) or the complemented (gray bar) strain were inoculated on both artificial membrane and host surface to evaluate appressorium formation and appressorium function, respectively. Appressorium formation was assessed as the number of germinated conidia which formed appressoria after 24 hours. Appressorium function was evaluated as the number of appressoria which formed penetration pegs/infectious hyphae after 48 hours. Mean values (+/- SD) presented as percentage points were derived from three independent experiments.

(**B**) Equal number of conidia of the wild-type or *pex6*Δ strain was inoculated on barley leaf explants. The number of papillary callose deposits (asterisk) and infection hyphae (arrow) were quantified after staining with aniline blue at 48 hours or 96 hours post inoculation. Scale bar represents 10 μm.

3.2.5   Loss of appressorial melanin layer in *pex6Δ*

Light microscopic observations revealed that compared to the wild-type, the *pex6Δ* mutant showed aberrant appressoria that appeared to lack the dark pigment melanin (Figure 7A). To perform a better analysis of the melanization and to determine why the *pex6Δ* appressoria were nonfunctional, thin-section electron microscopy (TEM) was performed on 24-hour old appressoria from these strains. In wild-type appressorial sections, an electron dense layer of melanin was distinctly observed and was uniformly deposited along the periphery of the entire cell (Figure 7B, WT). At higher magnifications, a distinct melanin layer was clearly seen between the appressorial cell wall and the plasma membrane. In all the sections of various *pex6Δ* appressoria (n=30) observed, this melanin layer was completely absent (Figure 7B). As a control for non-melanized appressoria, TEM was also conducted on appressoria formed by wild-type conidia in the presence of tricyclazole, a well-known inhibitor of melanin synthesis (Mares et al., 2006). As in *pex6Δ* appressoria, the melanin layer was also found to be absent in tricyclazole-treated appressoria. Furthermore, the melanin layer was restored in the complemented *pex6Δ* strain (Figure 7B, complemented).
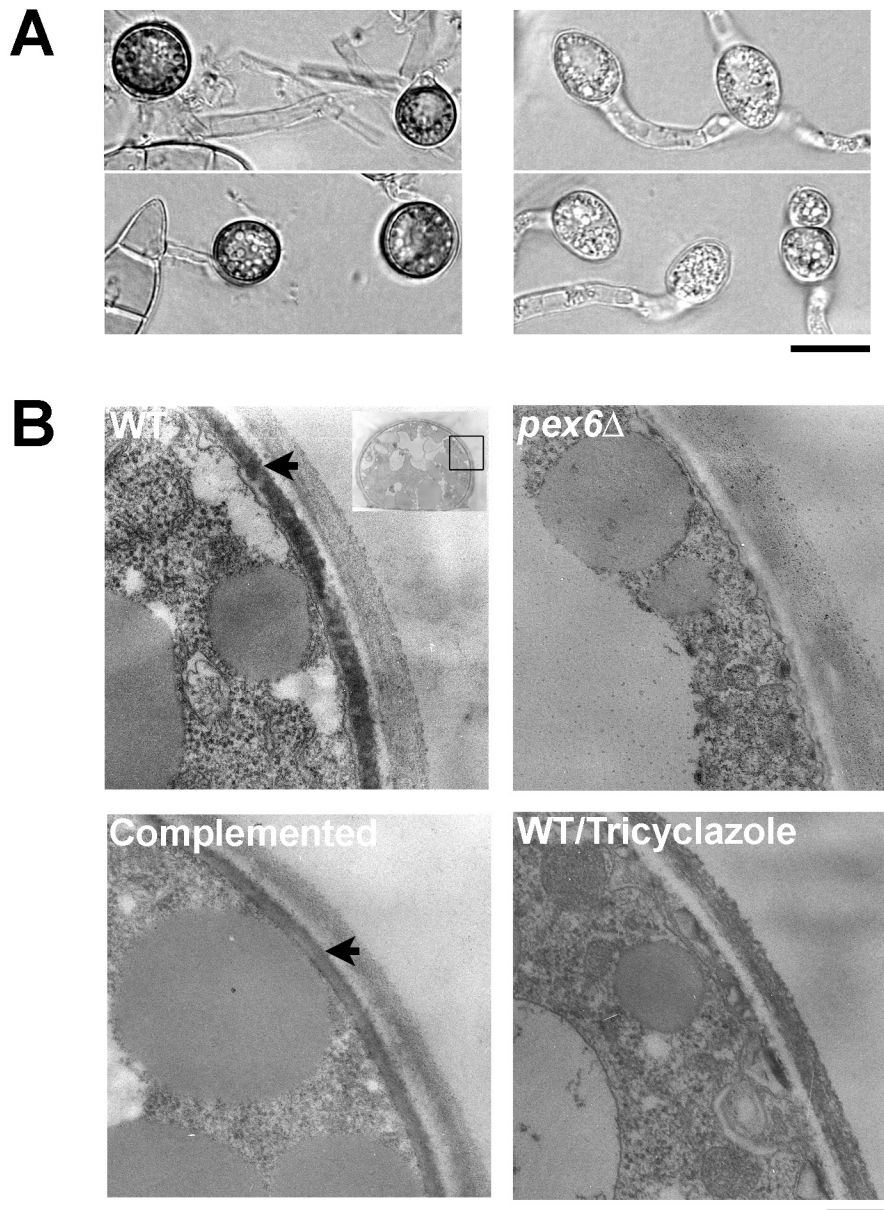
Figure 7. Loss of appressorial melanin layer in the *pex6Δ* strain.
(**A**) Conidia harvested from the wild-type (left panel) or the *pex6Δ* (right panel) strain were incubated on artificial inductive surfaces for 24 hours and observed by Hoffman modulation contrast optics based light microscopy. Bar = 10 μm.

(**B**) Twenty-four hour old appressoria of the wild-type, *pex6Δ* and complemented strains were processed for thin-section electron microscopy (TEM). As a control for non-melanized appressoria, wild-type conidia were allowed to form appressoria in the presence of tricyclazole. The melanin layer in the wild-type and complemented strains is indicated by the arrowhead. Boxed area in the inset demarcates the magnified region of the outer layers of the appressoria presented in the WT panel. Bar = 200 nm.

3.2.6 Loss of Woronin bodies in *pex6Δ*

In *pex6Δ*, about 40% of the appressoria exhibit abnormal shapes such as double-appressoria or bean-shaped appressoria (Figure 8A). The aberrant appressorial morphology is reminiscent of the misshapen appressoria observed in the *hex1Δ* mutant which lacks Woronin bodies (Soundararajan et al., 2004). Woronin bodies (WB) are peroxisome-derived organelles which function to maintain cellular integrity by sealing septal pores during stress conditions. The *pex6Δ* strain also exhibited compromised growth in osmotic stress conditions as shown by its poor growth in sorbose medium compared to wild-type (Figure 8B). This phenotypic defect was also observed in the *M. grisea hex1Δ* mutant (Soundararajan et al., 2004). These additional phenotypic defects of *pex6Δ* were therefore attributed to the loss of peroxisome-derived Woronin bodies.
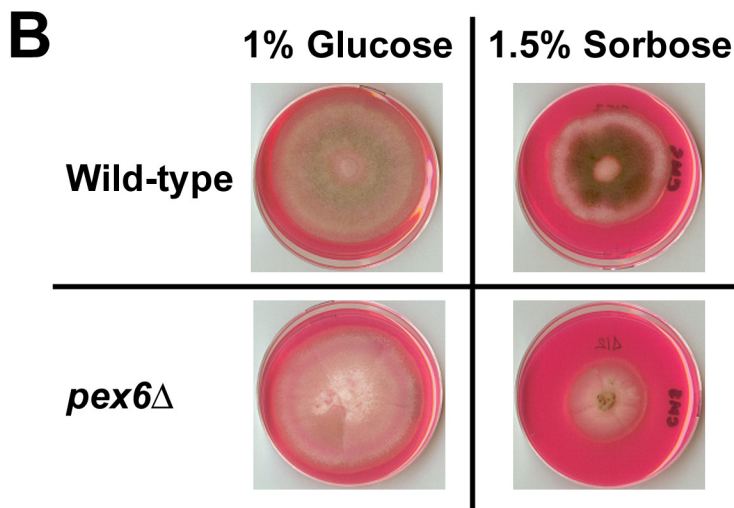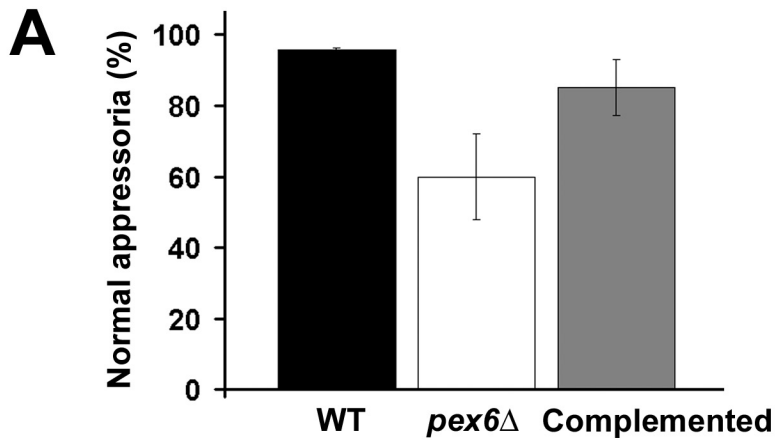
Figure 8. Phenotypic defects of *pex6Δ* which are associated with the loss of Woronin bodies.

(A) The frequency of normal (spherical) and misshapen (kidney-shaped, double) appressoria of wild-type, *pex6Δ* or *pex6Δ* complemented strain was assessed from 24-hr appressorial assays on barley leaf surface.

(B) To assess for sensitivity to osmotic stress, wildtype and *pex6Δ* strains were cultivated on complete medium with phloxine B containing either 1% glucose or 1.5% sorbose.

In *M. grisea* and other filamentous fungi, WBs are easily observed as 100-200 nm electron dense organelles usually localized near the septal pore (Momany et al., 2002; Soundararajan et al., 2004). To determine if there is a defect in WB formation in the *pex6Δ*, thin section electron micrographs of the fungal mycelia were analyzed. In the wild-type preparations, WBs were easily observed as single-membrane bound, electron dense vesicles measuring ~100 nm at the medial section of the septum (Figure 9A). However, WBs were never observed among all the medial sections of fungal mycelia of *pex6Δ* observed. In the *pex6Δ*-complemented strain, WBs were present at the same frequency as in the wild-type.
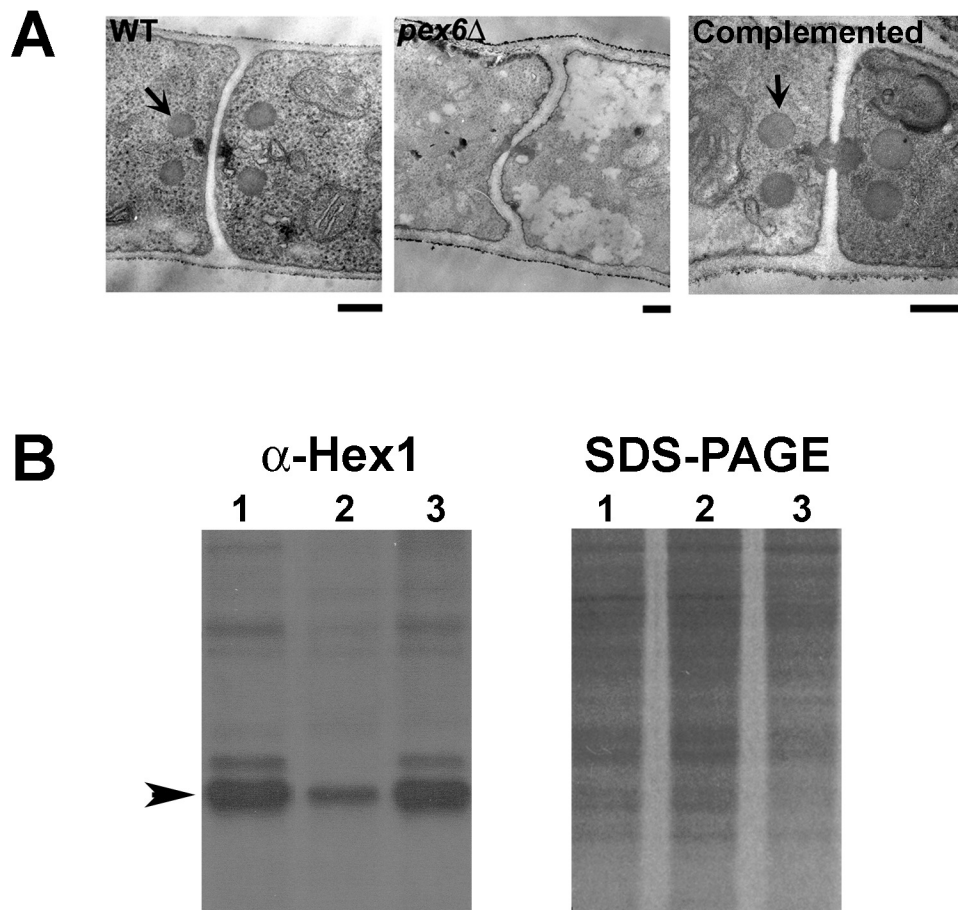
Figure 9. Loss of Woronin bodies and and reduction of Hex1p in the *pex6Δ* strain.
(A) Mycelia, harvested from 48-hour liquid cultures of the wild-type, *pex6Δ* or the *pex6Δ* complemented strain, were processed for TEM analysis. Woronin bodies (arrow) were found to be present only in the wild-type and complemented strains. Bar = 200 nm.

(B) Western analysis was performed on total protein extracts from wild-type (1), *pex6Δ* (2) and *pex6Δ* complemented strains with anti-Hex1. The *M. grisea* Hex1p is indicated by the arrowhead. The same protein samples were electrophoresed on an SDS-PAGE to ascertain that equal amounts of protein were loaded.

The core of WBs consists of the Hex1p (Jedd and Chua, 2000). The presence of a canonical PTS1 (tripeptide SKL) at the C-terminus of the Hex1p sequence indicates the protein's passage through the peroxisome for proper vesicle biogenesis. Using an antibody against the *Neurospora crassa* Hex1p, which cross-reacts with *M.grisea* Hex1p, a reduction in the levels of Hex1p was observed in the *pex6Δ* strain (Figure 9B). These observations demonstrate that WBs require a functional peroxisome organelle for biogenesis and that these vesicles are important for *M. grisea* during osmotic stress and for appressorium morphogenesis.

3.2.7 Identification of *M. grisea* carnitine acetyltransferases

It has been proposed that fungal melanin synthesis utilizes acetyl-CoA as precursor molecules (Chumley and Valent, 1990) and that peroxisomal beta-oxidation of fatty acids could be a potential source for acetyl-CoA biogenesis (Thines et al., 2000; Kimura et al., 2001). Since *pex6Δ* is unable to metabolize long chain fatty acids, it is likely that the transfer of fatty acids and acyl groups from peroxisomes to the cytoplasm and/or to the mitochondria, will either be sub-optimal or abolished in this mutant. In eukaryotes, the transfer of acyl groups across intracellular membranes is facilitated by carnitine. Hence, the role of carnitine acetyltransferases (CrAT; EC number 2.3.1.7), which play a role in the requisite modification and movement of acetyl-CoA between membrane-bound organelles and the cytoplasm, was investigated. In *Saccharomyces cerevisiae*, there are three CrAT enzymes with specific and overlapping localizations to the peroxisome, mitochondria and cytoplasm. A TBLASTN (Altschul et al., 1997) search of the *S. cerevisiae* CrATs against the *Magnaporthe* genome revealed that there are only two CrATs (designated

*CRAT1/*MG01721.4 and *CRAT2/*MG06981.4) encoded within the *M. grisea* genome

(Figure 10).

```
Cat2p  MRICHSRTLSNLKDLEITSRRAMHSAIVNHSTQKA-QFPVETNNGEHYWAEKENKFYQNKRENFQGITENKQQDL
Pth2p  --------------MASGSKRSSSSLEAGYVEDKS-KGPMLR----------------------------FQESL
CrAT2  --------------MPSQVRIFTPPKELGETLAEPDKDPVKAQQPLPRRQLKEMSKNHGGIEEEGGITFAAQDSL

Cat2p  PSLPVPELKSTLDKYLQEIRPFCNDVETFERQQLLCKDFS-EDMGEILQDRLKEYANDK--RNVMAKEWDEQSYL
Pth2p  PRLPVPTLEETAARYLRTLKPLLSKEELANSTKAVQEFVKPGGVGAKLQEKLIARRDPKHKNWIYEWWNEAAYL
CrAT2  PKLPIPDLERTCEKYLAALKPLQSPREHGETRNAVQEELR--EDGEELQEKLKKYAEGQT--SYIEQSWYDS-YL

Cat2p  QYNDPIVPYVSYFYSHMPLPNHLSKIDNDELIKATAIISTVVKFIEKIKDESLEVEIIKGMPFCMNSESLKFNTS
Pth2p  AYREPVVPYVSYFYSHR-----DDRRERDEAKRRAAITTAALEFKKMVDSGTLEPEYMKKLPICMDSYKWKFNAS
CrAT2  NFDNPVVLNLNPFFLLE---DDPTPARNNQVTRAASLVVSALEFVRAVRKEELPEDKVKNTPLCMYQYSRLFGEA

Cat2p  RLEGKPEDNCCTNIFYSVYENNFVTIAYKGKFYKLMTHDGNDKPLSENEIWRQIYSVVFQGSCS---DPKLGGIG
Pth2p  RVAAKE----AEYPVKFEAAQHKYIVAIRNNRFYKIEHEVGG-RQLNTSELEAQFRRVYELAGCE---AKMEPAVG
CrAT2  RVETEN----GCCQEQDPHSKHIVVMAHGQFYWFDALDDNSDVIMTEKDISINLQTIVDDASLTPIQEAAKGALG

Cat2p  SLTSLPRDQWREVHLELMKD--EISQDSLETIHKSSPMICLDLEQSPVTLEEKS----------RNCWHGDGINR
Pth2p  ALTSENRDVWTDARALLLSAG-EARKAALETIEASSFIVCLD-DAAEVTLEERA----------HAYLHGDGQNR
CrAT2  VLSTENRKVWSGLRDILTREEGSNNADCLGIIDSALFILCLDYTEPATAAELCQNMLCGTSEIEKGVQIGTCTNR

Cat2p  FYDKSLQELVTGNGSSGELAEHSKKDGTPTIELNNYVCQQLN--KLDVD-------------DFMRKVITFSSTV
Pth2p  WYDKPLQEIVNDNGTSGEMGEHSKKDGTPTHRLNDYVNDAIVNNKLDFS-------------DPSVESGLE----
CrAT2  WYDK-LQIIVCKNGSAGINFEHTGVDGHTVLRFASDVYTDTILRFARTINGHSPTLWASTSPDPSKRDPESFGDV

Cat2p  AMKPMELPEIITEKIHKAIESAQLQEKETIGEHDLRVWHYNKYGKTSIKRHGMSPDAEIQQVICLAVEKYLKRQL
Pth2p  --DPSPVRETVNEQLQSEIDRAKRDEDAVIGQHEIAVQSYQGYGKGLIKKFRCSPDAYVQNVICLAVHKNYGKNR
CrAT2  IPTPHKLEWDLVEEVSIEVRFAETRLADLIGRNEFECLDFSAYGKNEITSMGFSPDAEVQNAYQAAMYGLMGRAE

Cat2p  ETYBAASTRKYFKGRTETGRSVSTASLEEVSKWQNGEVEIDEKIQALKHSAKEHSTELKNEANGNGVDRHFEGLK
Pth2p  ETYESAATRREQQGRTEECRSVSEBSVAWCNAMADESAQDADKVKLFRAAIDSHVEYITAESDGKGVDRHLFGLK
CrAT2  CTYEPAMTKFELHGRTEAVRSVTDESINEIQNFW-AENEAEAKVEALRAACKKHVNMTKDCAKAQGCDRHLYALF

Cat2p  NMLK----------------------------------------------------SNDDQIP
Pth2p  RLLE------------------------------------------------------PGQ-AVP
CrAT2  CLWQRLVDEDAGTTTNGYSSGMSDNEGAVSERSPSPTATTATATGEKEKENGEGLRSRGESTSSSQRSVKYATLP

Cat2p  PLEKDPLFNYSSTWLISTSQLSSEYEDGYGWSQVNENGFGLAYELNNEWLHINIVNKPAKSGASVNRLHYYLSQA
Pth2p  EIYKDPAYSYSSSWYLSTSQLSSEYENGYGWSQVIEAGFGILAYMINENSTNFNIVSKGLAS----QRMSFYLNEA
CrAT2  LIEADPGWDKLNTTILSTSNCGNPSLRQFGFGPVSGDGFGIGYIIKDERISMCVASKHRQTKRFVDAEBSYLLEI

Cat2p  ADEIEDALENENKR-KAKL-------------------------------------------------------
Pth2p  AGDMRDLLMPTIEAPKSKL-------------------------------------------------------
CrAT2  RRILRLASRRAASSTADGGPLAGSIAEAKQQTTRAREVDDEQRQQYRRPSQQTNRLKSRGRMIAGPGLEGLMRSK

Cat2p  -------------------------------------------------------------------------
Pth2p  =========================================================================
CrAT2  SSMTGTTSPTSESLAMSEDDELGGYGFFDAGMLLQALKARNTHFDVGETRASERAAVQARRNNVGKKLRLIDY
```

Figure 10. Multiple sequence alignment of *M. grisea* carnitine acetyltransferases. ClustalW (Thompson et al., 1994) based amino acid sequence alignment for Cat2p (*S. cerevisiae*) with the two carnitine acetyl-transferases (Pth2p/CrAT1 and CrAT2) from *M. grisea*. Black background highlights identical amino acids, while similar residues are shown on a gray backdrop. Dashed lines or dots indicate the gaps in the alignment.

The MG01721.4 locus was re-annotated and the Crat1 protein showed the highest similarity to *S. cerevisiae CAT2* and shared 40% amino acid identity (e=-116). Cat2p localizes to both the mitochondrion and the peroxisome (Swiegers et al., 2001). *In silico* analysis of Crat1 using subcellular localization prediction programs (PSORTII and TargetP; (Nakai and Horton, 1999; Emanuelsson et al., 2000) failed to reveal any canonical mitochondrial localization motif. However, a distinct PTS1 (serine-lysine-leucine; SKL) signature was detected at its C-terminus, thus supporting a peroxisomal localization for the protein encoded by the *CRAT1/*MG01721 ORF. Since an uncharacterized mutation REMI (Restriction enzyme mediated insertion) termed *Pth2* (Sweigard et al., 1998) has been identified at the MG01721 locus, *CRAT1/*MG01721 was hereafter referred to as *PTH2*. MG06981, the other CrAT in *M. grisea* showed the highest similarity to *Neurospora crassa FacC* (e=-34, 55% amino acid identity). The *FacC* ortholog in *A. nidulans* has been well-studied and is predicted to localize to the cytoplasm (Stemple et al., 1998). MG06981.4 ORF will henceforth be referred to as *CRAT2* and its product as Crat2.

3.2.8 Pathogenesis-related defects in CrAT minus mutants

To determine the role of CrATs in *Magnaporthe* pathogenesis, deletion strains for the *PTH2* or *CRAT2* and a *PTH2/CRAT2* double mutant were generated in the B157 wild-type background. Using single step gene replacement strategy, the complete ORF of *PTH2* and *CrAT2* were replaced with the selection markers coding for hygromycin and bialaphos resistance, respectively. Polymerase chain reaction assisted specific amplifications, and Southern hybridizations confirmed that the correct gene replacement events had taken place in the selected single and double mutant

transformants. At least two independent deletion strains in each instance were used for all the phenotypic and functional analyses presented here.

The pathogenicity and pathogenesis-related traits of the different CrAT-delete mutants were assessed in detached barley leaf infection assays. Inoculations with increasing conidial loads of the *pth2Δ* and the *pth2Δ crat2Δ* strains demonstrated that both mutants were completely nonpathogenic (Figure 11). In contrast, the *crat2Δ* strain elicited disease symptoms similar to wild-type levels.

	Wildtype	*pth2Δ*	*crat2Δ*	*pth2Δ/ crat2Δ*
4000				
2000				
1000				
500				

Figure 11. Pathogenicity of carnitine acetyltransferase (CrAT) mutants.
Leaf explants from barley were inoculated with the indicated number of conidia from wild-type or the indicated CrAT mutants. Disease symptoms were assessed seven days post-inoculation.

The rate and frequency of appressorium formation, was assessed at different time-points during infection assays using the CrAT-delete mutants (Figure 12). Both *pth2Δ* and *pth2Δ crat2Δ* mutants exhibited a delay in appressorium formation during the early period of the process. At four hours after inoculation, the number of appressoria in these mutant strains was $50 \pm 1.5\%$ of those seen in the wild-type. At six hours post inoculation, appressorium formation had increased to $80 \pm 2.2\%$ of that observed for the wild-type. At the 24 hour timepoint, the overall number of appressoria was similar in the wild-type and in the *pth2Δ* and *pth2Δ crat2Δ* mutants. Appressorium formation of *crat2Δ* was similar to the wild-type rate throughout the duration of the process.
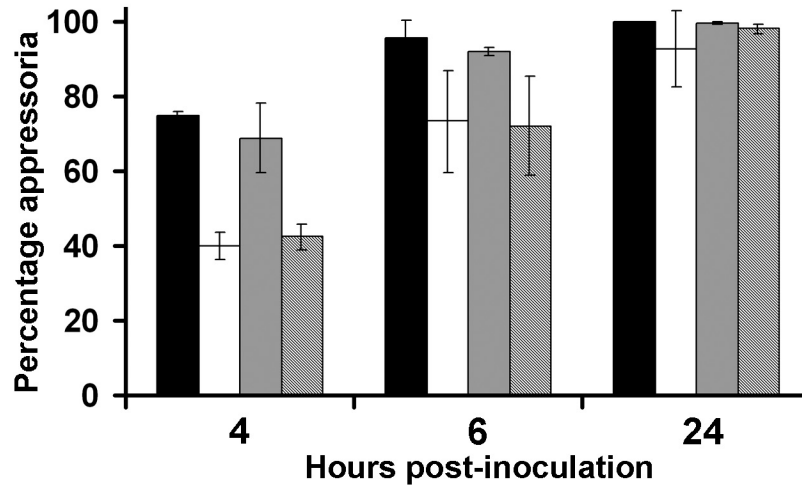
Figure 12. Rate and frequency of appressorium formation in the carnitine acetyl-transferase (CrAT) mutants.

Conidial preparations from wild-type (black bar), *pth2Δ* (open bar), *crat1Δ* (gray bar) and *pth2Δcrat1Δ* (stippled bar) mutants were inoculated for appressorial assays. Appressoria was counted from samples taken at 4-, 6- and 24-hours after inoculation.

Observations and quantifications for host penetration capability as judged by aniline blue staining for callose deposits and penetration hyphae revealed that the *pth2Δ* like the *pex6Δ* produced nonfunctional appressoria that failed to elaborate any penetration pegs or infection/penetration hyphae (Figure 13). At the 48-hour, and even the 96-hour time-point, these mutant appressoria did not elaborate any host penetration structures. Thus, *pth2* activity plays a major and essential role during the host penetration step of the rice-blast infection cycle.
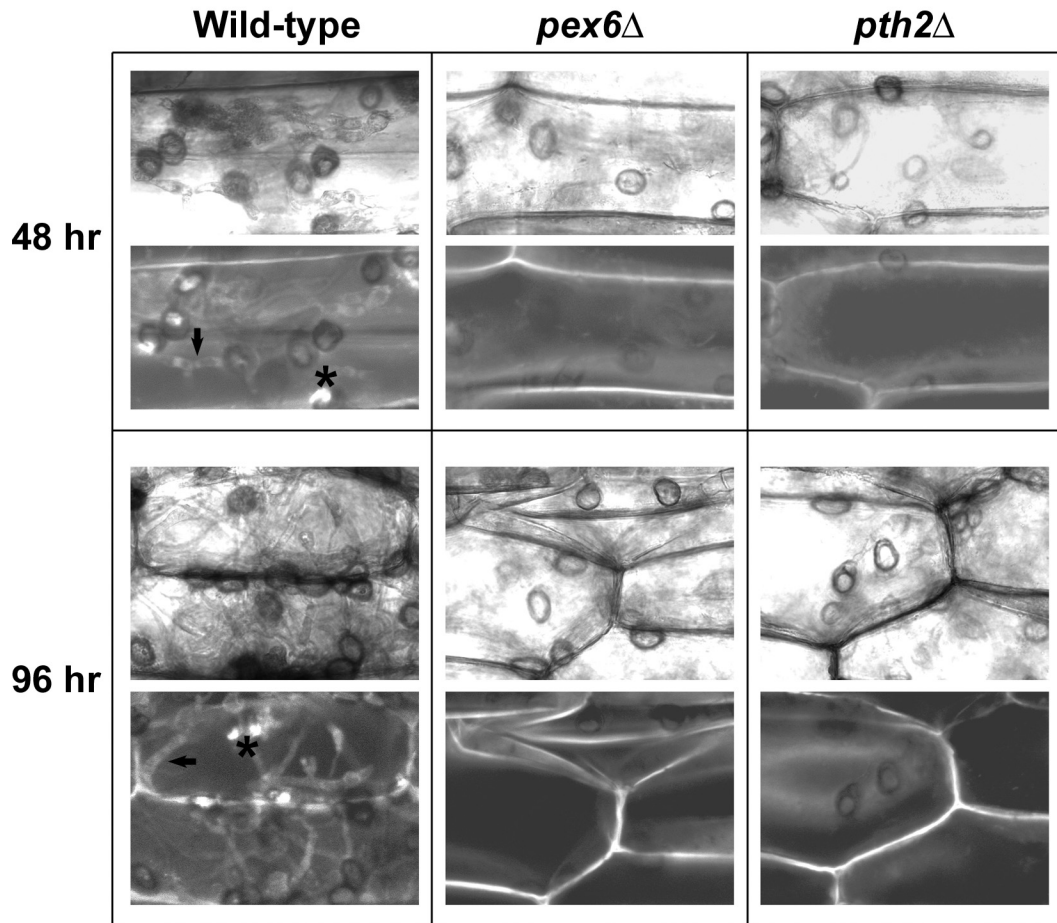
Figure 13. Host penetration defects of *pex6Δ* and *pth2Δ* mutants.
Equal number of conidia from the wild-type, *pex6Δ* or the *pth2Δ* strain was inoculated on barley leaf explants. The number of papillary callose deposits (asterisk) and infection hyphae (arrow) were visualized by staining with aniline blue at 48 hours or 96 hours post inoculation. Scale bar represents 10 μm.

3.2.9 Contribution of PTH2 to appressorial melanization

Since the host penetration defects observed during appressorium function of *pth2Δ* mutant were remarkably similar to the ones shown by the *pex6Δ* appressoria, the appressorial melanization in the *pth2Δ*, *crat2Δ* and *pth2Δ crat2Δ* mutants was evaluated. The *pth2Δ* mutant appressoria showed a significant reduction in the overall melanization of the appressoria (Figure 14). Such reduction in melanin deposition was not seen in the *crat2Δ* mutants, whereas the decreased melanization was again evident in the appressoria formed by the *pth2Δcrat2Δ* double mutant. These results indicate that Pth2 activity is involved in efficient melanization of appressoria, and that the defect observed in the appressoria function could be a consequence of this reduction of melanin. It is however possible that the loss of pathogenicity in the *pth2Δ* mutant may not be due solely to such a reduction in pigmentation. Combinatorial defects in the fatty acid utilization pathway, improper melanization in appressoria, or the general defect in acetyl CoA transport as observed in the *pth2Δ* mutant could result in the phenotypic defects observed therein.
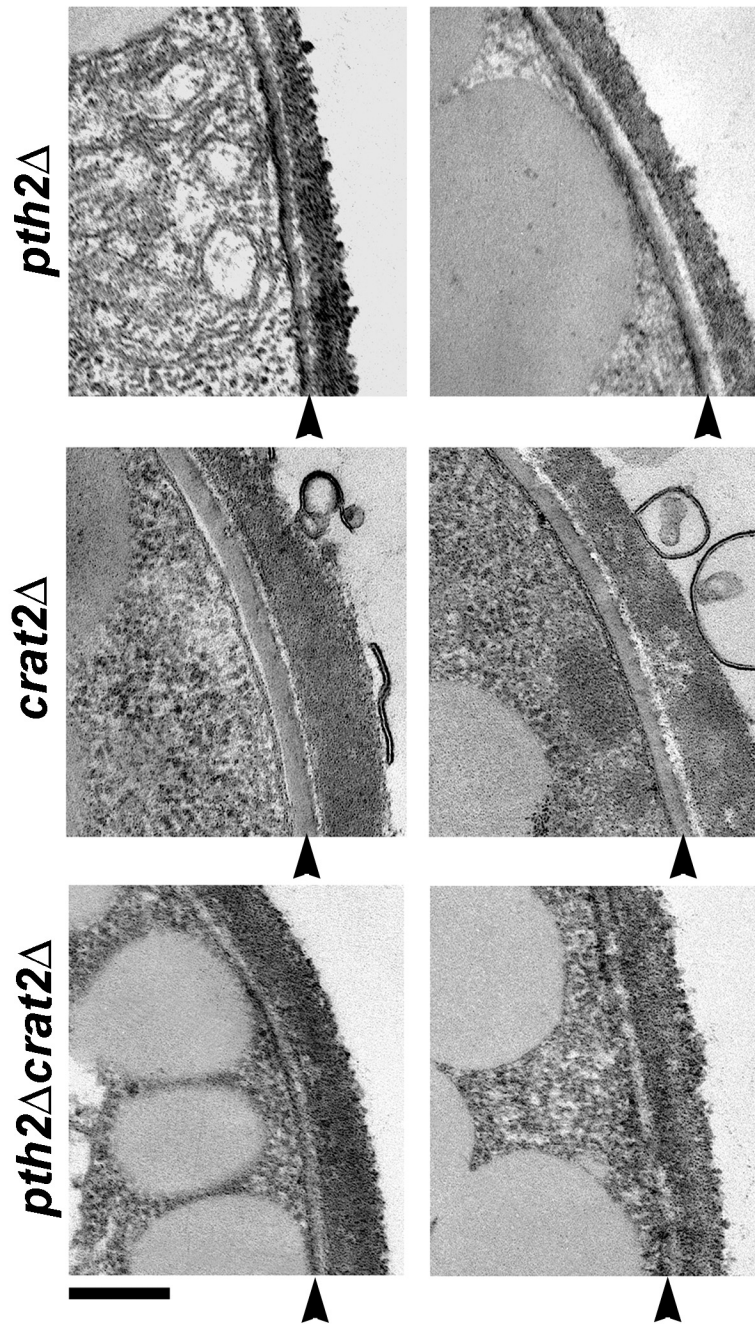
Figure 14. Reduction of appressorial melanization in the carnitine acetyltransferase (CrAT) mutants.

Conidiospores from the CrAT mutants (*pth2Δ, crat2Δ* and the *pth2Δcrat2Δ*) were spotted onto artificial inductive membranes and allowed to incubate for 24 hours and then processed for TEM analysis as described. Bar = 200 nm. Representative images from two independent appressoria from each mutant strain are depicted.

3.2.10 Metabolic function of *M. grisea* carnitine acetyltransferases

Carnitine acetyltransferase assays utilizing acetyl-CoA as a substrate were conducted to quantify and compare the total levels of CrAT enzyme activity in the wild-type, *pth2*Δ, *crat2*Δ and the *pth2*Δ *crat2*Δ mutant (Figure 15). In the wild-type strain, the total CrAT activity (specific activity 24.5 ± 1.1 nmol/min/mg protein) was induced by olive oil and acetate but was not repressed by glucose. In the *pth2*Δ mutant, CrAT activity was found to be significantly reduced (specific activity 1.6 ± 0.8 nmol/min/mg protein) and could not be elevated by either olive oil or acetate. In the *crat2*Δ, olive oil and acetate treatment elicited a slight induction in the enzyme activity although not as effectively as in the wild-type strain. CrAT activity was similar in wild-type and *crat2*Δ (specific activity 22.8 ± 1.6 nmol/min/mg protein) strains during glucose treatment. The *pth2*Δ*crat2*Δ double mutant strain showed negligible amounts (0.09 ± 0.21 nmol/min/mg protein) of overall CrAT activity.
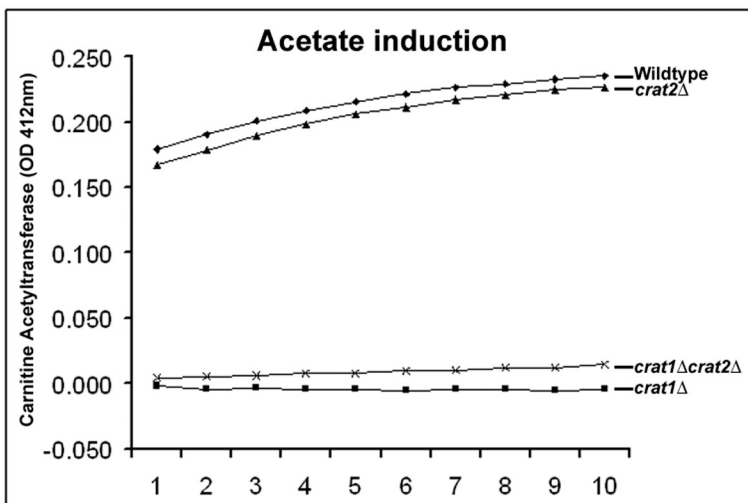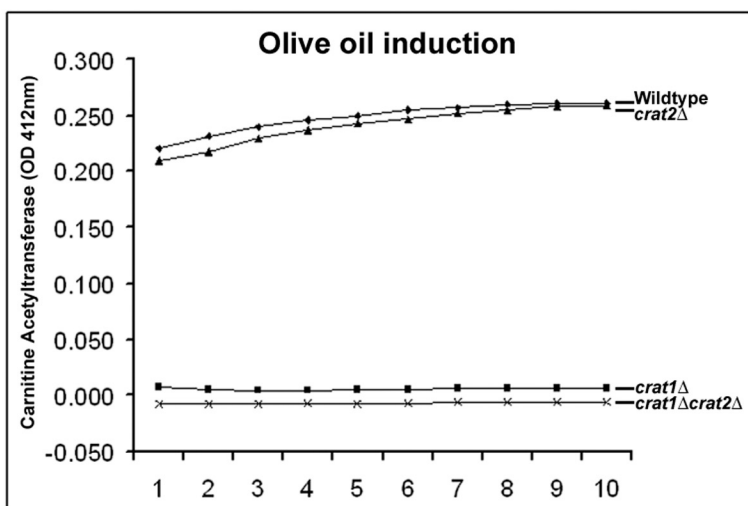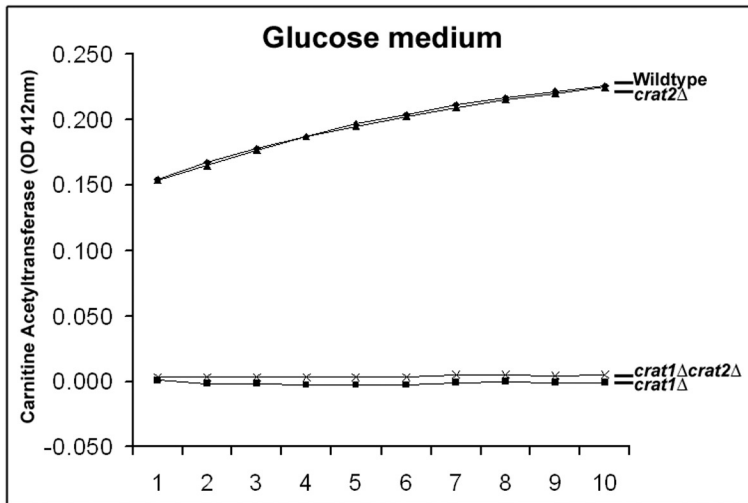
Figure 15. Carnitine acetyltransferase activity of CrAT mutants.
Total protein extracts used for the assay were prepared from mycelia of wild-type, *pth2Δ* (*crat1Δ*), *crat2Δ* and *pth2Δ crat2Δ* strains which were pre-cultured in glucose medium for three days and subsequently induced for four hours in a medium containing 1% glucose or 1% olive oil or 50 mM acetate.

The ability to metabolize different carbon sources was evaluated for the CrAT-minus mutants (Table 2). Wild-type strain utilized glucose and olive oil equally efficiently, whereas acetate was consumed to a lesser extent. The *pth2Δ* and the *pth2Δ crat2Δ* mutant grew normally on glucose containing medium but were unable to utilize olive oil or acetate. There were no discernable differences between the growth of *crat2Δ* strain and the wild-type on all the carbon sources tested. These results demonstrate that *PTH2* function provides the major carnitine acetyltransferase activity in *M. grisea* and it also regulates the utilization of fatty acids and acetate as carbon source. The contribution of Crat2 to cellular carnitine acetyltransferase levels and its role in fatty acid or acetate utilization were inferred to be insignificant.

Strains	Carbon Source		
	Glucose	Olive oil	Acetate
Wild-type	+++	+++	+
pth2Δ	+++	-	-
crat2Δ	+++	+++	+
pth2Δ/crat2Δ	+++	-	-

Table 2. Growth of carnitine acetyltransferase (CrAT) mutants on different carbon sources.

M. grisea wild-type and the indicated CrAT mutant strains were cultured on basal medium containing either 1% glucose or 1% olive oil or 50 mM acetate as sole carbon source. Growth was assessed after ten days. +++:Good growth; +:Poor growth; -:No growth.

In order to assess whether the CrAT activity of the two predicted carnitine acetyltransferases is regulated at the transcriptional level, semi-quantitative RT-PCR was conducted to assess the relative amounts of each transcript. Such semi-quantitative RT-PCR based analyses revealed that the transcription of *PTH2* and *CRAT2* was induced by olive oil and acetate in the wild-type strain (Figure 16). Additionally, these results likewise indicate that CrAT2 is actively transcribed and thus is not a pseudogene.
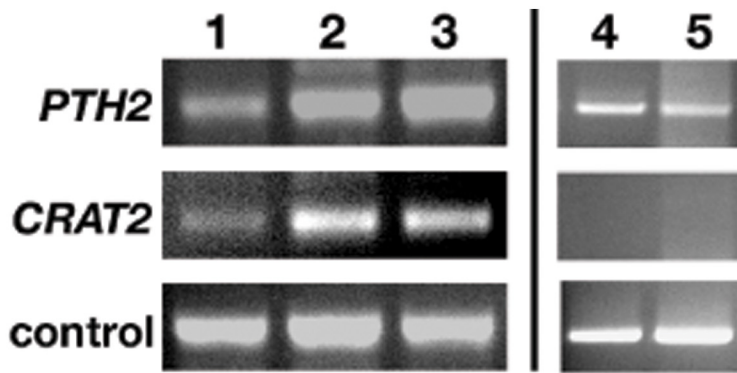
Figure 16. Expression analysis of *PTH2* and *CRAT2* transcripts.
RT-PCR was perfomed on RNA extracted from wild-type during vegetative growth on different carbon sources (lanes 1-3) and during pathogenic development (lanes 4 and 5). For the vegetative growth,wild-type was cultivated on 1% glucose (1), 1% olive oil (2) or 50 mM acetate (3). For pathogenesis, RNA was extracted 4 (4) and 24 (5) hours after inoculation. Amplification for the β-tubulin gene and *MPG1* served as loading control for the total RNA from vegetative or pathogenic growth, respectively.

3.2.11 Subcellular localization of Crat1p/Pth2p

In silico predictions suggested a peroxisomal location for Pth2p, but the findings that Pth2 was essential for acetate utilization raised the possibility that Pth2 might also be present in a non-peroxisomal pool. A detailed analysis of the subcellular localization of a Pth2-RFPSKL fusion protein during growth in olive oil or acetate containing medium was conducted. The subcellular location of the Pth2-RFPSKL protein was the same as that observed for the GFP-PTS1 signal, with both the fusion proteins co-localizing predominantly within the peroxisomes (Figure 17). Such co-localization pattern of the Pth2-RFPSKL and the GFP-PTS1 did not differ significantly when compared between growth on olive oil or acetate. However, under both the conditions, a separate albeit limited subcellular localization (inferred to be cytosolic) of Pth2-RFPSKL was evident which was distinct from the GFP-PTS1 containing compartments (Figure 17, magnified insets). This cytoplasmic pool appeared to be more prominent when acetate was present as the primary carbon source (Figure 17, arrowhead). These results demonstrate that *PTH2* transcription is induced by fatty acids and acetate and that Pth2 is predominantly peroxisomal but could also be present in the cytosol although in very limited amounts.

It has been reported previously that Cat2, the *S. cerevisiae* ortholog of Pth2, encodes a protein, which contains a mitochondrial targeting signal (MTS) at the N-terminus and a type 1 peroxisome targeting signal (PTS1) at the C-terminus. Cat2 can be targeted to either the mitochondria or the peroxisomes depending on the growth conditions (Elgersma et al., 1995). Acetate- or glycerol-grown cells produce a longer Cat2 transcript, which contains the MTS. Whereas, during growth on oleate, a shorter Cat2 variant lacking the MTS is produced. As mentioned above, our re-annotation of the

MG01721.4 sequence revealed the presence of a PTS1 at the C-terminus of the Pth2p indicating a peroxisomal localization. However, inspection of sequences upstream of the predicted ATG site revealed the presence of another ATG at -602 basepairs. The upstream ATG was found to be in-frame with the first predicted ATG and translation from the upstream ATG results in an additional 21 amino acids. Results from anaylsis of the new protein sequence using MitoProtII predicted a 0.9918 probability of export to the mitochondria, with cleavage site at amino acid 30. To determine the subcellular location of MgPth2p, C-terminus tagging with RFP of the protein was undertaken. To preserve the function of the innate C-terminal PTS1 of Pth2, the tagging construct was designed such that an RFP-SKL tag was inserted at the extreme C-terminus and replaced the sequences coding for the innate –SKL and the stop codon. Transformation of the Pth2-tagging construct was performed in strains already expressing the peroxisomal marker GFP-PTS1. Mycelia were first grown on glucose for three days and then transferred to either olive oil or acetate medium for another 16 hours before imaging. In mycelia cultured in olive oil, there is a clear colocalization between Pth2-RFP and GFP-PTS1. This demonstrates that Pth2 is targeted to peroxisomes during growth on fatty acids. During growth on acetate, Pth2-RFP still colocalizes predominantly with GFP-PTS1. There is faint cytoplasmic RFP fluorescence, which may be attributed to either background fluorescence or Pth2p cytosolic localization. The faint cytoplasmic fluorescence appeared diffuse and did not resemble mitochondrial structures which appear as filaments when stained with Mitotracker dyes. These results argue for a predominant peroxisomal localization of Pth2p during growth on fatty acids or acetate.
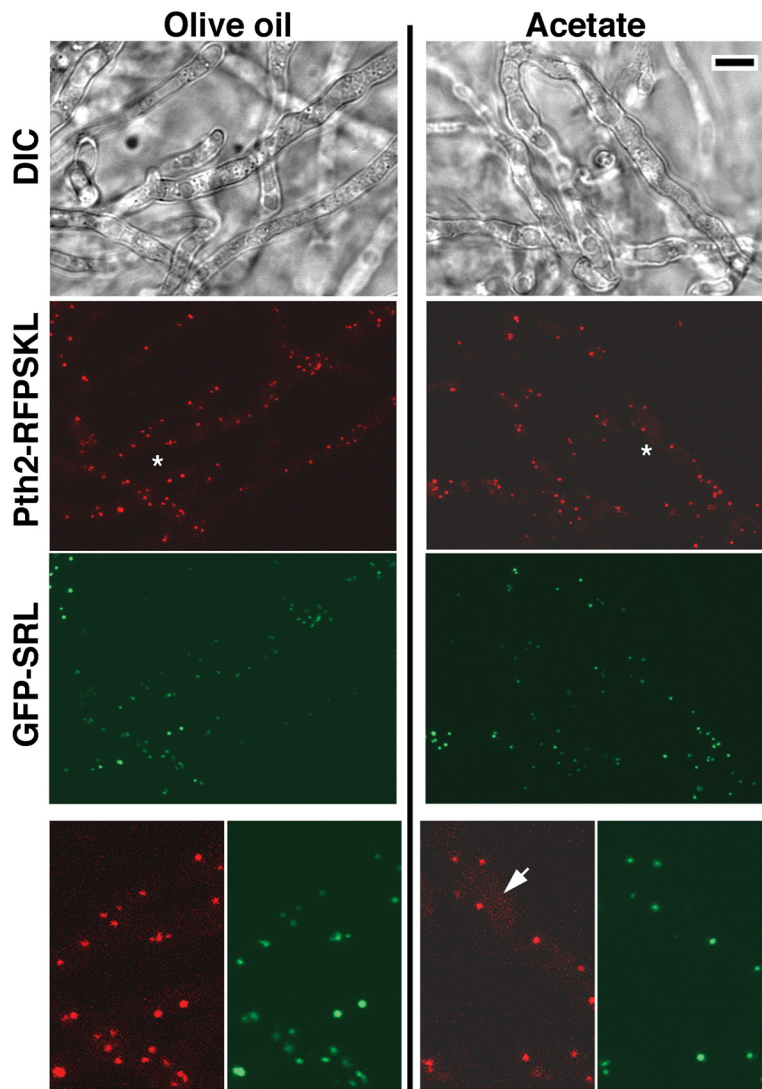
Figure 17. Subcellular localization of Pth2-RFPSKL.
M. grisea strain B1173 (relevant genotype *PTH2*:RFP-SKL;GFP-PTS1) was cultured in medium containing either olive oil or acetate as the sole source of carbon. Laser scanning confocal microscopy using appropriate filters (or DIC) was then performed on the mycelia to image GFP and RFP epifluorescence. Scale bar depicts 5 μm. The lower panels represent 4X magnifications of the regions denoted by the asterisk in each instance together with their respective GFP counterparts. The arrow indicates the presence of a possible Pth2 cytoplasmic pool during growth on acetate.

3.2.12 Role of peroxisomal acetyl-CoA in *M. grisea* pathogenesis

Studies in some lower eukaryotes have shown that acetyl-CoA produced by beta-oxidation in the peroxisomes is transported to the mitochondrion to replenish the intermediates of the citric acid cycle. However, the transport of the products of beta-oxidation out of the peroxisomes and into the mitochondria is not well understood (Hooks, 2002). Products of the peroxisomal beta-oxidation are also routed into gluconeogenesis via the glyoxylate cycle, through which two carbon compounds are assimilated into the tricarboxylic acid (TCA) cycle. The *pex6Δ* mutant might be unable to supply such products and/or their precursors. Additionally, glucose metabolism supplies some of the intermediates of the citric acid cycle in a peroxisome independent manner. Appressorial function in the *pex6Δ* and the *pth2Δ* mutant in the presence of excess metabolic intermediates such as glucose, citrate, malate or succinate was then investigated. Appressorium-mediated host penetration and blast disease elaboration was normal in the WT strain in the presence (or absence) of glucose or citrate (Figure 18A). On the other hand and rather interestingly, the presence of glucose (but not citrate or malate or succinate) caused a slight remediation of the host penetration defect in the *pth2Δ* mutant. Upon quantification, such limited restoration of appressorium function in the *pth2Δ* was found to be about 18.8 ± 0.4% (Figure 18B). However, the resultant penetration hyphae in the glucose treated *pth2Δ* samples were found to be incapable of proper proliferation within the host tissue (Figure 18C). Rather surprisingly, treatment with either glucose or citrate did not restore the appressorial function (of host penetration) in the *pex6Δ* mutant, thus maintaining the *pex6Δ* mutant's inability to gain entry into (and to elicit disease symptoms) on host leaf surfaces.
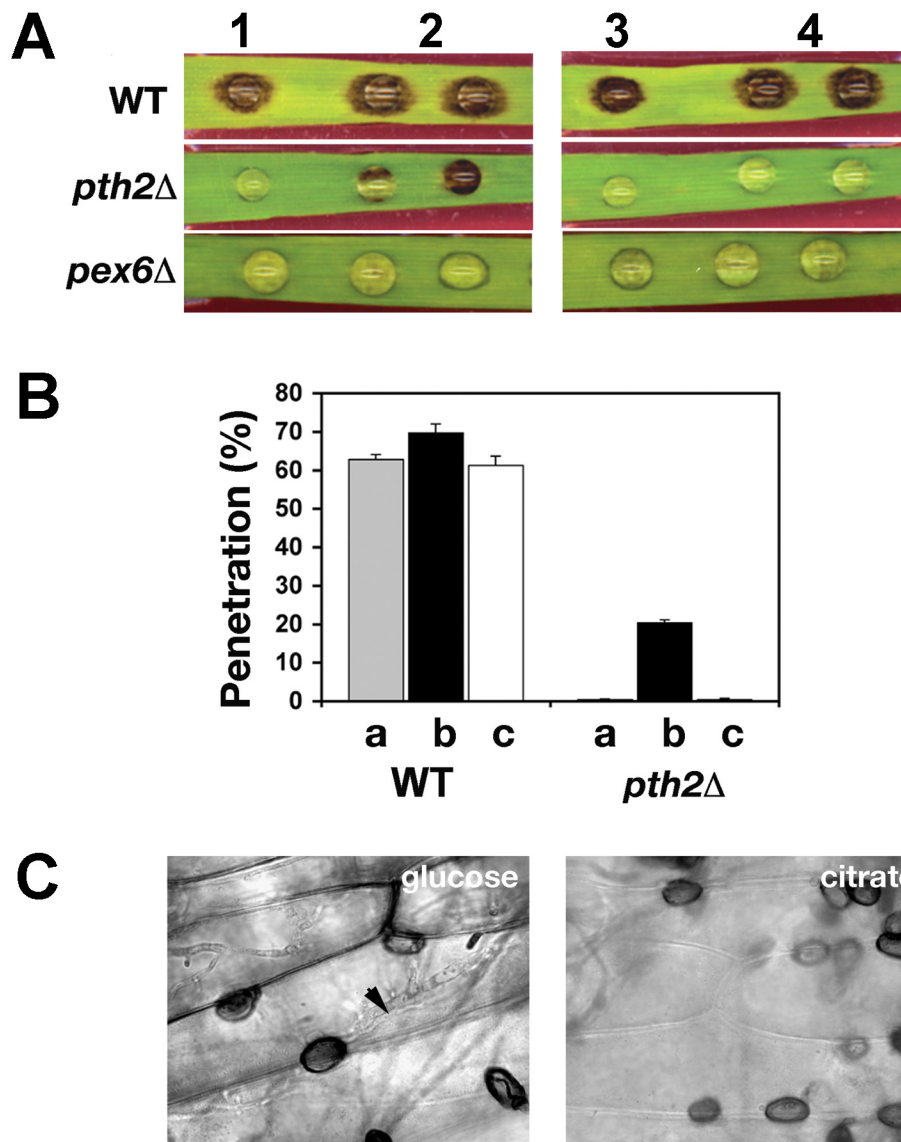
Figure 18. **Partial remediation of pathogenicity defect by chemical supplementation.**

(**A**) Wild-type, *pth2Δ* and *pex6Δ* strains were inoculated on barley leaves in the presence of exogenous glucose (2) or citrate (4). Untreated control samples are represented by inoculations (1) and (3).

(**B**) Quantitation of penetration pegs and infectious hyphae in the wild-type (WT) and *pth2Δ* strains during untreated (gray bar), glucose supplementation (black bar) or citrate supplementation (open bar) conditions.

(**C**) Light microscopic analysis of acid fuchsin stained fungal structures in the chemical remediation experiments described in panels (A) and (B) above. Glucose-induced infectious hyphae is indicated by an arrowhead.

Earlier results (Figure 14) hinted at a significant reduction in overall thickness of the appressorial cell walls in the *pth2Δ* mutant. Tests were then conducted to determine whether cell wall integrity was compromised in these mutants. To this end, the sensitivity of the wild type, the *pex6Δ* and the *pth2Δ* strains to cell-wall-perturbing agents such as Calcofluor white and Congo red was assessed. Compared to the wild-type strain, the *pth2Δ* and the *pex6Δ* mutant were found to be significantly sensitive to Calcofluor white (Figure 19) whereas the *pex6Δ* showed increased sensitivity to cell wall perturbations with Congo red. Based on these results, it can be concluded that the *pth2Δ* and the *pex6Δ* mutant possess weakened cell walls. It is possible that the reduced cell wall integrity (or biosynthesis) in a glucose-deficient environment is the likely cause of the loss of appressorial function in the *pth2Δ* and the *pex6Δ* mutant. These results suggest that acetyl-CoA generated by peroxisomal activity likely feeds into the glyoxylate cycle and gluconeogenic pathway for cell wall synthesis during penetration-peg formation.

In summary, the characterization of mutants, defective in peroxisome biogenesis (*pex6Δ*) and export of peroxisomal acetyl-CoA (*pth2Δ*) demonstrated that peroxisomal metabolic function is essential during *M. grisea* pathogenesis. Fatty acid beta-oxidation within the peroxisomes generates acetyl-CoA, which is likely utilized in the polyketide pathway for melanin synthesis. Moreover, peroxisomal acetyl-CoA is also most probably directed through the gluconeogenesis pathway for the synthesis of cell wall components of penetration pegs.
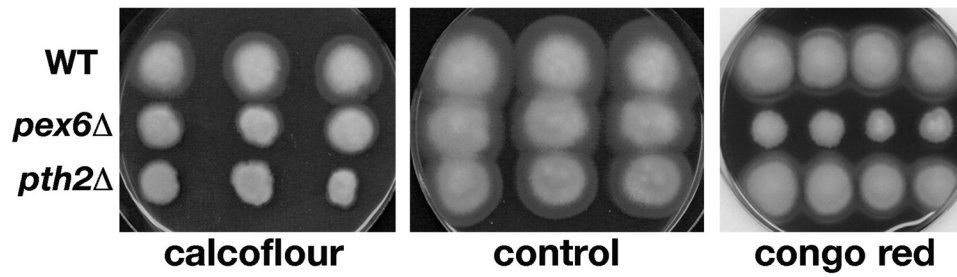
Figure 19. Weakening of fungal cell walls due to loss of *PEX6* or *PTH2* function. Conidia from the wild-type, *pex6Δ* or the *pth2Δ* strain were cultured in the absence (control) or presence of cell wall destabilizing agents (100 µg/ml of Calcofluor white or Congo red) using prune agar as basal medium. Growth was assessed five days after inoculation.

CHAPTER IV IMPORTANCE OF PEROXISOMAL AND MITOCHONDRIAL FATTY ACID BETA-OXIDATION DURING *Magnaporthe* PATHOGENESIS

4.1 Introduction

Lipid metabolism plays a key role during fungal pathogenicity. Mutations in genes, which encode enzymes of primary or auxiliary lipid metabolic pathways, result in loss of pathogenicity or attenuation of virulence in both plant (Idnurm and Howlett, 2002; Wang et al., 2003) and animal pathogens (Lorenz and Fink, 2001; Piekarska et al., 2006). Cellular lipid metabolism is accomplished via the beta-oxidation of fatty acids (Kunau et al., 1995). Depending on the organism, fatty acid beta-oxidation occurs in peroxisome and/or mitochondria. In fungi, owing to extensive studies in yeasts, it is generally accepted that fatty acid oxidation is exclusive to the peroxisome organelle (Hiltunen et al., 2003). However, recent studies have demonstrated the presence of a mitochondrial beta-oxidation pathway in *S. pararoseus* (Feron et al., 2005) and in the filamentous fungus *A. nidulans* (Maggio-Hall and Keller, 2004). Because my previous work alluded to the importance of the peroxisomal beta-oxidation pathway in *M. grisea* pathogenicity, I decided to investigate whether mitochondrial beta-oxidation occurs in *M. grisea* and if so, what is the contribution of the peroxisomal or mitochondrial pathway during pathogenesis.

4.2   Results

4.2.1   Identification of peroxisomal multifunctional beta-oxidation enzyme ortholog in *M. grisea*

In order to delineate whether the *pex6Δ* defects were due to loss of organellar integrity or loss of metabolic function of beta-oxidation, a *M. grisea* ortholog of a specific peroxisome-associated beta-oxidation enzyme was sought. A known distinct characteristic of the enzymology of the peroxisome-based beta-oxidation machinery is the presence of a multifunctional enzyme possessing both a dehydrogenase and a dehydratase activity (Hashimoto, 2000). A well-characterized multifunctional protein, which catalyzes the second and third steps of the beta-oxidation cycle in the peroxisome, has homologs in yeast (Fox2 in *Saccharomyces cerevisiae*, (Hiltunen et al., 1992); Mfe2 in *Yarrowia lipolytica*, (Smith et al., 2000)), filamentous fungi (in *N. crassa* Fox2 and *A. nidulans* FoxA, (Thieringer and Kunau, 1991b; Maggio-Hall and Keller, 2004)) and mammals (Mfe2;(Jiang et al., 1996)). The *Magnaporthe* genome was then searched using the BLAST algorithm for orthologs of the *A. nidulans* FoxA (AN7111.2). The BLAST search yielded 42 hits, of which the first ten were closely examined (Table 3).   MG06148.4 showed the highest percent identity (63%) and highest percent similarity (Positives = 74%) to AN7111.2. A perusal of the available HMMER predicted domains of these loci in *M. grisea* showed that only MG06148 contained both the dehydrogenase and dehydratase domains (Table 3). For the other nine loci, only one of either a dehydrogenase or a dehydratase domain was predicted. Because of its high similarity to AN7111.2 and the prediction of two requisite enzymatic domains from its amino acid sequence, MG06148.4 was selected for further characterization.

MG Locus	% Identity	% Positive	HMMER-predicted Domains
	Relative to AN7111.2		
MG06148.4	63	74	adh-short; adh-short; MaoC
MG04839.4	29	43	MaoC
MG07216.4	32	48	adh-short
MG06494.4	32	51	adh-short
MG03016.4	28	48	adh-short
MG02252.4	31	51	adh-short
MG03290.4	26	45	adh-short
MG07514.4	31	47	adh-short
MG09415.4	26	42	adh-short
MG00697.4	30	45	adh-short

Table 3. Sequence comparison for *A. nidulans* FoxA orthologs in *M. grisea*.
A BLAST search of the *A.nidulans* multifunctional beta-oxidation protein FoxA (AN7111.2) against the *M. grisea* genome identified more than 20 hits of which ten are listed here. The identified HMMER-predicted domains correspond to short-chain acyl-CoA dehydrogenase (adh-short) and dehydratase (MaoC).

A comparison of the predicted conserved domains of six characterized beta-oxidation multifunctional proteins and MG06148 was done (Figure 20). The presence of two short chain dehydrogenase domains (ADH) and one dehydratase domain (MaoC) appears to be conserved in fungi as these domains were identified in all fungal enzymes as well as MG06148. In comparison, the human Mfe2 (HsMfe2) possesses only one dehydrogenase domain and one dehydratase domain. Among all the enzymes, only the *Glomus mosseae* GmFox2 (Requena et al., 1999) and HsMfe2 has a sterol carrier protein domain (SCP2).
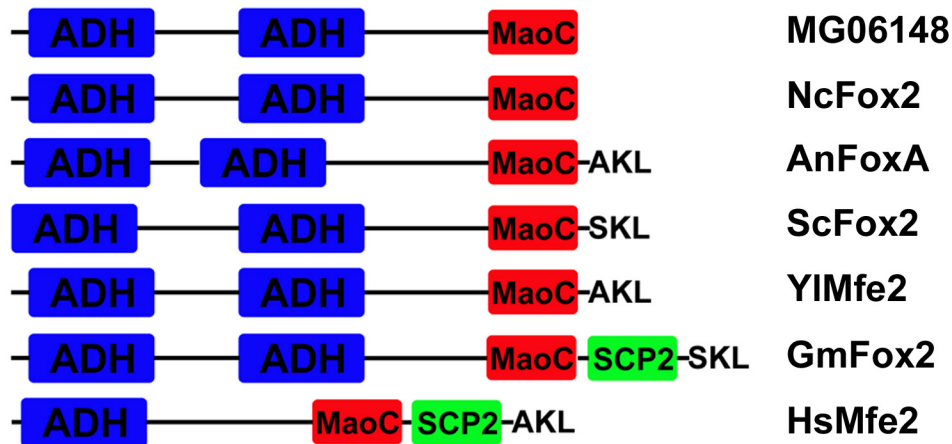
Figure 20. Conserved protein domains in diverse multifunctional beta-oxidation enzymes.

The enzymatic domains of acyl-CoA dehydrogenase (ADH), dehydratase (MaoC) and sterol-carrier protein domains in the protein sequences of filamentous fungi (*M. grisea* MG06148, *N. crassa* NcFox2, *A. nidulans* AnFoxA), yeasts (*S. cerevisiae* ScFox2, *Yarrowia lipolytica* YlMfe2), arbuscular mycorrhizal fungus *Glomus mosseae* GmFox2 and *Homo sapiens* HsMfe2 were identified through the Conserved Domains Database of the National Center for Biotechnology Information. Presence of the carboxy terminus tripeptide peroxisome targeting sequence I (PTSI), -A/S-K-L, is indicated in some of the proteins.

A consensus peroxisomal targeting tripeptide sequence (S/A-K-L) was identified at the C-terminus end of all the protein sequences analyzed except for the orthologs in *N. crassa* and *Magnaporthe* (Figure 20). Previous reports on the characterization of the *S. cerevisiae* (ScFox2) (Hiltunen et al., 1992), human (HsMfe2) (Jiang et al., 1996) and *A. nidulans* (AnFoxA) (Maggio-Hall and Keller, 2004) enzymes have confirmed the localization of these proteins to peroxisomes. The subcellular localization of the NcFox2, which lacked a peroxisomal targeting sequence, was demonstrated to be in catalase-free microbodies (Thieringer and Kunau, 1991a). A phylogenetic analysis of the different multifunctional enzymes showed that MG06148 was most closely related to NcFox2 (Figure 21).
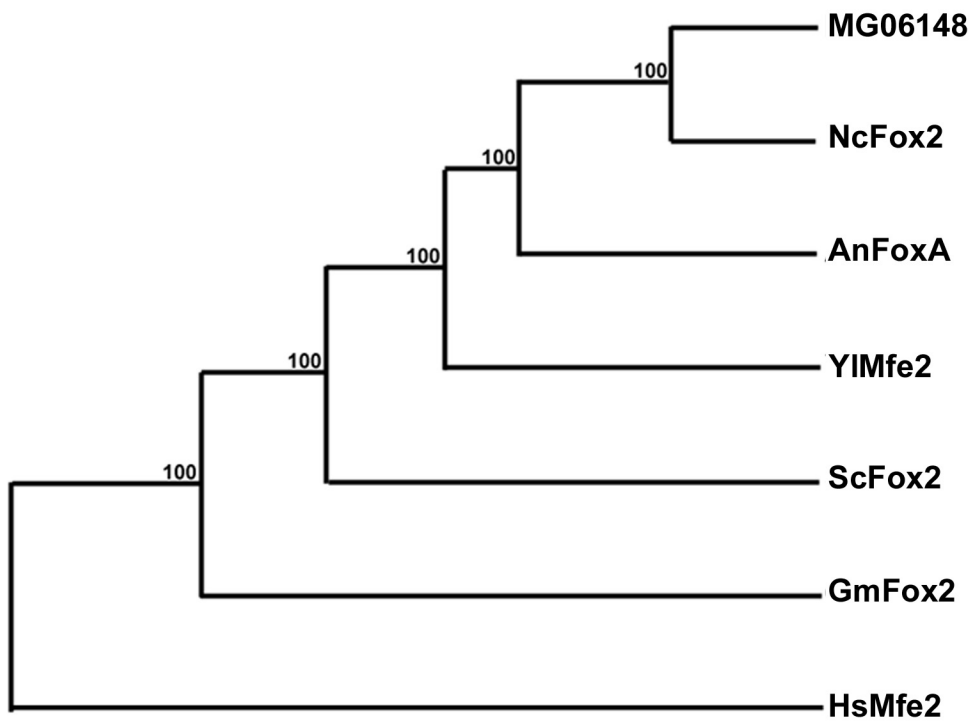
Figure 21. Phylogenetic analysis of diverse multifunctional proteins (MFP) involved in beta-oxidation.

The protein sequences of the MFP from filamentous fungi (*M. grisea* MG06148, *N. crassa* NcFox2, *A. nidulans* AnFox2), yeasts (*S. cerevisiae* ScFox2, *Yarrowia lipolytica* YlMfe2), arbuscular mycorrhizal fungus (*Glomus mosseae* GmFox2) and human (*Homo sapiens* HsMfe2) were analyzed analyzed using the cluster algorithm of the Tree Top Phylogenetic Tree Prediction program. Bootstrap values (100 iterations) are given at the nodes of the branches.

Based on the results of this *in silico* analysis, MG06148 is the best candidate for a *M. grisea* peroxisome-associated multifunctional beta-oxidation enzyme. Hereafter, the protein encoded by MG06148 is referred to as MgFox2.

To determine if MgFox2 is indeed a peroxisome-localized beta-oxidation enzyme, MgFox2 was chromosomally tagged with a Red Fluorescent Protein (RFP) at its C-terminus in a strain expressing GFP-PTS1. The resultant *FOX2*-RFP/GFP-PTS1 strain was cultivated in olive oil medium and analyzed by epifluorescence microscopy. MgFox2-RFP showed perfect colocalization with GFP-PTS1 (Figure 22). This demonstrates that even though MgFox2 lacks the conserved C-terminal PTS1 it is still targeted to the peroxisomes.
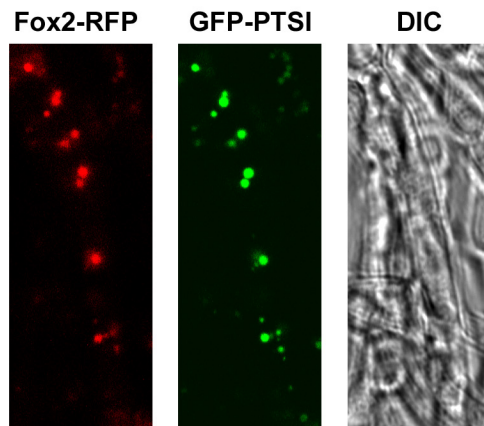
Figure 22. Subcellular localization of MgFox2.
The Fox2 ORF was tagged at the C-terminus with red fluorescent protein (RFP) in a strain expressing GFP-PTS1. Mycelia used for imaging were cultured in fatty acid medium.

4.2.2   Identification of mitochondrial beta-oxidation enzyme orthologs in *M. grisea*

As two independent beta-oxidation pathways exist in the mitochondria and the peroxisomes (Kunau et al., 1995), a concurrent investigation of both pathways is required to better ascertain the role of lipid metabolism during *M. grisea* pathogenesis. Appressorial assays using an *M. grisea* strain expressing GFP-PTS1 and stained with Mitofluor594 enabled the visualization of both peroxisome and mitochondrial organelles during appressorium morphogenesis. Both peroxisomes and mitochondria were found to be abundant within the developing appressoria (Figure 23). Recently, a mitochondria-based beta-oxidation pathway in *A. nidulans* has been described (Maggio-Hall and Keller, 2004). In this filamentous fungus, the mitochondrial enzyme enoyl-CoA hydratase A (*echA*) was shown to be required for the metabolism of short chain fatty acids. A BLAST search of the *Magnaporthe* genome with the *A. nidulans echA* (An*echA*) (GenBank Accession AN5916.2) identified the following six loci: MG06272.4, MG03335.4, MG07309.4, MG04012.4, MG08775.4 and MG0359.4. Based on analyses with the PSORTII subcellular localization program (Nakai and Horton, 1999), only MG06272, MG03335 and MG0359 are predicted to be mitochondrial. However, a peroxisomal localization is possible for MG07309 and MG00359 based on the well-conserved PTS1 signal, -AKL and –HKL (Gould et al., 1989) respectively. A phylogenetic tree was generated using Tree Top algorithm at the Web Gene Bee services of the Belozersky Institute of Moscow State University ([www.genebee.msu.su)](www.genebee.msu.su). The phylogenetic analysis showed that MG06272 is the closest ortholog of the *A. nidulans* EchA (Figure 24). The calculated distance between MG06272 and AN5916.2 is 0.39, whereas that of next closest protein, MG03335, is already 0.789 (Table 4). The percent identity of the

103

amino acid sequences is likewise highest between AN5916 and MG06272, i.e. 61%. While the other five *M. grisea* loci analyzed had sequence identity ranging from 25.2-16.8% with AN5916. Based on its close phylogenetic relationship to An*echA* and on the PSORTII mitochondrial prediction, MG06272 was selected for further characterization.

DIC   **GFP-PTS1**   **MF594**
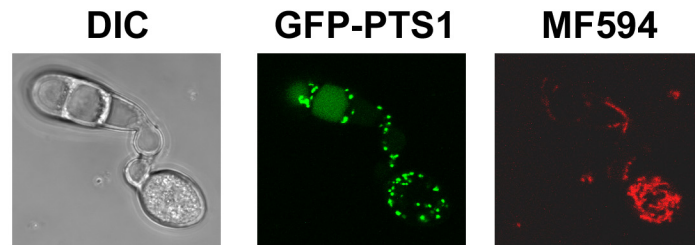
Figure 23 . Peroxisomes and mitochondria in a developing appressorium.
To visualize the organelles, 6 hr old appressorial assays on coverslips were processed for epifluorescence microscopy. The *M. grisea* strain used in the experiment expressed GFP tagged with a peroxisome targeting signal 1 (GFP-PTS1) to show the peroxisome structures. To visualize mitochondria, the appressorial assays were stained with Mitofluor594.
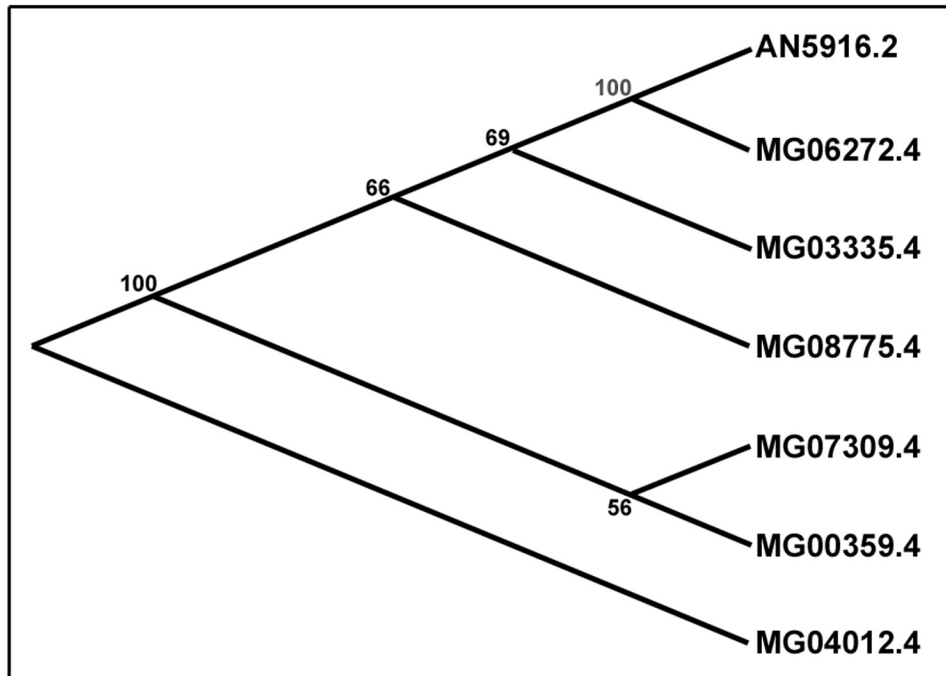
Figure 24. Phylogenetic analysis of the enoyl-CoA hydratase (EchA) of *A. nidulans* and its putative orthologs in *M. grisea*.

The amino acid sequence of *A.nidulans* EchA (AN5916.2) and the most similar proteins from *M. grisea* (MG06272.4, MG03335.4, MG08775.4, MG07309.4, MG00359.4 and MG04012.4), as obtained by BLAST, were analyzed using the cluster algorithm of the Tree Top Phylogenetic Tree Prediction program. Bootstrap support values (100 iterations) are given at the nodes of the branches.

Phylogenetic Distance

	AN5916.2	MG06272.4	MG03335.4	MG07309.4	MG04012.4	MG08775.4	MG00359.4
AN5916.2		0.395	0.789	0.805	0.879	0.833	0.872
MG06272.4	61.0		0.758	0.770	0.924	0.796	0.851
MG03335.4	25.2	25.7		0.899	0.917	0.838	0.973
MG07309.4	17.5	20.4	16.1		0.977	0.900	0.859
MG04012.4	17.5	20.9	14.6	17.2		0.971	0.993
MG08775.4	17.4	19.2	17.8	13.0	16.4		0.964
MG00359.4	16.8	16.8	15.7	16.1	13.2	15.4	

Percent Identity

Table 4. Phylogenetic distance and percent identity between the enoyl-CoA hydratase of *A. nidulans* and putative orthologs in *M. grisea*.
The protein sequences of *A. nidulans* EchA (AN5916.2) and its *M. grisea* orthologs (MG06272.4, MG03335.4, MG08775.4, MG07309.4, MG00359.4 and MG04012.4) were analyzed using the multiple sequence alignment program of the European Bioinformatics Institute (EBI).

Sequence analysis of the annotated MG06272 locus, encoding a 1424 amino acid product, revealed that there was misannotation of the sequence. A Reverse Position Specific Blast of MG06272, via the World Wide Web at the National Centre for Biotechnology Information, to identify conserved domains (Marchler-Bauer et al., 1999; Marchler-Bauer et al., 2002) in the amino acid sequence showed that the enoyl-CoA hydratase domain in MG06272 encompassed only amino acids 47 to 208. In addition, two zinc finger domains and one SH3 domain were identified in the last 424 amino acids of the sequence. After analysis using the EMBOSS pairwise alignment algorithms of the European Bioinformatics Institute, only the first 292 amino acids of MG06272 aligned with AN5916. Based on these *in silico* analyses, MG06272 was re-annotated and named as Mg*ECHA*. The re-annotated Mg*ECHA* includes only the first 292 amino acids of the published MG06272 sequence and was used for further experiments. In the *Magnaporthe grisea* genome database version 5.0, the MG06272.4 locus had been re-annotated and split into two: MGG_12869.5 which is 3646 bp in length and MGG_12868.5. The domain for the enoyl-CoA hydratase/isomerase family was identified in MGG12868.5.

The human and rat ECH enzyme is composed of 290 amino acids with a putative amino-terminal mitochondrial targeting sequence of 29 residues (Minami-Ishii et al., 1989; Kanazawa et al., 1993). Glutamic acid residues at positions 144 and 164 are conserved in members of hydratase/isomerase families and are critical for the enzyme's catalytic activities (Muller-Newen et al., 1995; Kiema et al., 1999). Both Glu144 and Glu164 are conserved in Mg*ECHA*. An additional phylogenetic analysis of MG06272 with the enoyl-CoA hydratases of *N. crassa* (NCU06448.1), *A. nidulans*

(AN5916.2) and human (P30084) showed that the *M.grisea* EchA has the closest relationship with the *N. crassa* counterpart (Figure 25).

Results of the analysis of the amino acid sequence of MG06272 using the subcellular localization prediction programs PSORTII and TargetP strongly indicated mitochondrial localization for the protein. To confirm the subcellular location, MgEchA was fused to GFP at the carboxy terminus. However, the resultant MG06272-GFP transformants exhibited impaired growth on fatty acid medium. This phenotypic defect suggests that tagging of the MG06272 with a GFP at its carboxy terminus compromises the function of the protein.
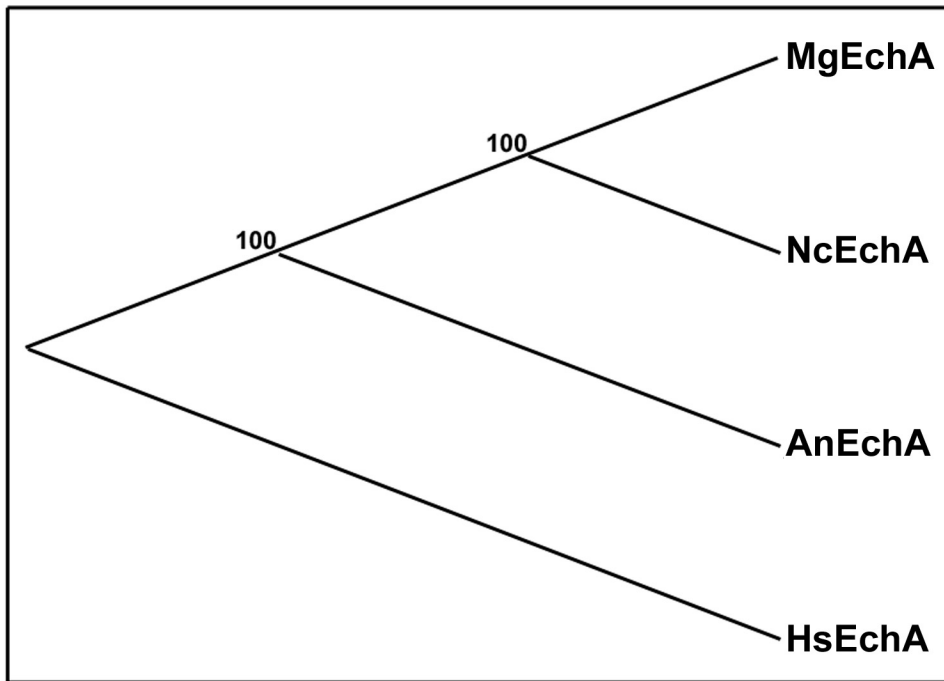
Figure 25. Phylogenetic analysis of diverse enoyl-CoA hydratases.
The amino acid sequence of EchA from *M. grisea* (MgEchA), *N. crassa* (NcEchA), *A. nidulans* (AnEchA) and *Homo sapiens* (HsEchA) were analyzed using the were analyzed using the cluster algorithm of the Tree Top Phylogenetic Tree Prediction program. Bootstrap values (100 iterations) are given at the nodes of the branches.

4.2.3 Creation of Mg*FOX2* and Mg*ECHA* deletion and complementation strains

To characterize the biological function of Mg*FOX2* and Mg*ECHA*, independent gene-deletion mutants were created, by replacing the entire ORF with selection markers for hygromycin and bialaphos resistance, respectively (Figure 26, 27). Molecular confirmation of the targeted deletion was performed by Southern analysis. For Mg*FOX2*, a 3'probe detected two bands in the wild-type (Figure 26, lane 1), 2.777 and 3.679 kb, of which the former was diagnostic. In the Mg*FOX2* knockout (Figure 26, lane 2), the 3.679 kb band was retained and a 989 bp band was detected due to an internal *Nco*I site in the selection marker. For Mg*ECHA*, a 5' probe detected a 1.879 kb band in the wild-type (Figure 27, lane 1). In the Mg*ECHA* knockout (Figure 27, lane 2), the loss of an internal *Pvu*I site in the ORF, which was replaced by the selection marker resulted in the disappearance of the 1.879 kb and the appearance of a 6.839 kb fragment due to a downstream *Eco*RV site.
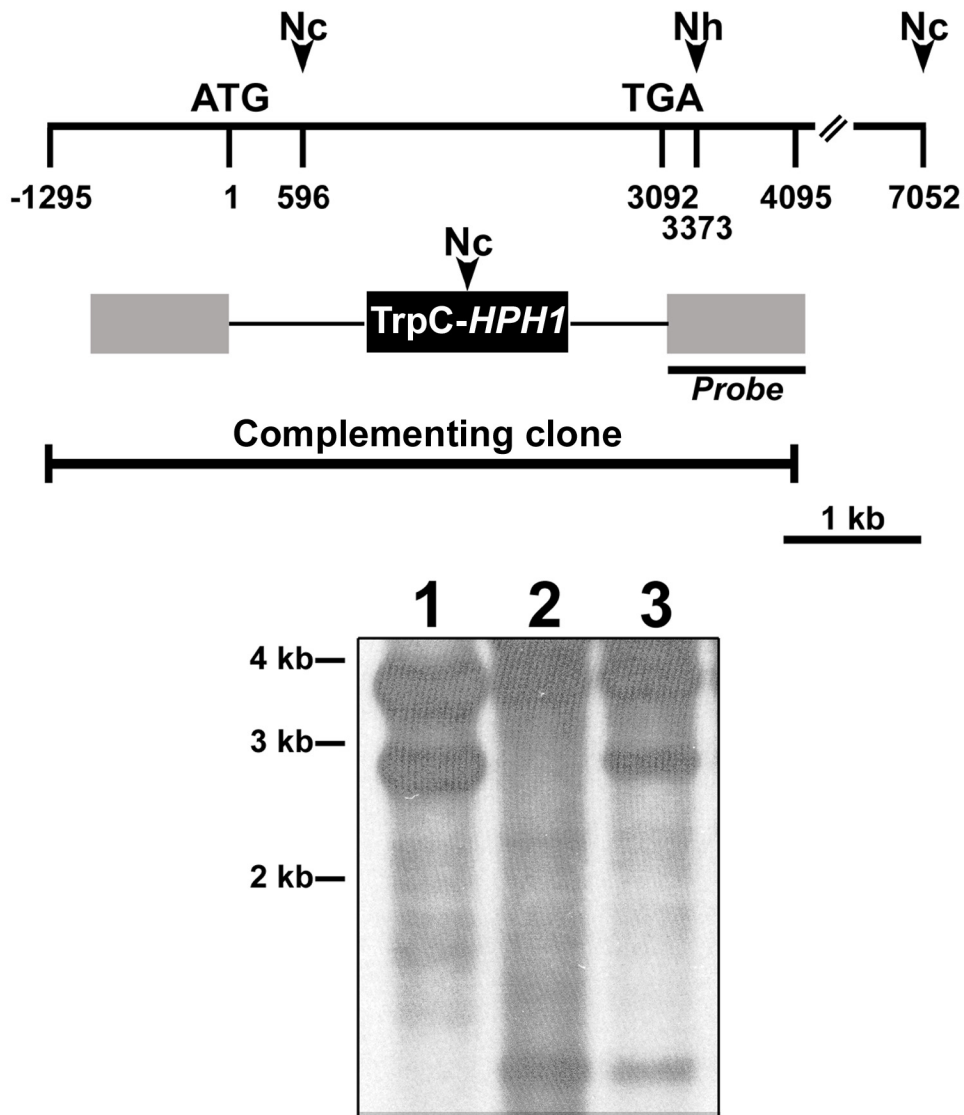
Figure 26. Annotation and gene deletion of Mg*FOX2*.
About 1 kb each of upstream and downstream sequences (gray boxes) were used as homology sites to direct the replacement of the *FOX2* ORF with a hygromycin resistance cassette (TrpC-*HPH1*). The resulting deletion strain was genetically complemented by ectopic insertion of the Complementing (Genomic) fragment. Southern blot analysis was performed on the wild-type (1), deletion (lane 2) and complemented (3) strains to confirm the gene replacement and complementation events. DNA blots contained genomic DNA double-digested with *Nco*I (Nc) and *Nhe*I (Nh) and hybridized with the indicated Probe fragment.
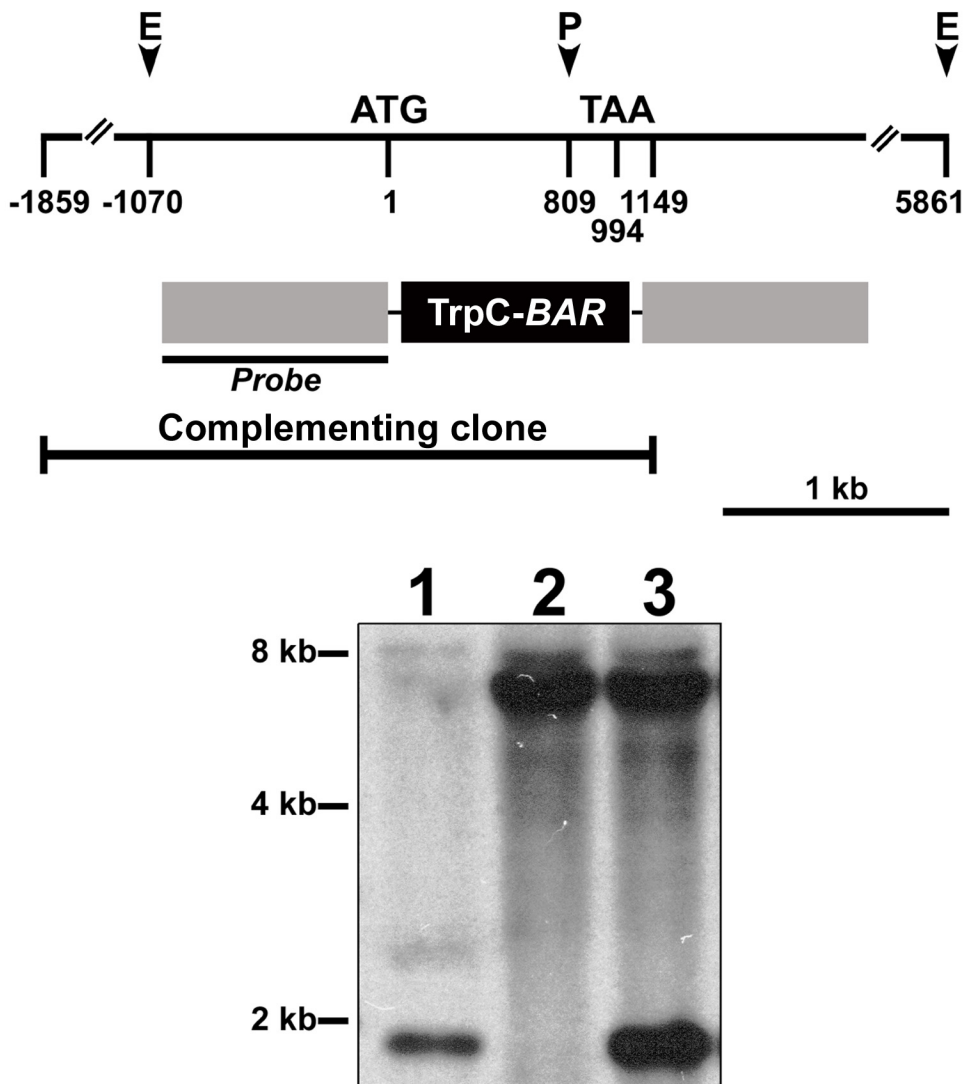
Figure 27. Annotation and gene deletion of Mg*ECHA*.
About 1 kb of upstream and downstream sequences (gray boxes) were used as homology sites to direct the replacement of the *ECHA* ORF with an ammonium glufosinate resistance cassette (TrpC-*BAR*). The resulting deletion strain was genetically complemented by ectopic insertion of the Complementing fragment. Southern blot analysis was performed on wild-type (1), deletion (lane 2) and complemented strains (3) to confirm the gene replacement and complementation events. DNA blots contained genomic DNA double-digested with *Eco*RV (E) and *Pvu*I (P) and were hybridized with the indicated Probe fragment.

To be certain that the observed phenotypic defects were due solely to the disruption of either Mg*FOX2* or Mg*ECHA*, genetic complementation of both deletion strains was done. In each instance, PCR fragment encompassing the entire ORF and at least 1 kb of upstream sequences was used to complement the respective deletion mutant (Figure 26, 27). Southern analysis was conducted to confirm the complemented strains. In both Mg*FOX2* and Mg*ECHA* complemented strains, the diagnostic band of 2.777 or 1.879 kb, respectively, was regained (Figure 26, lane 3 and Figure 27, lane 3).

4.2.4 Characterization of lipid metabolism of *echA*Δ and *fox2*Δ

To determine the role of Mg*FOX2* and Mg*ECHA* in lipid metabolism, the deletion strains were cultured on medium containing either glucose or olive oil as sole carbon source (Figure 28). On glucose-containing medium, *fox2*Δ and the genetically complemented deletion strains grew similar to wild type. However, *echA*Δ grew slower and had a less dense colony. Both the deletion strains failed to grow on olive oil medium, whereas the growth of the wild type and the respective complemented strains were comparable.
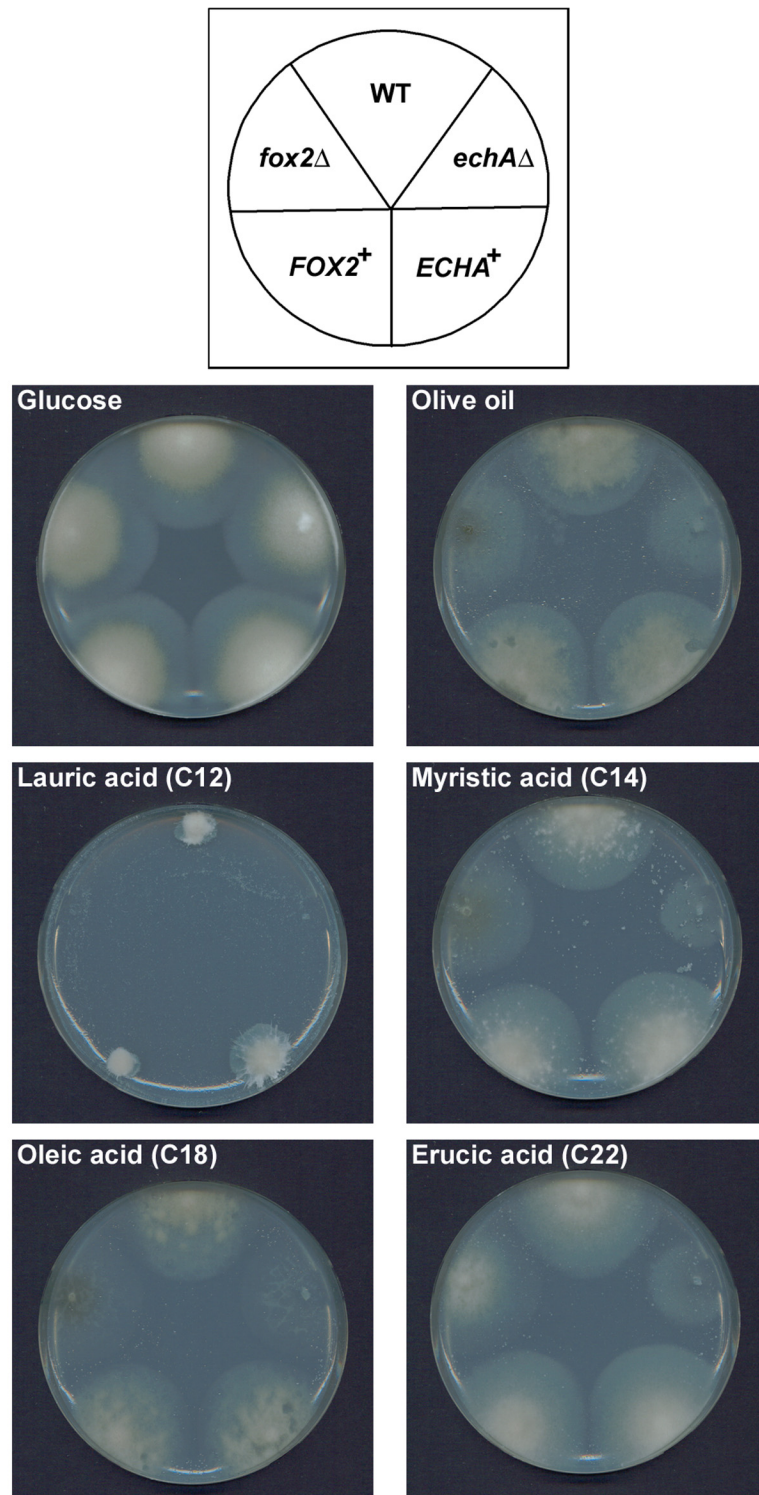
Figure 28. Fatty acid utilization of *fox2Δ* and *echAΔ* mutants.
Mycelial plugs of wild-type (WT), deletion mutants (*fox2Δ*, *echAΔ*) and genetically complemented strains (*FOX2+*, *ECHA+*) were inoculated on basal medium containing either 1% glucose or 1% olive oil or equivalent carbon concentrations of fatty acids of different chain lengths (C12, C14, C18, C22) as sole carbon source.

To examine the requirements for Mg*FOX2* and Mg*ECHA* for the catabolism of different types of fatty acids, the deletion strains were cultivated on fatty acids of different chain lengths (Figure 28). Equivalent carbon content as adjusted by the molar concentrations of the following fatty acids was used: hexanoic acid (C6), octanoic acid (C8), decanoic acid (C10), lauric acid (C12), myrisitic acid (C14), palmitic acid (C16) and erucic acid (C22). At the concentrations used, hexanoic, octanoic and decanoic fatty acids were toxic to wild-type *M. grisea*. On lauric acid, the wild type grew in an abnormal and restricted manner. The *fox2*Δ and *echA*Δ were both unable to metabolize myristic, palmitic and erucic acid. Based on these results, it was not possible to differentiate between the peroxisomal and mitochondrial capability or specificity to utilize fatty acids of different chain lengths.

To further investigate the role of these beta-oxidation genes during lipid metabolism, the transcription of both genes upon induction with different carbon sources was evaluated by RT-PCR (Figure 29). During growth in glucose, Mg*ECHA* transcripts could not be detected whereas Mg*FOX2* transcripts were clearly visible. Though olive oil induced the transcription of both genes, Mg*FOX2* was significantly upregulated compared to Mg*ECHA*. This is consistent with a peroxisomal localization for MgFox2, as fatty acids have been shown to induce the expression of nuclear-encoded genes regulating peroxisomal beta-oxidation (Hiltunen et al., 2003). Acetate treatment also resulted in the transcriptional upregulation of Mg*FOX2* and to a lesser extent Mg*ECHA*.
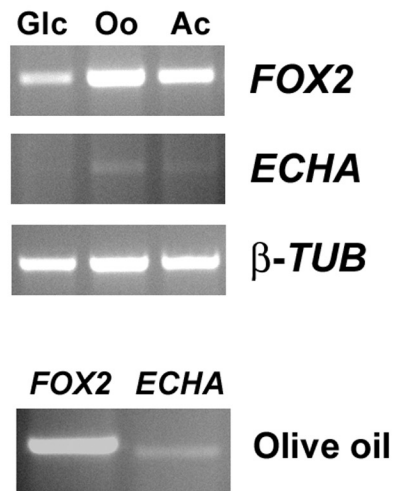
Figure 29. RT-PCR analyses of *FOX2* and *ECHA* transcripts.
RNA was harvested from mycelial cultures that had been pre-grown in 1% glucose for three days and then further incubated in either 1% glucose (Glc) or 1% olive oil (Oo) or 50 mM sodium acetate (Ac) for another 16 hours. The RT-PCR products from olive oil grown cultures were reloaded (bottom gel) to shown the difference between the transcription levels of *FOX2* and *ECHA*. RT-PCR amplification of the β-tubulin transcript was used as a loading control.

Taken together, these results suggest that although Mg*echA* and Mg*fox2* are required for fatty acid metabolism, their distinct enzyme activities may contribute differently to other metabolic requirements of the fungus.

4.2.5   Vegetative growth defect of *echA*Δ

To further examine the observed compromised growth of *echA*Δ on glucose medium, a conidial dilution series was inoculated on standard culture medium (prune agar medium) (Figure 30). In wild-type and *fox2*Δ, even with the lowest conidial concentration, mycelial growth was substantial at three days post-inoculation. These colonies from different conidial concentrations were fast growing and at day five had reached equivalent colony diameters and density. However, with *echA*Δ inoculations, at day three, only the highest conidial dilution exhibited growth and was comparable to the colony in the lowest conidial inoculations of either the wild-type or the *fox2*Δ. The *echA*Δ colony grew slowly and at day five had a smaller diameter than any of the colonies of the other two strains tested. Some slight growth could be observed from the second highest conidial dilution of *echA*Δ at day five. These results indicate that mitochondrial enoyl-CoA hydratase activity is required for optimal fungal vegetative growth.
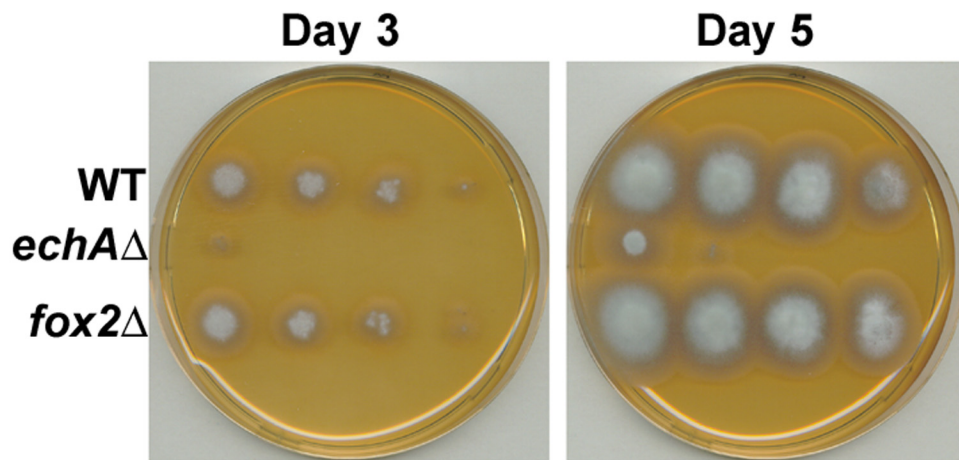
Figure 30. Vegetative growth defect of *echA*Δ.
A serial dilution of conidial suspension of wild-type or *echA*Δ or *fox2*Δ strains was inoculated on prune agar medium. Growth was assessed three and five days after inoculation.

4.2.6 Mitochondrial morphology of mutants

The vegetative growth defect of *echAΔ* is reminiscent of the slow growth phenotype of *S. cerevisiae* petite mutants, which are known to have defects in mitochondrial respiration (Tzagoloff and Dieckmann, 1990). As mitochondrial morphology has been shown to be important for the respiratory capacity of these organelles (Skulachev, 2001), the mitochondria of the mutants were stained with Mitofluor 594 and observed using epifluorescence microscopy. The mitochondrial structures of both wild type and the *fox2Δ* consisted of long tubular networks (Figure 31). In contrast, the mitochondria of *echAΔ* resembled spherical or short spiral structures. These results suggest that normal mitochondrial morphology is perturbed in the *echAΔ* and may be the cause of the growth defect observed during vegetative growth.
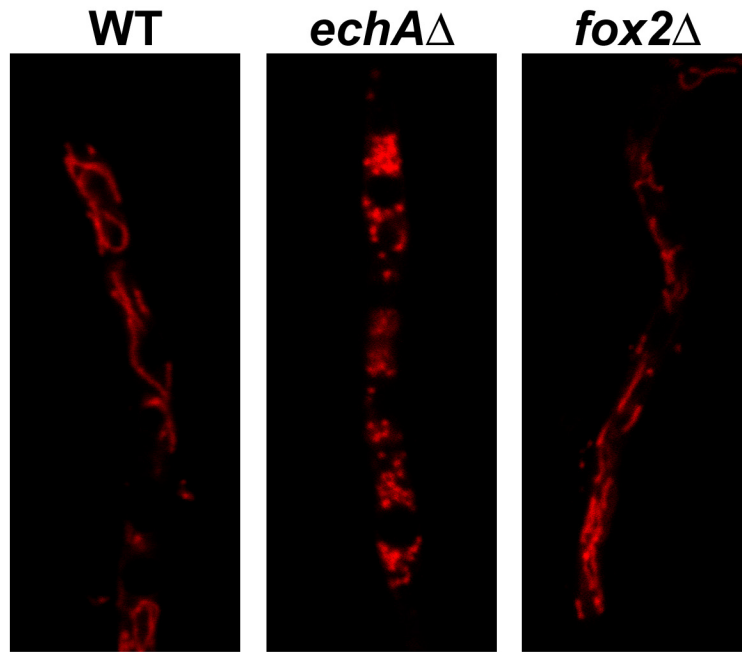
Figure 31. Aberrant mitochondrial morphology in *echAΔ*.
Mycelia of wild-type (WT), *echAΔ* and *fox2Δ* strains were stained with Mitofluor594 and viewed under fluorescence microscopy.

4.2.7. Pathogenicity and pathogenic lipid metabolism

The overall pathogenicity of the Mg*FOX2* and Mg*ECHA* deletion and complemented strains was evaluated on a detached barley leaf infection assay (Figure 32). Inoculation of barley leaf explants with 20 µl droplets containing 3000 conidia was sufficient for the development of blast lesions by the wild-type and the respective complemented strains. The formation of spreading lesions was visible starting at three days post-inoculation in the inoculations with the wild type and the complemented strains. On the other hand, both *fox2*Δ and *echA*Δ mutants failed to elicit any disease lesions on the inoculated barley leaves.

Figure 32. Pathogenicity of *fox2*Δ and *echA*Δ mutants.
Conidial preparations of wild-type (1), *echA*Δ (2), complemented *echA*Δ (3), *fox2*Δ (4) and complemented *fox2*Δ (5) strains were inoculated on detached barley leafs. Assessment of disease lesions was done seven days post-inoculation.

During *M. grisea* pathogenesis, lipid bodies in the germinating conidium are transported to the developing appressorium where they are immediately utilized/ degraded (Thines et al., 2000). Similar lipid mobilization and breakdown events have been observed in other fungal pathogens (Both et al., 2005) and suggest that the oxidation of storage fatty acids contributes essential metabolites during early pathogenesis. The role of Mg*FOX2* and Mg*ECHA* during pathogenic lipid metabolism was investigated by observing the fate of lipid bodies in the maturing appressorium. Nile red stained lipid droplets were no longer detectable in wild-type appressoria at 24 hours, in contrast to the *fox2Δ* and the *echAΔ* appressoria where they accumulated in large numbers (Figure 33). The ultrastructural detail of wild-type appressoria consisted of a large central vacuole and few small lipid bodies (Figure 33). In contrast, abundant lipid bodies were observed in thin electron microscopic sections of both the *fox2Δ* and *echAΔ* mutant appressoria. Hence, lipid breakdown during early pathogenic development and subsequent *in planta* infection requires both Mg*FOX2* and Mg*ECHA*.

Wild-type

***fox2*Δ**

***echA*Δ**
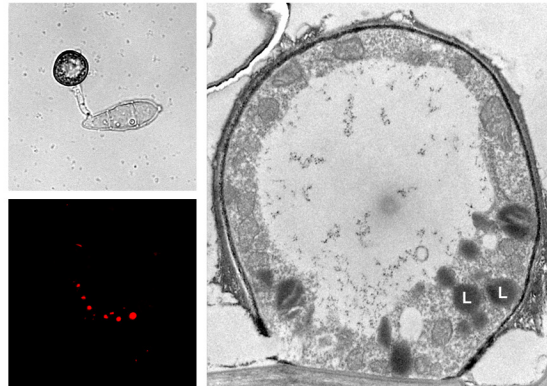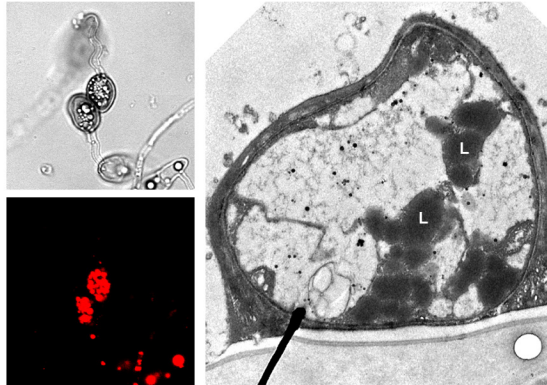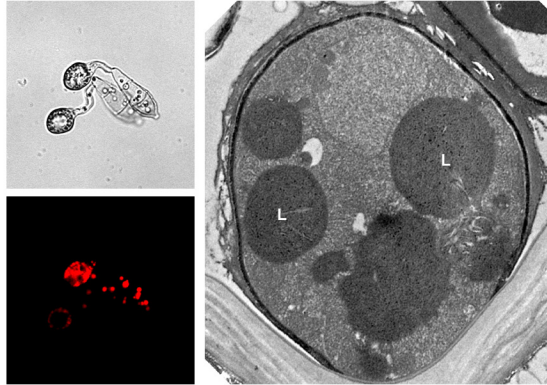
Figure 33. Mobilization of lipid bodies in the appressoria.
To observe lipid bodies (L) 24-hr old appressoria of the wild-type or the indicated mutant strains were either stained with Nile red (left panels) or processed for TEM (right panels). Scale bar for nile red staining = 10 μm, scale bar for TEM = 1 μm.

4.2.8   Pathogenicity-related traits

To better characterize the loss-of-pathogenicity phenotype of *fox2Δ* and *echAΔ*, appressorium morphogenesis and appressorium-mediated host penetration were carefully investigated. In addition, glucose supplementation was done during the assays to check for possible remediation of observed defects. Fatty acid oxidation serves as a crucial energy source during different developmental processes (Schulz, 1991). If the phenotypic defects observed could be attributed to the loss of energy source, then they could be remediated upon supplementation with an easily metabolizable energy source such as glucose.

From light microscopic observations of appressorium assays on artificial membranes, it was found that *fox2Δ* and *echAΔ* had a high frequency, 50-60%, of abnormal-looking appressoria (Figure 34). Whereas most wild-type appressoria were spherical, darkly-pigmented and had a uniform protoplasmic content punctuated with small vesicles, the abnormal appressoria of the mutants were misshapen, more transparent and had large vesicles clustered within the cytoplasm. Addition of high concentrations of glucose (final concentration = 2.5%) at the start of appressorium assays resulted in the formation of normal appressoria at wild-type frequency in the mutants (Figure 34). These results suggest that mitochondrial and peroxisomal beta-oxidation of fatty acids provides a crucial energy source during appressorium morphogenesis.
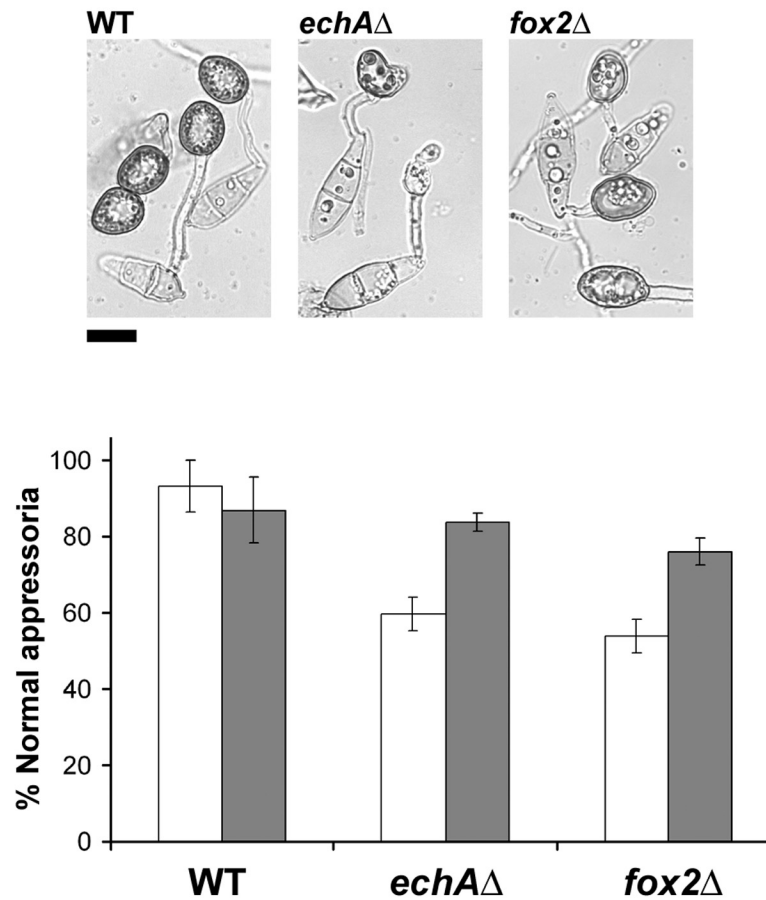
Figure 34. Defects in appressorium morphogenesis of *echA*Δ and *fox2*Δ.
A high percentage (~30%) of *echA*Δ and *fox2*Δ appressoria exhibit abnormal development having a less pigmented and vacuolated appearance (top panel). Scale bar = 10 μm. The appressorial morphology was quantitatively assessed (bottom panel) in untreated (open bar) and in the presence of 2.5% glucose (gray bar) at 24-hours post inoculation.

The *M. grisea* pathogen invades its host by forcing a thin penetration peg from the appressorium through the leaf epidermis (Talbot, 2003). As part of the plant's defense mechanism, callose material is deposited at the entry site of the fungal penetration peg (Jacobs et al., 2003). This plant-derived callose deposition can be visualized by aniline blue staining and is taken as a measure of fungal penetration peg formation (Vogel and Somerville, 2000). At 48 hours post-inoculation, ~83% of wild-type appressoria formed penetration pegs (Figure 35). These penetration pegs developed into infectious hyphae, which ramified and colonized neighboring plant cells at 96 hours post-inoculation. Less than 1% of appressoria from either *echAΔ* or *fox2Δ* formed penetration pegs. However, there was no infectious hyphae formation from the mutant appressoria even at 96 hours post-inoculation. Addition of glucose during infection assays resulted in an increased frequency of callose deposition underneath the appressoria of both mutants indicating a partial remediation of penetration peg formation (Figure 35). However, typical infectious hyphae did not develop further from these glucose-induced penetration pegs. Interestingly, a low frequency of abnormal infectious hyphae was observed in *echAΔ*, but not in *fox2Δ* (Figure 36). These results suggest that fatty acid metabolism, in addition to providing an energy source, produces other secondary metabolites which are essential for appressorium mediated host penetration and host proliferation.
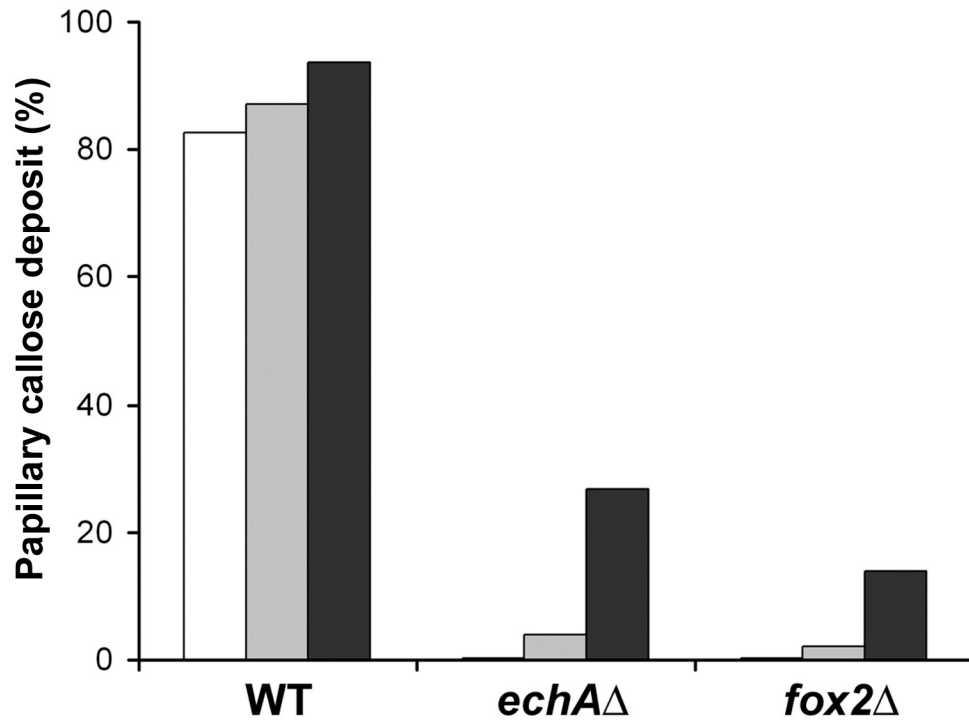
Figure 35. Host penetration defects of *echA*Δ and *fox2*Δ mutants.
The presence of aniline blue stained callose underneath the site of appresoria in barley leaf inoculations was taken as a measure of host penetration capability. Data was obtained from untreated samples 96 hr post-inoculation (open bar), in the presence of 2.5% glucose 48 hr post-inoculation (gray bar) and in the presence of 2.5% glucose 96 hr post-inoculation (black bar).
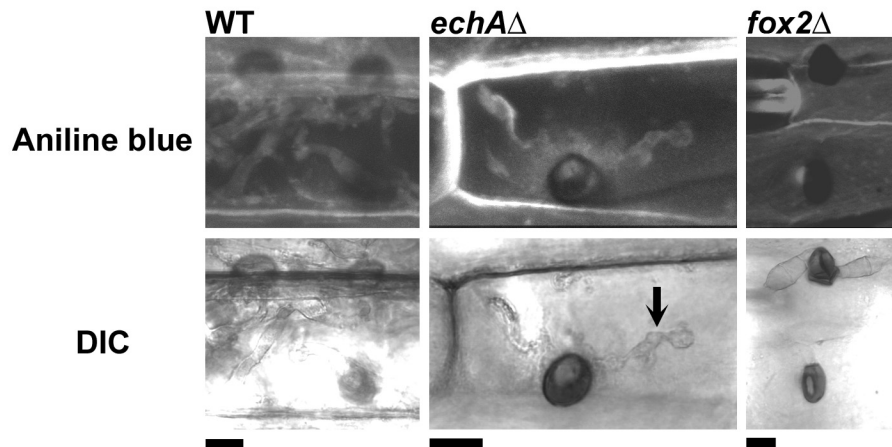
Figure 36. Host proliferation defect of *echA*Δ.
Wild-type, *echA*Δ and *fox2*Δ strains were inoculated on barley leaves in the presence of exogenous glucose and were processed by aniline blue staining at the 96 hr timepoint. Glucose-induced infectious hyphae (arrow) which failed to proliferate within the host tissue was observed in the *echA*Δ inoculations. Scale bar = 10 μm.

The appressorial melanin layer in the *fox2Δ* and *echAΔ* was assessed by thin section electron microscopy since the experiments on the *PEX6* and *PTH2* deletion mutants implicated a role for peroxisomal metabolism for appressorial melanin synthesis. In the wild type and *echAΔ* strains, the melanin layer was easily visible as a uniform electron dense layer between the appressorial cell wall and the plasma membrane (Figure 37). In contrast, the appressorial melanin layer in the *fox2Δ* appeared greatly reduced. The reduction in the appressorial melanin layer of the *fox2Δ* mutant is consistent with the defects in melanin deposition in the *pex6Δ* and *pth2Δ* appressoria and supports the hypotheses that peroxisomal metabolism provides the precursor acetyl-CoA molecules utilized for melanin synthesis. The presence of an intact melanin layer in the *echAΔ* appressoria suggests that the acetyl-CoA molecules produced during mitochondrial fatty acid oxidation do not contribute to the melanin polyketide synthesis pathway.
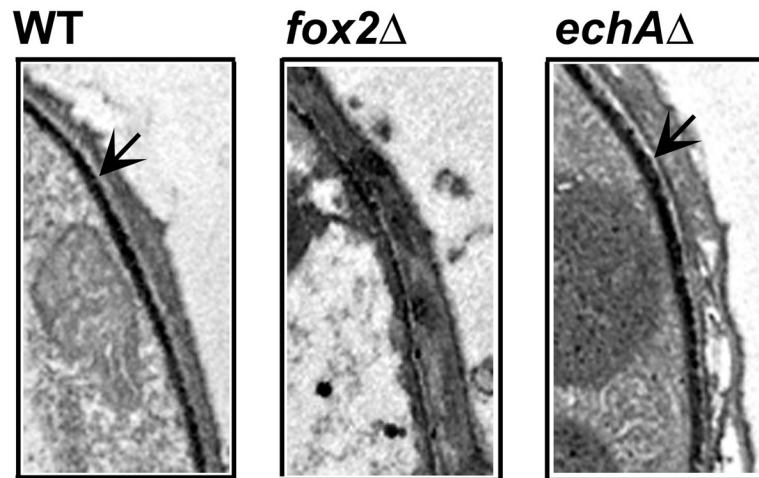
Figure 37. Appressorial melanization in the *fox2*Δ and *echA*Δ mutants.
To analyze the melanin layer in the appressorium, 24 hour old appressorial assays of the wild-type (WT), *fox2*Δ and *echA*Δ strains were processed for thin section electron microscopy. The electron dense appressorial melanin layer (arrow) is comparable between the wild-type and *echa*Δ but appears greatly reduced in the *fox2*Δ.

CHAPTER V DISCUSSION

The extensive analysis of various metabolic mutants helped establish the role of lipid catabolism via peroxisomal and mitochondrial beta-oxidation pathways during *M. grisea* pathogenesis (Figure 38). Targeted deletions of genes required or essential for peroxisome biogenesis (*PEX6*), for carnitine-mediated acetyl-CoA transport (*PTH2*) and for peroxisomal beta-oxidation (*FOX2*) demonstrated that acetyl-CoA generated from peroxisomal fatty acid beta-oxidation is utilized for synthesis of appressorial melanin and likely for the biogenesis of the cell wall components in penetration pegs. The presence of an additional fatty acid catabolism pathway in the mitochondria of *M. grisea* was demonstrated through the creation and characterization of a strain lacking the mitochondrial beta-oxidation enzyme *ECHA*. The mitochondrial component of lipid catabolism is essential for utilization of fatty acids and is required during the appressorium morphogenesis, host penetration and host proliferation stages of pathogenic development. Exogenous addition of glucose only partially remediates the host penetration defect in the mutants (*pth2Δ*, *fox2Δ* and *echAΔ*) and thus indicates that acetyl-CoA is compartmentalized or its availability is temporally controlled. Furthermore, these studies revealed that during pathogenesis metabolic pathways are strictly regulated.
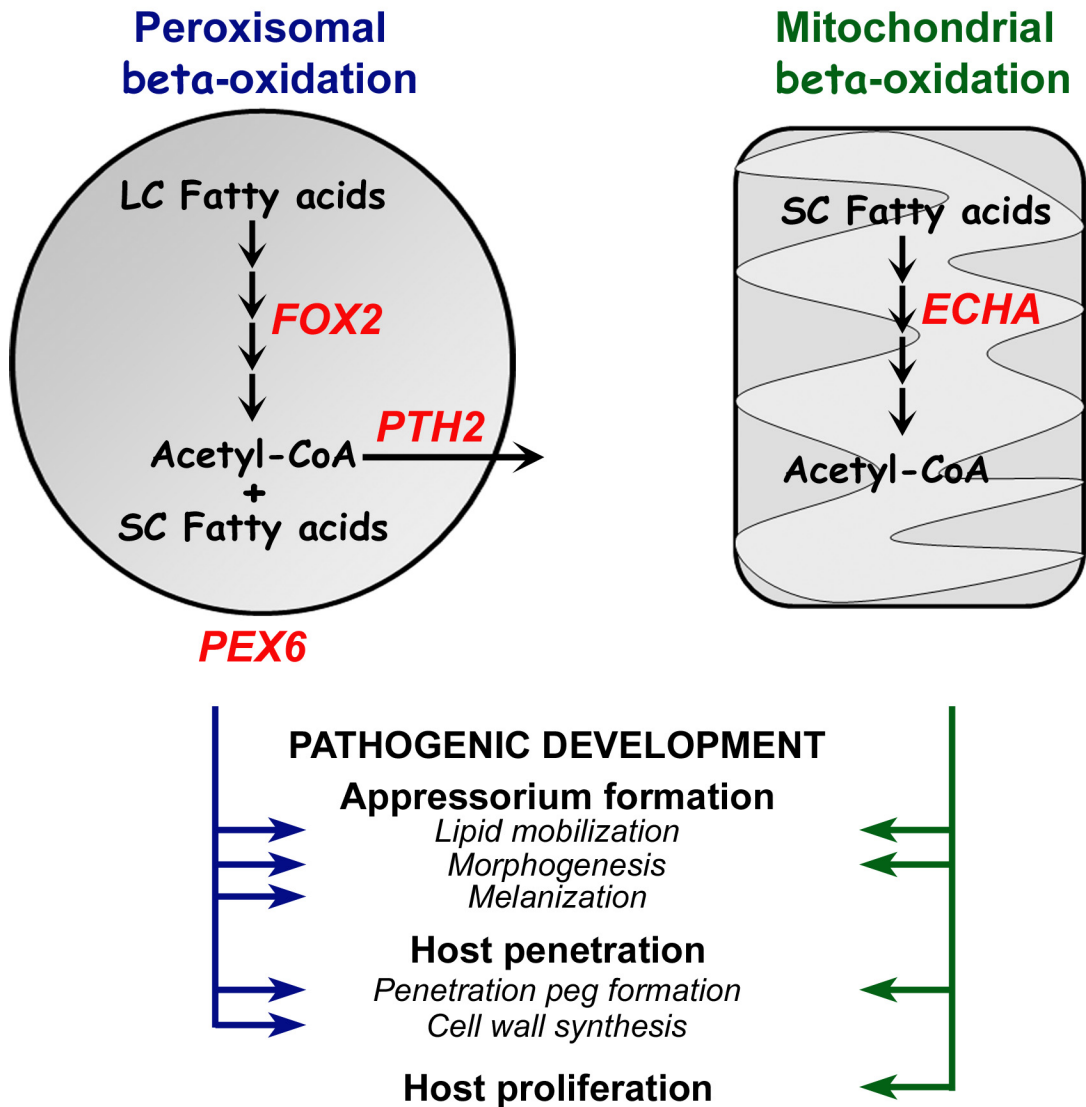
Figure 38. Model illustrating the metabolic contributions of peroxisomal and mitochondrial fatty acid beta-oxidation to pathogenic development in *M. grisea*. Through the functional characterization of genes which are involved in peroxisome biogenesis (*PEX6*), peroxisomal beta-oxidation (*FOX2*), acetyl-CoA transport (*PTH2*) and mitochondrial beta-oxidation (*ECHA*), exclusive and cooperative contributions during stages of pathogenesis can be assigned to peroxisomal and mitochondrial fatty acid catabolism. Peroxisomal beta-oxidation of long-chain (LC) fatty acids yields acetyl-CoA and chain-shortened (SC) fatty acids. The SC fatty acids are thought to depend on mitochondrial beta-oxidation for complete oxidation. Lipid mobilization, appressorium morphogenesis and penetration peg elaboration during pathogenic development require the fatty acid catabolic function of both peroxisomes and mitochondria. On the other hand, appressorial melanization and synthesis of cell wall components of penetration pegs requires only peroxisome-derived acetyl-CoA.

5.1 Lipid metabolism plays a key role during fungal pathogenesis

5.1.1 Accumulation and mobilization of lipid stores

Triacylglycerols are the most efficient form of storage lipids in many organisms (Murphy, 2001). These neutral lipids accumulate within the hydrophobic core of single membrane bound organelles called lipid bodies. Upon mobilization, the stored lipids provide an important source of chemical energy and precursors for membrane phospholipids for the cell (Wagner and Daum, 2005). Lipid bodies are abundant in the asexual spores (conidia) of *M. grisea* (Weber et al., 2001). During pathogenic development, these lipid bodies are transported from the germinated conidium into the tip of the germ tube (Thines et al., 2000). As the appressorium formed and matured from the germ tube tip, these lipid bodies are rapidly degraded. The metabolism of endogenous lipid stores is sufficient to provide the energy and biosynthetic requirements of the developing appressoria. Ultrastructural analysis of the dormant conidia of the anthracnose fungus *Colletotrichum lagenarium* demonstrated the presence of abundant lipid bodies (Kimura et al., 2001). In the germinating spores of the mycorrhizal fungus *Glomus caldenonius*, there is a sharp decline in the amount of triacylglycerols with a concomitant increase in the free fatty acid content (Beilby and Kidby, 1980). In the watermold *Blastocladiella emersonii*, a remarkable loss of endogenous lipids in the zoospores is seen within the first 15 minutes of germination (Smith and Silverman, 1973).

The preference to metabolize different types of energy sources has also been observed in other fungal species. During germination and growth, the ascospores of *Neurospora tetrasperma* utilize a combination of carbohydrate and lipid metabolism

(Lingappa and Sussman, 1959). For the initial stage of germination and germ tube protrusion, endogenous carbohydrate reserves are immediately metabolized. Five hours after the initiation of germination, an accelerated degradation of endogenous lipid reserves takes place. In *M. grisea*, both glycogen and lipid storage reserves are translocated from the germinated conidium into the developing appressorium where they are rapidly degraded. However, though enzymatic activities for both carbohydrate and lipid catabolism are present in the germinating conidium, only triacylglycerol lipase activity increases significantly during appressorium maturation (Thines et al., 2000). In some fungi, such as the root rot fungus *Phymatotrichum*, glycogen reserves represent the predominant energy source for germination of the sclerotia (Ergle, 1948).

In other fungi, metabolism of endogenous lipid or carbohydrate reserves is insufficient to support germination and an exogenous supply of nutrients is necessary to initiate germination. In the damping-off disease causing fungus *Fusarium roseum*, the germination of macroconidial spores requires an exogenous source of carbon, nitrogen and inorganic nutrients (Sisler and Cox, 1954). In *Fusarium solani*, despite an accumulation of lipid reserves in spores during vegetative growth on rich medium, spores do not germinate in the absence of exogenous glucose (Cochrane et al., 1963). Moreover, only a small fraction of the lipid stores is degraded during spore germination.

5.1.2   Upregulation of genes related to lipid catabolism

The importance of lipid metabolism during pathogenic development is indicated by the upregulation of genes and the increased activity of enzymes of lipid metabolism

and its auxiliary pathways. Transcriptional profiling of different pathogenic stages of the barley powdery mildew pathogen *Blumeria graminis* demonstrated that genes involved in the degradation of lipids are upregulated during the early stages of pathogenesis (Both et al., 2005). In *M. grisea*, the enzyme activity of triacylglycerol lipase, which is the primary enzyme for mobilization of stored lipids, increases during early pathogenesis (Thines et al., 2000). During the critical stage of host macrophage sequestration during the pathogenesis of *Candida albicans* and *Cryptococcus neoformans*, there is an increased transcription of genes coding for enzymes of the glyoxylate cycle (Lorenz and Fink, 2001; Rude et al., 2002). As an auxiliary pathway to lipid metabolism, the glyoxylate cycle enables the utilization of fatty acid oxidation products for energy generation and macromolecular synthesis.

5.1.3 Loss or reduction in pathogenicity resulting from mutations in genes involved in lipid metabolism

In this study, the loss of pathogenicity resulting from the independent deletion of four different genes (*PEX6*, *PTH2*, *FOX2* and *ECHA*) related to lipid metabolism emphasizes the indispensable nature of this metabolic process to *M. grisea* pathogenicity. The contribution of peroxisomal metabolic functions is underscored by the pathogenicity-related defects of the *pex6Δ*, *pth2Δ* and *fox2Δ* mutants. The host penetration defect and the loss of the appressorial melanin in the *M. grisea pex6Δ* is comparable to the defects observed in the *pex6Δ* strain of *C. lagenarium* (Kimura et al., 2001). Acetyl-CoA produced from fatty acid catabolism within the peroxisomes most likely contributes to the synthesis of appressorial melanin in both fungi. A drastic reduction in the appressorial melanin layer was also observed in the *pth2Δ* mutant which is defective in transporting acetyl-CoA out of the peroxisome. The

137

deletion of genes encoding for specific fatty acid beta-oxidation enzymes in the peroxisome (*FOX2*) and mitochondria (*ECHA*) also results in the loss of pathogenicity. Both genes are essential for utilization of fatty acid substrates. The characterization of an *Ustilago maydis* mutant in the peroxisomal MFP2 reports the consequences of the disruption of beta-oxidation enzymes on fungal pathogenesis (Klose and Kronstad, 2006). The pathogenicity defect In the *U. maydis mfp2Δ* strain is likely to be related to the impairment of *in planta* proliferation, which leads to a reduction in virulence (Klose and Kronstad, 2006). The attenuation in virulence was likewise observed in the *C. albicans fox2Δ* strain (Piekarska et al., 2006).

The importance of lipid catabolism during pathogenesis is mostly inferred from the identification of pathogenicity mutants defective in the glyoxylate cycle, which serves as an auxiliary pathway of lipid metabolism. In general, the disruption of the glyoxylate cycle in different fungal phyto-pathogens results in the inability to utilize fatty acids as sole carbon source in vitro (Idnurm and Howlett, 2002; Wang et al., 2003). During pathogenesis, the impairment in the mobilization and degradation of lipid bodies in the spores is also observed in these mutants (Wang et al., 2003; Solomon et al., 2004). The common defect in conidial germination observed among the different fungal species, either low germination rate (Idnurm and Howlett, 2002; Solomon et al., 2004) or delayed germination (Wang et al., 2003), suggests that lipid metabolism is required at a very early stage during pathogenesis. In addition, defects in specific stages of pathogenic development were identified in these different glyoxylate cycle mutants. The loss of the isocitrate lyase (Icl1) function in the blackleg disease fungus *Leptosphaeria maculans* results in an acute impairment of pathogenicity due to reduced hyphal growth at infection sites (Idnurm and Howlett,

138

2002). As the *icl1Δ* is incapable of utilizing fatty acids as sole carbon source *in vitro*, a defect in carbon (fatty acid) utilization on the plant surface may be the cause of limited hyphal growth. On the other hand, the attenuation in virulence of a similar *icl1Δ* in *M. grisea* is ascribed to a delay in the development of infection stages such as appressorial maturation and host penetration (Wang et al., 2003). The disruption of the glyoxylate pathway through the loss of malate synthase 1 (*MLS1*) function in the wheat pathogen *Stagonospora nodorum* results in the failure of spores to germinate in the absence of exogenous carbon (Solomon et al., 2004). In *C. albicans*, loss of *ICL1* function leads to reduced virulence and decreased survival within host macrophages (Lorenz and Fink, 2001). The crucial role of the glyoxylate pathway during pathogenesis, however, does not seem to be universal. In *Cryptococcus neoformans*, no defect in virulence or growth within macrophages was associated with the targeted deletion of the single *ICL* gene (Rude et al., 2002).

Given the importance of lipid catabolic pathways to numerous cellular processes, the possibility of a negative effect on the general fitness of *Magnaporthe* due to the mutations in *PEX6*, *PTH2*, *ECHA* and *FOX2* was always considered. This could imply that the observed pathogenicity defect is not specific to pathogenicity and could be due to secondary effects resulting from the impairment of fitness. Traits used to assess the overall fitness of the mutants include: vegetative growth on standard medium or in the presence of cell wall inhibiting chemicals and conidiation. Among the mutants characterized, *pth2Δ* and *fox2Δ* exhibited wild-type levels of conidiation and mycelial growth. On the other hand, the *pex6Δ* and *echAΔ* mutants did exhibit some defects in these nonpathogenesis-related traits. Both mutants had reduced

growth on glucose medium and exhibited reduced levels of conidiation. In *pex6Δ*, these vegetative phase defects may be a consequent of the inability to form functional peroxisomes. As peroxisomes are known to be important in many processes, in addition to fatty acid beta-oxidation, it is not surprising that pleiotropic effects are observed. In *echAΔ*, these vegetative phase defects may be due to impairment of the mitochondrial respiratory pathway or even to the inability to maintain functional mitochondrial structures. However, defects observed during vegetative growth may not necessarily be relevant to pathogenic development as these two life cycle phases may be relying on different metabolic pathways.

5.2   Establishment of mitochondrial beta-oxidation pathway in *M. grisea*

Mitochondrial fatty acid beta-oxidation machinery has been documented in many but not all organisms. Complete oxidation of fatty acids requires the presence of beta-oxidation systems within the peroxisomes and the mitochondria (Schulz, 1991). The peroxisomal beta-oxidation cycle acts as a chain-shortening step during fatty acid catabolism. Chain-shortened fatty acids and acetyl-CoA molecules are then routed to the mitochondrial pathway for complete oxidation. It has been recently demonstrated in *A. nidulans* (Maggio-Hall and Keller, 2004) that the mitochondrial beta-oxidation pathway is required for the utilization of short chain fatty acids. In the present study, through the mutational analysis of a mitochondrial beta-oxidation enzyme, *ECHA*, the presence of a mitochondrial beta-oxidation system was demonstrated in *M. grisea*. In *M. grisea*, mitochondrial beta-oxidation is required for metabolism of fatty acid and for the host penetration stage during pathogenesis. The *echAΔ* appressoria are unable to form penetration pegs but are completely melanized. This phenotypic defect suggests that the products and intermediates of mitochondrial beta-oxidation

contribute to the synthesis of pathogenicity-related metabolites other than melanin. In humans, mitochondrial beta-oxidation provides a major source of energy for respiration. It is possible that glycolysis can replenish acetyl-CoA products in mitochondria through pyruvate and rescue the energy deficiency. Supplementation with the easily utilizable energy source glucose, however, can only partially remediate the host penetration defect of *echA*Δ. Exogenous supply of high concentrations of glucose has been shown to be insufficient for full restoration of pathogenicity. Glucose supplementation of *C. lagenarium pex6*Δ mutant resulted in incomplete restoration of pathogenicity, up to only 20% host penetration (Kimura et al., 2001). This indicates that acetyl-CoA from glycolysis is not efficiently utilized to compensate for acetyl-CoA generated by lipid breakdown. Moreover, the glucose-induced penetration pegs in *echA*Δ do not develop into normal invasive infectious hyphae. For pathogenic development, mitochondrial beta-oxidation may be important in producing secondary metabolites essential for host penetration and may be a key metabolic pathway, which is required during *in planta* proliferation.

5.3 The contributions of lipid oxidation to pathogenesis

5.3.1 Lipid metabolism as an energy source

In germinating lettuce embryos, the acetyl-CoA generated from beta-oxidation of short-chain (hexanoate) and long-chain (palmitate) fatty acids is directed to the tricarboxylic acid cycle, and hence contributes mainly to energy production (Salon et al., 1988). Only 5% of the total level of acetyl-CoA metabolized through the tricarboxylic acid cycle is directed through the glyoxylate cycle. In human hepatoma G2 cells, a significant fraction of the acetyl-CoA from mitochondrial beta-oxidation is incorporated into intermediates of the tricarboxylic acid cycle (Wong et al., 2004). In

mammals, mitochondrial fatty acid oxidation represents the key mechanism by which energy is derived from metabolism of fatty acids (Coates and Tanaka, 1992). Thus, physiological defects associated with the loss of mitochondrial beta-oxidation, such as cardiac myopathy, are aggravated during periods of prolonged fasting (Kurtz et al., 1998).

5.3.2 Contribution of lipid metabolism to melanin biosynthesis

In *M. grisea*, melanin is composed of polymers of 1,3,6,8-tetrahydroxynapthalene, which is synthesized via the polyketide pathway. Malonyl-CoA, which is formed from the carboxylation of acetyl-CoA, serves as the starter unit in pentaketide synthesis (Fujii et al., 2000). Loss of appressorial melanin in the *pex6Δ*, indicated that acetyl-CoA derived from peroxisomal beta-oxidation comprises the major pool of precursors for melanin synthesis. A block in the transport of peroxisomal acetyl-CoA (*pth2Δ*) or a disruption of peroxisomal fatty acid beta-oxidation (*fox2Δ*) results only in the drastic reduction of the appressorial melanin layer. These results indicate that there may be other metabolic processes, which compensate for the loss of a peroxisome-derived acetyl-CoA pool or other mechanisms, which enable the export of peroxisomal metabolites. In addition to peroxisomal fatty acid oxidation, there are a number of other metabolic pathways, which generate acetyl-CoA within the cell. The enzyme ATP citrate lyase (ACL) produces cytosolic acetyl-CoA in a catalytic reaction involving citrate and coenzyme A (Fatland et al., 2002). In plants, ACL-derived acetyl-CoA has been shown to be carboxylated to malonyl-CoA and then utilized for the synthesis of metabolites, which are essential for development (Fatland et al., 2005). The fatty acid beta-oxidation pathway within the mitochondria also generates acetyl-CoA can be re-routed to the cytosol either directly or through TCA

intermediates such as citrate (Bartlett and Eaton, 2004). Studies on the Arabidopsis *acl* knock down line suggest that the generation and utlization of acetyl-CoA pools is strictly compartmentalized (Fatland et al., 2005). On the other hand, the expression of a heterologous acetyl-CoA hydrolase in the mitochondria has been shown to result in an increase in the overall levels of acetyl-CoA within the transgenic plants (Bender-Machado et al., 2005). This therefore indicates that a compensatory reaction operates during alterations in the concentration of acetyl-CoA pools and results in redirecting carbon fluxes within the cell.

5.3.3 Lipid metabolism for synthesis of cell wall precursors

Exogenous glucose could partially restore the formation of penetration pegs in the *pth2Δ* mutant suggests that peroxisomal acetyl-CoA is utilized in gluconeogenesis pathways. It is possible that the carbohydrate cell wall components of penetration pegs are produced through gluconeogenesis. Consequently, the *pth2Δ* and *pex6Δ* mutants exhibit enhanced sensitivity to cell wall destabilizing agents. In plants, the carbon flux from lipid catabolism has been shown to be important during cell wall morphogenesis. In the endosperm tissue of *Arabidopsis thaliana* seedlings, experiments with radioactive carbon demonstrate that the acetate moiety is not respired but is incorporated into sucrose through dicarboxylic acids generated via the glyoxylate cycle (Canvin and Beevers, 1961). In fungi and plants, the cytoplasmic pool of the nucleotide sugar uridinediphosphoglucose (UDP-glucose) is used as the precursor for the synthesis of cell wall polysaccharides (Seitz et al., 2000; Latge et al., 2005). The enzymes responsible for the interconversion of nucleotide sugars to commit them for cell wall synthesis are thought to interact metabolically with the glycolytic and gluconeogenic pathways (Seifert, 2004). In *A. thaliana*, a defect in

143

starch degradation results in altered composition of cell walls and upregulation of lipid mobilization and gluconeogenesis genes (Gomez et al., 2006).

5.3.4 Lipid metabolism for glycerol synthesis

The possible metabolic source of glycerol within the developing appressoria of *Magnaporthe* has been previously addressed (Thines et al., 2000). In this work, the activity of enzymes related to lipid catabolism was found to be elevated during appressorium maturation. In comparison, the activity of enzymes related to carbohydrate metabolism was found to be present at steady levels throughout the process. These results imply that lipid catabolic pathways may be more important for glycerol synthesis during appressorium development. The possible role of the loss of the different lipid catabolic gene functions investigated in this thesis to appressorial glycerol synthesis was considered. Enyzmatic quantitations from bulk appressorial extracts have estimated the internal glycerol concentration to be 3.2 M (De Jong et al., 1997). However, the most accepted method to indirectly assess glycerol concentrations within the appressoria is through the appressorium cytorrhysis (cellular collapse) assay (Howard et al., 1991a). This assay involved the incubation of mature appressoria in various concentrations of glycerol (1-5 M). Upon incubation of appressoria in an external glycerol concentration, which is higher than the internal concentration, appressoria collapse and are readily observed by light microscopy. Cellular collapse of 50% of the appressoria were observed in an external glycerol solution of 3.2 M which provides an estimate of 2-4 M of internal glycerol concentration (Dixon et al., 1999). An attempt to determine possible changes in the appressorial glycerol levels of the *Magnaporthe* mutants in this study was technically unsuccessful. An unexpectedly high percentage (~70%) of collapsed wild-type

144

appressoria was observed even at relatively low external glycerol concentrations (~2 M). For future work, assessment of internal appressorial glycerol content may be carried out through more sensitive quantitation methods such as high performance liquid chromatography (HPLC) or mass spectrophotometry (MS), which would require much lower amounts of appressorial extracts.

5.3.5 Lipid metabolism for organellar homeostasis

The critical metabolic functions of an organelle may exert a role in the maintenance of its morphology, size and abundance. The mechanism by which this regulation is achieved, however, is still uncertain. The loss of the multifunctional fatty acid beta-oxidation enzyme MFE2 in the yeast *Yarrowia lipolytica* results in the formation of predominantly larger peroxisomes (Smith et al., 2000). This aberrant peroxisome size is attributed to the increased production of other beta-oxidation enzymes, such as thiolase. On the other hand, in *S. cerevisiae*, the specific inhibition of medium chain fatty acid oxidation either through the loss of a catalytic enzyme function or the impairment of substrate provision induces the formation of only a few giant peroxisomes (van Roermund et al., 2000). It was then thought that metabolites derived from the oxidation of medium chain fatty acids act as signaling molecules, which regulate peroxisome proliferation. In humans, larger peroxisomes with a five-fold reduction in abundance are also associated with a general deficiency in peroxisomal beta-oxidation machinery (Chang et al., 1999). In plants, the biogenesis of glyoxysomes, which are specialized peroxisomes, is thought to be regulated at least partially by the transcriptional and posttranscriptional regulation of the glyoxysomal enzymes isocitrate lyase and malate synthase (Comai et al., 1989).

Loss or inhibition of mitochondrial beta-oxidation also results in aberrations in mitochondrial morphology. In *Drosophila*, deletion of *Scully*, which encodes the third enzyme of the beta-oxidation pathway, results in the formation of fewer and smaller mitochondria with reduced and swollen cristae (Torroja et al., 1998). Human and rat liver slices which had been treated with inhibitors of mitochondrial beta-oxidation exhibit aberrations in mitochondrial ultrastructure characterized by enlarged, C- or O-shaped mitochondria with crystalline and granular inclusions (Vickers et al., 2006). Quite interestingly, the mitochondria of the *echA*Δ mutant consists of spherical and short tubular structures which are in marked contrast to the reticulate network of the mitochondria in the wild-type strain. In addition, *echA*Δ grows much slower than wild type on normal medium, which may be indicative of a respiratory defect. These phenotypic defects are reminiscent of yeast petite mutants, which are incapable of growth on nonfermentable carbon sources and exhibit morphological aberrations in their mitochondrial membranes (Heslot et al., 1970).

5.4 Lipotoxicity as a possible consequence of the disruption of the beta-oxidation pathway

It is possible that some of the phenotypic defects observed in the beta-oxidation mutants, result from the accumulation of long chain fatty acids or toxic metabolic intermediates. In human pathologies associated with increased risk to Type2 diabetes, mitochondrial beta-oxidation of fatty acids is diminished and results in excessive release of fatty acids from adipocytes (Maassen et al., 2006). Accumulation of branched long-chain and very long chain fatty acids was recorded in patients showing a deficiency in the peroxisomal multifunctional protein 2 (Huyghe et al., 2006a). However, it is important to note that given the range of metabolic capacity amongst

different fungi, the inhibitory effect of fatty acids on fungal growth has been shown to vary depending on the fatty acid chain length and the fungal species. Acetic acid has been shown to be toxic to the mycorrhizal fungus *Boletus* (at 1-2 nm) and to the litter fungus *Marasmius* (at 8 mM) (Lindeberg and Lindeberg, 1974). *Aspergillus nidulans*, however, grows well on 50 mM acetate as sole carbon source (Hynes et al., 2006). In my study, I found that *Magnaporthe* grew poorly on either 50 mM or 5 mM sodium acetate as sole carbon source. As acetate proved not to be an optimal carbon source for *Magnaporthe*, further consideration of acetate metabolism in the beta-oxidation mutants was not included. Medium chain fatty acids (C6, C8, C10 and C12) are fungitoxic to the blue mold cheese fungus *Penicillum crustosum* (Hatton and Kinderlerer, 1991). Endogenous respiration of *Boletus* species is inhibited by C2-C12 fatty acids with the inhibitory effect increasing in proportion to chain length (Pedersen, 1970). *A. nidulans*, however, grows well on medium containing either C4 (10 mM), C5 (10 mM) and C6 (5 mM) as sole carbon source (Hynes et al., 2006). I have observed that fatty acids C6, C8 and C10, even at 5 mM concentrations, were very toxic to *Magnaporthe*. *Magnaporthe* also failed to grow on media containing a combination of either of these fatty acids and either glucose or lactose. However on growth medium containing C12-fatty acids, *Magnaporthe* was able to grow although the colony morphology appeared to be restricted and unusually fluffy. It is possible that the block in the beta-oxidation pathway leads to the accumulation of such toxic fatty acids in the *echAΔ* and *fox2Δ* in *Magnaporthe.* The accumulation of these toxic metabolites may contribute to some of the observed phenotypic defects such as the compromised vegetative growth of *echAΔ*. However, the abnormal appressorium morphogenesis defect observed in both *echAΔ* and *fox2Δ* was rescued by exogenous glucose. This would suggest that this particular phenotypic defect is most likely

associated with the inability of the mutant to metabolize lipids for energy source. For future work, it would be interesting if a metabolic profiling of different lipid catabolic mutants created in this study would be undertaken to address the possible role of toxic metabolite accumulation in fungal development as well as to identify novel metabolites important for pathogenicity.

REFERENCES

Adachi, K., and Hamer, J.E. (1998). Divergent cAMP signaling pathways regulate growth and pathogenesis in the rice blast fungus Magnaporthe grisea. Plant Cell 10, 1361-1374.

Adamski, J., Husen, B., Marks, F., and Jungblut, P.W. (1992). Purification and properties of oestradiol 17 beta-dehydrogenase extracted from cytoplasmic vesicles of porcine endometrial cells. Biochem J 288 (Pt 2), 375-381.

Altschul, S.F., Madden, T.L., Schaffer, A.A., Zhang, J., Zhang, Z., Miller, W., and Lipman, D.J. (1997). Gapped BLAST and PSI-BLAST: a new generation of protein database search programs. Nucleic Acids Res 25, 3389-3402.

Amchenkova, A.A., Bakeeva, L.E., Chentsov, Y.S., Skulachev, V.P., and Zorov, D.B. (1988). Coupling membranes as energy-transmitting cables. I. Filamentous mitochondria in fibroblasts and mitochondrial clusters in cardiomyocytes. J Cell Biol 107, 481-495.

Antonenkov, V.D., Van Veldhoven, P.P., Waelkens, E., and Mannaerts, G.P. (1997). Substrate specificities of 3-oxoacyl-CoA thiolase A and sterol carrier protein 2/3-oxoacyl-CoA thiolase purified from normal rat liver peroxisomes. Sterol carrier protein 2/3-oxoacyl-CoA thiolase is involved in the metabolism of 2-methyl-branched fatty acids and bile acid intermediates. J Biol Chem 272, 26023-26031.

Arakawa, H., Takiguchi, M., Amaya, Y., Nagata, S., Hayashi, H., and Mori, M. (1987). cDNA-derived amino acid sequence of rat mitochondrial 3-oxoacyl-CoA thiolase with no transient presequence: structural relationship with peroxisomal isozyme. Embo J 6, 1361-1366.

Avila-Adame, C., and Koller, W. (2003). Characterization of spontaneous mutants of Magnaporthe grisea expressing stable resistance to the Qo-inhibiting fungicide azoxystrobin. Curr Genet 42, 332-338.

Baker, A., Graham, I.A., Holdsworth, M., Smith, S.M., and Theodoulou, F.L. (2006). Chewing the fat: beta-oxidation in signalling and development. Trends Plant Sci 11, 124-132.

Balhadere, P.V., Foster, A.J., and Talbot, N.J. (1999). Identification of pathogenicity mutants of the rice blast fungus *Magnaporthe grisea* by insertional mutagenesis. Molecular Plant -Microbe Interactions 12, 129-142.

Bartlett, K., and Eaton, S. (2004). Mitochondrial beta-oxidation. Eur J Biochem 271, 462-469.

Beilby, J.P., and Kidby, D.K. (1980). Biochemistry of ungerminated and germinated spores of the vesicular-arbuscular mycorrhizal fungus, Glomus caledonius: changes in neutral and polar lipids. J Lipid Res 21, 739-750.

Bell, A.A., and Wheeler, M.H. (1986). Biosynthesis and functions of fungal melanins. Annual Review of Phytopathology 24, 411-451.

Bell, A.F., Feng, Y., Hofstein, H.A., Parikh, S., Wu, J., Rudolph, M.J., Kisker, C., Whitty, A., and Tonge, P.J. (2002). Stereoselectivity of enoyl-CoA hydratase results from preferential activation of one of two bound substrate conformers. Chem Biol 9, 1247-1255.

Bender-Machado, L., Bäuerlein, M., Carrari, F., Schauer, N., Lytovchenko, A., Gibon, Y., Kelly, A., Loureiro, M., Müller-Röber, B., Willmitzer, L., and Fernie, A. (2005). Expression of a yeast acetyl CoA hydrolase in the mitochondrion. Plant Molecular Biology 55, 645-662.

Birschmann, I., Rosenkranz, K., Erdmann, R., and Kunau, W.H. (2005). Structural and functional analysis of the interaction of the AAA-peroxins Pex1p and Pex6p. Febs J 272, 47-58.

Birschmann, I., Stroobants, A.K., van den Berg, M., Schafer, A., Rosenkranz, K., Kunau, W.H., and Tabak, H.F. (2003). Pex15p of Saccharomyces cerevisiae provides a molecular basis for recruitment of the AAA peroxin Pex6p to peroxisomal membranes. Mol Biol Cell 14, 2226-2236.

Bode, K., Hooks, M.A., and Couee, I.I. (1999). Identification, separation, and characterization of acyl-coenzyme A dehydrogenases involved in mitochondrial beta-oxidation in higher plants. Plant Physiol 119, 1305-1314.

Bohnert, H.U., Fudal, I., Dioh, W., Tharreau, D., Notteghem, J.L., and Lebrun, M.H. (2004). A putative polyketide synthase/peptide synthetase from Magnaporthe grisea signals pathogen attack to resistant rice. Plant Cell 16, 2499-2513.

Boisnard, S., Zickler, D., Picard, M., and Berteaux-Lecellier, V. (2003). Overexpression of a human and a fungal ABC transporter similarly suppresses the differentiation defects of a fungal peroxisomal mutant but introduces pleiotropic cellular effects. Mol Microbiol 49, 1287-1296.

Both, M., Csukai, M., Stumpf, M.P., and Spanu, P.D. (2005). Gene expression profiles of Blumeria graminis indicate dynamic changes to primary metabolism during development of an obligate biotrophic pathogen. Plant Cell 17, 2107-2122.

Bruno, K.S., Tenjo, F., Li, L., Hamer, J.E., and Xu, J.R. (2004). Cellular localization and role of kinase activity of PMK1 in Magnaporthe grisea. Eukaryot Cell 3, 1525-1532.

Canvin, D.T., and Beevers, H. (1961). Sucrose synthesis from acetate in the germinating castor bean: kinetics and pathway. J Biol Chem 236, 988-995.

Chang, C.C., South, S., Warren, D., Jones, J., Moser, A.B., Moser, H.W., and Gould, S.J. (1999). Metabolic control of peroxisome abundance. J Cell Sci 112 (Pt 10), 1579-1590.

Choi, W., and Dean, R.A. (1997). The adenylate cyclase gene MAC1 of Magnaporthe grisea controls appressorium formation and other aspects of growth and development. Plant Cell 9, 1973-1983.

Chumley, F.G., and Valent, B. (1990). Genetic analysis of melanin-deficient, nonpathogenic mutans of *Magnaporthe grisea.* Molecular Plant -Microbe Interactions 3, 135-143.

Clergeot, P.H., Gourgues, M., Cots, J., Laurans, F., Latorse, M.P., Pepin, R., Tharreau, D., Notteghem, J.L., and Lebrun, M.H. (2001). PLS1, a gene encoding a tetraspanin-like protein, is required for penetration of rice leaf by the fungal pathogen Magnaporthe grisea. Proc Natl Acad Sci U S A 98, 6963-6968.

Coates, P.M., and Tanaka, K. (1992). Molecular basis of mitochondrial fatty acid oxidation defects. J Lipid Res 33, 1099-1110.

Cochrane, V.W., Cochrane, J.C., Collins, C.B., and Serafin, F.G. (1963). Spore germination and carbon metabolism in Fusarium solani. II. Endogenous respiration in relation to germination. American Journal of Botany 50, 806-814.

Collins, C.S., Kalish, J.E., Morrell, J.C., McCaffery, J.M., and Gould, S.J. (2000). The peroxisome biogenesis factors pex4p, pex22p, pex1p, and pex6p act in the terminal steps of peroxisomal matrix protein import. Mol Cell Biol 20, 7516-7526.

Comai, L., Dietrich, R.A., Maslyar, D.J., Baden, C.S., and Harada, J.J. (1989). Coordinate expression of transcriptionally regulated isocitrate lyase and malate synthase genes in Brassica napus L. Plant Cell 1, 293-300.

Cooper, T.G., and Beevers, H. (1969). Beta oxidation in glyoxysomes from castor bean endosperm. J Biol Chem 244, 3514-3520.

De Jong, J.C., McCormack, B.J., Smirnoff, N., and Talbot, N.J. (1997). Glycerol generates turgor in rice blast. Nature 389, 244-245.

De Lucas, J.R., Dominguez, A.I., Valenciano, S., Turner, G., and Laborda, F. (1999). The acuH gene of Aspergillus nidulans, required for growth on acetate and long-chain fatty acids, encodes a putative homologue of the mammalian carnitine/acylcarnitine carrier. Arch Microbiol 171, 386-396.

De Vos, K., Goossens, V., Boone, E., Vercammen, D., Vancompernolle, K., Vandenabeele, P., Haegeman, G., Fiers, W., and Grooten, J. (1998). The 55-kDa tumor necrosis factor receptor induces clustering of mitochondria through its membrane-proximal region. J Biol Chem 273, 9673-9680.

Dean, R.A., Talbot, N.J., Ebbole, D.J., Farman, M.L., Mitchell, T.K., Orbach, M.J., Thon, M., Kulkarni, R., Xu, J.R., Pan, H., Read, N.D., Lee, Y.H., Carbone, I., Brown, D., Oh, Y.Y., Donofrio, N., Jeong, J.S., Soanes, D.M., Djonovic, S., Kolomiets, E., Rehmeyer, C., Li, W., Harding, M., Kim, S., Lebrun, M.H., Bohnert, H., Coughlan, S., Butler, J., Calvo, S., Ma, L.J., Nicol, R., Purcell, S., Nusbaum, C., Galagan, J.E.,

and Birren, B.W. (2005). The genome sequence of the rice blast fungus Magnaporthe grisea. Nature 434, 980-986.

Dieuaide-Noubhani, M., Novikov, D., Baumgart, E., Vanhooren, J.C., Fransen, M., Goethals, M., Vandekerckhove, J., Van Veldhoven, P.P., and Mannaerts, G.P. (1996). Further characterization of the peroxisomal 3-hydroxyacyl-CoA dehydrogenases from rat liver. Relationship between the different dehydrogenases and evidence that fatty acids and the C27 bile acids di- and tri-hydroxycoprostanic acids are metabolized by separate multifunctional proteins. Eur J Biochem 240, 660-666.

Dixon, K.P., Xu, J.R., Smirnoff, N., and Talbot, N.J. (1999). Independent signaling pathways regulate cellular turgor during hyperosmotic stress and appressorium-mediated plant infection by Magnaporthe grisea. Plant Cell 11, 2045-2058.

Dyall, S.D., Brown, M.T., and Johnson, P.J. (2004). Ancient invasions: from endosymbionts to organelles. Science 304, 253-257.

Eastmond, P.J., and Graham, I.A. (2001). Re-examining the role of the glyoxylate cycle in oilseeds. Trends Plant Sci 6, 72-78.

Eastmond, P.J., Germain, V., Lange, P.R., Bryce, J.H., Smith, S.M., and Graham, I.A. (2000). Postgerminative growth and lipid catabolism in oilseeds lacking the glyoxylate cycle. Proc Natl Acad Sci U S A 97, 5669-5674.

Ebbole, D.J., Jin, Y., Thon, M., Pan, H., Bhattarai, E., Thomas, T., and Dean, R. (2004). Gene discovery and gene expression in the rice blast fungus, Magnaporthe grisea: analysis of expressed sequence tags. Mol Plant Microbe Interact 17, 1337-1347.

Elgersma, Y., van Roermund, C.W., Wanders, R.J., and Tabak, H.F. (1995). Peroxisomal and mitochondrial carnitine acetyltransferases of Saccharomyces cerevisiae are encoded by a single gene. Embo J 14, 3472-3479.

Elgersma, Y., Elgersma-Hooisma, M., Wenzel, T., McCaffery, J.M., Farquhar, M.G., and Subramani, S. (1998). A mobile PTS2 receptor for peroxisomal protein import in Pichia pastoris. J Cell Biol 140, 807-820.

Elgersma, Y., Kwast, L., van den Berg, M., Snyder, W.B., Distel, B., Subramani, S., and Tabak, H.F. (1997). Overexpression of Pex15p, a phosphorylated peroxisomal integral membrane protein required for peroxisome assembly in S.cerevisiae, causes proliferation of the endoplasmic reticulum membrane. Embo J 16, 7326-7341.

Elliott, C.E., and Howlett, B.J. (2006). Overexpression of a 3-ketoacyl-coathiolase in Leptosphaeria maculans causes reduced pathogenicity on Brassica napus. Mol Plant Microbe Interact 19, 588-596.

Emanuelsson, O., Nielsen, H., Brunak, S., and von Heijne, G. (2000). Predicting subcellular localization of proteins based on their N-terminal amino acid sequence. Journal of Molecular Biology 300, 1005-1016.

Engel, C.K., Kiema, T.R., Hiltunen, J.K., and Wierenga, R.K. (1998). The crystal structure of enoyl-CoA hydratase complexed with octanoyl-CoA reveals the structural adaptations required for binding of a long chain fatty acid-CoA molecule. J Mol Biol 275, 847-859.

Ergle, D.R. (1948). The carbohydrate metabolism of germinating Phymatotrichum sclerotia with special reference to glycogen. Phytopathology 38, 142-151.

Faber, K.N., Heyman, J.A., and Subramani, S. (1998). Two AAA family peroxins, PpPex1p and PpPex6p, interact with each other in an ATP-dependent manner and are associated with different subcellular membranous structures distinct from peroxisomes. Mol Cell Biol 18, 936-943.

Fatland, B.L., Nikolau, B.J., and Wurtele, E.S. (2005). Reverse genetic characterization of cytosolic acetyl-CoA generation by ATP-citrate lyase in Arabidopsis. Plant Cell 17, 182-203.

Fatland, B.L., Ke, J., Anderson, M.D., Mentzen, W.I., Cui, L.W., Allred, C.C., Johnston, J.L., Nikolau, B.J., and Wurtele, E.S. (2002). Molecular characterization of a heteromeric ATP-citrate lyase that generates cytosolic acetyl-coenzyme A in Arabidopsis. Plant Physiol 130, 740-756.

Feron, G., Blin-Perrin, C., Krasniewski, I., Mauvais, G., and Lherminier, J. (2005). Metabolism of fatty acid in yeast: characterisation of beta-oxidation and ultrastructural changes in the genus Sporidiobolus sp. cultivated on ricinoleic acid methyl ester. FEMS Microbiol Lett 250, 63-69.

Filppula, S.A., Sormunen, R.T., Hartig, A., Kunau, W.H., and Hiltunen, J.K. (1995). Changing stereochemistry for a metabolic pathway in vivo. Experiments with the peroxisomal beta-oxidation in yeast. J Biol Chem 270, 27453-27457.

Flynn, C.R., Mullen, R.T., and Trelease, R.N. (1998). Mutational analyses of a type 2 peroxisomal targeting signal that is capable of directing oligomeric protein import into tobacco BY-2 glyoxysomes. Plant J 16, 709-720.

Fong, J.C., and Schulz, H. (1977). Purification and properties of pig heart crotonase and the presence of short chain and long chain enoyl coenzyme A hydratases in pig and guinea pig tissues. J Biol Chem 252, 542-547.

Foster, A.J., Jenkinson, J.M., and Talbot, N.J. (2003). Trehalose synthesis and metabolism are required at different stages of plant infection by Magnaporthe grisea. Embo J 22, 225-235.

Fujii, I., Mori, Y., Watanabe, A., Kubo, Y., Tsuji, G., and Ebizuka, Y. (2000). Enzymatic synthesis of 1,3,6,8-tetrahydroxynaphthalene solely from malonyl coenzyme A by a fungal iterative type I polyketide synthase PKS1. Biochemistry 39, 8853-8858.

Furuta, S., Miyazawa, S., Osumi, T., Hashimoto, T., and Ui, N. (1980). Properties of mitochondria and peroxisomal enoyl-CoA hydratases from rat liver. J Biochem (Tokyo) 88, 1059-1070.

Gomez, L.D., Baud, S., Gilday, A., Li, Y., and Graham, I.A. (2006). Delayed embryo development in the ARABIDOPSIS TREHALOSE-6-PHOSPHATE SYNTHASE 1 mutant is associated with altered cell wall structure, decreased cell division and starch accumulation. Plant J 46, 69-84.

Gould, S.J., and Valle, D. (2000). Peroxisome biogenesis disorders: genetics and cell biology. Trends Genet 16, 340-345.

Gould, S.J., Keller, G.A., Hosken, N., Wilkinson, J., and Subramani, S. (1989). A conserved tripeptide sorts proteins to peroxisomes. J Cell Biol 108, 1657-1664.

Gray, M.W. (1989). The evolutionary origins of organelles. Trends Genet 5, 294-299.

Gray, M.W., Burger, G., and Lang, B.F. (1999). Mitochondrial evolution. Science 283, 1476-1481.

Hamer, J.E., and Talbot, N.J. (1998). Infection-related development in the rice blast fungus Magnaporthe grisea. Curr Opin Microbiol 1, 693-697.

Hashiguchi, N., Kojidani, T., Imanaka, T., Haraguchi, T., Hiraoka, Y., Baumgart, E., Yokota, S., Tsukamoto, T., and Osumi, T. (2002). Peroxisomes are formed from complex membrane structures in PEX6-deficient CHO cells upon genetic complementation. Mol Biol Cell 13, 711-722.

Hashimoto, T. (2000). Peroxisomal beta-oxidation enzymes. Cell Biochem Biophys 32 Spring, 63-72.

Hatton, P., and Kinderlerer, J. (1991). Toxicity of medium chain fatty acids to Penicillium crustosum Thom and their detoxification to methyl ketones. Journal of applied bacteriology 70, 401-407.

Hayashi, M., Toriyama, K., Kondo, M., Kato, A., Mano, S., De Bellis, L., Hayashi-Ishimaru, Y., Yamaguchi, K., Hayashi, H., and Nishimura, M. (2000). Functional transformation of plant peroxisomes. Cell Biochem Biophys 32 Spring, 295-304.

Heslot, H., Goffeau, A., and Louis, C. (1970). Respiratory metabolism of a "petite negative"yeast Schizosaccharomyces pombe 972h. J Bacteriol 104, 473-481.

Hettema, E.H., and Tabak, H.F. (2000). Transport of fatty acids and metabolites across the peroxisomal membrane. Biochim Biophys Acta 1486, 18-27.

Hettema, E.H., Girzalsky, W., van Den Berg, M., Erdmann, R., and Distel, B. (2000). Saccharomyces cerevisiae pex3p and pex19p are required for proper localization and stability of peroxisomal membrane proteins. Embo J 19, 223-233.

Hettema, E.H., van Roermund, C.W., Distel, B., van den Berg, M., Vilela, C., Rodrigues-Pousada, C., Wanders, R.J., and Tabak, H.F. (1996). The ABC transporter proteins Pat1 and Pat2 are required for import of long-chain fatty acids into peroxisomes of Saccharomyces cerevisiae. Embo J 15, 3813-3822.

Hijikata, M., Wen, J.K., Osumi, T., and Hashimoto, T. (1990). Rat peroxisomal 3-ketoacyl-CoA thiolase gene. Occurrence of two closely related but differentially regulated genes. J Biol Chem 265, 4600-4606.

Hiltunen, J.K., and Qin, Y. (2000). beta-oxidation - strategies for the metabolism of a wide variety of acyl-CoA esters. Biochim Biophys Acta 1484, 117-128.

Hiltunen, J.K., Palosaari, P.M., and Kunau, W.H. (1989). Epimerization of 3-hydroxyacyl-CoA esters in rat liver. Involvement of two 2-enoyl-CoA hydratases. J Biol Chem 264, 13536-13540.

Hiltunen, J.K., Wenzel, B., Beyer, A., Erdmann, R., Fossa, A., and Kunau, W.H. (1992). Peroxisomal multifunctional beta-oxidation protein of Saccharomyces cerevisiae. Molecular analysis of the fox2 gene and gene product. J Biol Chem 267, 6646-6653.

Hiltunen, J.K., Mursula, A.M., Rottensteiner, H., Wierenga, R.K., Kastaniotis, A.J., and Gurvitz, A. (2003). The biochemistry of peroxisomal beta-oxidation in the yeast Saccharomyces cerevisiae. FEMS Microbiol Rev 27, 35-64.

Hoepfner, D., van den Berg, M., Philippsen, P., Tabak, H.F., and Hettema, E.H. (2001). A role for Vps1p, actin, and the Myo2p motor in peroxisome abundance and inheritance in Saccharomyces cerevisiae. J Cell Biol 155, 979-990.

Hoepfner, D., Schildknegt, D., Braakman, I., Philippsen, P., and Tabak, H.F. (2005). Contribution of the endoplasmic reticulum to peroxisome formation. Cell 122, 85-95.

Holroyd, C., and Erdmann, R. (2001). Protein translocation machineries of peroxisomes. FEBS Lett 501, 6-10.

Hooks, M.A. (2002). Molecular Biology, enzymology, and the physiology of B-oxidation. In Plant Peroxisomes, A. Baker and I.A. Graham, eds (London: Kluwer Academic Publishers), pp. 19-55.

Howard, R.J., and Ferrari, M.A. (1989). Role of melanin in appressorium function. Experimental Mycology 13, 403-418.

Howard, R.J., Bourett, T.M., and Ferrari, M.A. (1991a). Infection by Magnaporthe grisea: an in vitro analysis. In Electron microscopy of plant pathogens., K. Mendgen and D.E. Lesemann, eds (Berlin, Germany: Springer-Verlag), pp. 251–264.

Howard, R.J., Ferrari, M.A., Roach, D.H., and Money, N.P. (1991b). Penetration of hard substrates by a fungus employing enormous turgor pressures. Proc Natl Acad Sci U S A 88, 11281-11284.

Hu, J., Aguirre, M., Peto, C., Alonso, J., Ecker, J., and Chory, J. (2002). A role for peroxisomes in photomorphogenesis and development of Arabidopsis. Science 297, 405-409.

Hutchinson, C.R., and Fujii, I. (1995). Polyketide synthase gene manipulation: a structure-function approach in engineering novel antibiotics. Annu Rev Microbiol 49, 201-238.

Huyghe, S., Mannaerts, G.P., Baes, M., and Van Veldhoven, P.P. (2006a). Peroxisomal multifunctional protein-2: the enzyme, the patients and the knockout mouse model. Biochim Biophys Acta 1761, 973-994.

Huyghe, S., Schmalbruch, H., Hulshagen, L., Veldhoven, P.V., Baes, M., and Hartmann, D. (2006b). Peroxisomal multifunctional protein-2 deficiency causes motor deficits and glial lesions in the adult central nervous system. Am J Pathol 168, 1321-1334.

Hynes, M.J., Murray, S.L., Duncan, A., Khew, G.S., and Davis, M.A. (2006). Regulatory genes controlling fatty acid catabolism and peroxisomal functions in the filamentous fungus Aspergillus nidulans. Eukaryot Cell 5, 794-805.

Ichas, F., Jouaville, L.S., and Mazat, J.P. (1997). Mitochondria are excitable organelles capable of generating and conveying electrical and calcium signals. Cell 89, 1145-1153.

Idell-Wenger, J.A. (1981). Carnitine:acylcarnitine translocase of rat heart mitochondria. Competition for carnitine uptake by carnitine esters. J Biol Chem 256, 5597-5603.

Idnurm, A., and Howlett, B.J. (2002). Isocitrate lyase is essential for pathogenicity of the fungus Leptosphaeria maculans to canola (Brassica napus). Eukaryot Cell 1, 719-724.

Ikeda, Y., Okamura-Ikeda, K., and Tanaka, K. (1985). Purification and characterization of short-chain, medium-chain, and long-chain acyl-CoA dehydrogenases from rat liver mitochondria. Isolation of the holo- and apoenzymes and conversion of the apoenzyme to the holoenzyme. J Biol Chem 260, 1311-1325.

Ishii, N., Hijikata, M., Osumi, T., and Hashimoto, T. (1987). Structural organization of the gene for rat enoyl-CoA hydratase:3-hydroxyacyl-CoA dehydrogenase bifunctional enzyme. J Biol Chem 262, 8144-8150.

Izai, K., Uchida, Y., Orii, T., Yamamoto, S., and Hashimoto, T. (1992). Novel fatty acid beta-oxidation enzymes in rat liver mitochondria. I. Purification and properties of very-long-chain acyl-coenzyme A dehydrogenase. J Biol Chem 267, 1027-1033.

Jacobs, A.K., Lipka, V., Burton, R.A., Panstruga, R., Strizhov, N., Schulze-Lefert, P., and Fincher, G.B. (2003). An Arabidopsis Callose Synthase, GSL5, Is Required for Wound and Papillary Callose Formation. Plant Cell 15, 2503-2513.

Jedd, G., and Chua, N.H. (2000). A new self-assembled peroxisomal vesicle required for efficient resealing of the plasma membrane. Nat Cell Biol 2, 226-231.

Jiang, L.L., Kobayashi, A., Matsuura, H., Fukushima, H., and Hashimoto, T. (1996). Purification and properties of human D-3-hydroxyacyl-CoA dehydratase: medium-chain enoyl-CoA hydratase is D-3-hydroxyacyl-CoA dehydratase. J Biochem (Tokyo) 120, 624-632.

Jiang, L.L., Kurosawa, T., Sato, M., Suzuki, Y., and Hashimoto, T. (1997). Physiological role of D-3-hydroxyacyl-CoA dehydratase/D-3-hydroxyacyl-CoA dehydrogenase bifunctional protein. J Biochem (Tokyo) 121, 506-513.

Jogl, G., and Tong, L. (2003). Crystal structure of carnitine acetyltransferase and implications for the catalytic mechanism and fatty acid transport. Cell 112, 113-122.

Johnson, D.R., Knoll, L.J., Levin, D.E., and Gordon, J.I. (1994). Saccharomyces cerevisiae contains four fatty acid activation (FAA) genes: an assessment of their role in regulating protein N-myristoylation and cellular lipid metabolism. J Cell Biol 127, 751-762.

Johnson, T.L., and Olsen, L.J. (2003). Import of the peroxisomal targeting signal type 2 protein 3-ketoacyl-coenzyme a thiolase into glyoxysomes. Plant Physiol 133, 1991-1999.

Kamijo, T., Aoyama, T., Miyazaki, J., and Hashimoto, T. (1993). Molecular cloning of the cDNAs for the subunits of rat mitochondrial fatty acid beta-oxidation multienzyme complex. Structural and functional relationships to other mitochondrial and peroxisomal beta-oxidation enzymes. J Biol Chem 268, 26452-26460.

Kanazawa, M., Ohtake, A., Abe, H., Yamamoto, S., Satoh, Y., Takayanagi, M., Niimi, H., Mori, M., and Hashimoto, T. (1993). Molecular cloning and sequence analysis of the cDNA for human mitochondrial short-chain enoyl-CoA hydratase. Enzyme Protein 47, 9-13.

Karpichev, I.V., and Small, G.M. (1998). Global regulatory functions of Oaf1p and Pip2p (Oaf2p), transcription factors that regulate genes encoding peroxisomal proteins in Saccharomyces cerevisiae. Mol Cell Biol 18, 6560-6570.

Kastaniotis, A.J., Autio, K.J., Sormunen, R.T., and Hiltunen, J.K. (2004). Htd2p/Yhr067p is a yeast 3-hydroxyacyl-ACP dehydratase essential for mitochondrial function and morphology. Mol Microbiol 53, 1407-1421.

Keller, G.A., Krisans, S., Gould, S.J., Sommer, J.M., Wang, C.C., Schliebs, W., Kunau, W., Brody, S., and Subramani, S. (1991). Evolutionary conservation of a microbody targeting signal that targets proteins to peroxisomes, glyoxysomes, and glycosomes. J Cell Biol 114, 893-904.

Kerner, J., and Hoppel, C. (2000). Fatty acid import into mitochondria. Biochim Biophys Acta 1486, 1-17.

Kiel, J.A., Hilbrands, R.E., van der Klei, I.J., Rasmussen, S.W., Salomons, F.A., van der Heide, M., Faber, K.N., Cregg, J.M., and Veenhuis, M. (1999). Hansenula polymorpha Pex1p and Pex6p are peroxisome-associated AAA proteins that functionally and physically interact. Yeast 15, 1059-1078.

Kiema, T.R., Engel, C.K., Schmitz, W., Filppula, S.A., Wierenga, R.K., and Hiltunen, J.K. (1999). Mutagenic and enzymological studies of the hydratase and isomerase activities of 2-enoyl-CoA hydratase-1. Biochemistry 38, 2991-2999.

Kimura, A., Takano, Y., Furusawa, I., and Okuno, T. (2001). Peroxisomal metabolic function is required for appressorium-mediated plant infection by Colletotrichum lagenarium. Plant Cell 13, 1945-1957.

Kionka, C., and Kunau, W.H. (1985). Inducible beta-oxidation pathway in Neurospora crassa. J Bacteriol 161, 153-157.

Kispal, G., Cseko, J., Alkonyi, I., and Sandor, A. (1991). Isolation and characterization of carnitine acetyltransferase from S. cerevisiae. Biochim Biophys Acta 1085, 217-222.

Kispal, G., Sumegi, B., Dietmeier, K., Bock, I., Gajdos, G., Tomcsanyi, T., and Sandor, A. (1993). Cloning and sequencing of a cDNA encoding Saccharomyces cerevisiae carnitine acetyltransferase. Use of the cDNA in gene disruption studies. J Biol Chem 268, 1824-1829.

Klein, A.T., Barnett, P., Bottger, G., Konings, D., Tabak, H.F., and Distel, B. (2001). Recognition of peroxisomal targeting signal type 1 by the import receptor Pex5p. J Biol Chem 276, 15034-15041.

Klose, J., and Kronstad, J.W. (2006). The Multifunctional {beta}-oxidation Enzyme Is Required for Full Symptom Development by the Biotrophic Maize Pathogen Ustilago maydis. Eukaryot Cell.

Koller, A., Spong, A.P., Luers, G.H., and Subramani, S. (1999). Analysis of the peroxisomal acyl-CoA oxidase gene product from Pichia pastoris and determination of its targeting signal. Yeast 15, 1035-1044.

Kornberg, H.L., and Krebs, H.A. (1957). Synthesis of cell constituents from C2-units by a modified tricarboxylic acid cycle. Nature 179, 988-991.

Kragler, F., Lametschwandtner, G., Christmann, J., Hartig, A., and Harada, J.J. (1998). Identification and analysis of the plant peroxisomal targeting signal 1 receptor NtPEX5. Proc Natl Acad Sci U S A 95, 13336-13341.

Kunau, W.H., Dommes, V., and Schulz, H. (1995). beta-oxidation of fatty acids in mitochondria, peroxisomes, and bacteria: a century of continued progress. Prog Lipid Res 34, 267-342.

Kunau, W.H., Buhne, S., de la Garza, M., Kionka, C., Mateblowski, M., Schultz-Borchard, U., and Thieringer, R. (1988). Comparative enzymology of beta-oxidation. Biochem Soc Trans 16, 418-420.

Kurtz, D.M., Rinaldo, P., Rhead, W.J., Tian, L., Millington, D.S., Vockley, J., Hamm, D.A., Brix, A.E., Lindsey, J.R., Pinkert, C.A., O'Brien, W.E., and Wood, P.A. (1998). Targeted disruption of mouse long-chain acyl-CoA dehydrogenase gene reveals crucial roles for fatty acid oxidation. Proc Natl Acad Sci U S A 95, 15592-15597.

Lang, B.F., Seif, E., Gray, M.W., O'Kelly, C.J., and Burger, G. (1999). A comparative genomics approach to the evolution of eukaryotes and their mitochondria. J Eukaryot Microbiol 46, 320-326.

Langfelder, K., Streibel, M., Jahn, B., Haase, G., and Brakhage, A.A. (2003). Biosynthesis of fungal melanins and their importance for human pathogenic fungi. Fungal Genet Biol 38, 143-158.

Latge, J.P., Mouyna, I., Tekaia, F., Beauvais, A., Debeaupuis, J.P., and Nierman, W. (2005). Specific molecular features in the organization and biosynthesis of the cell wall of Aspergillus fumigatus. Med Mycol 43 Suppl 1, S15-22.

Latruffe, N., Vamecq, J., and Cherkaoui Malki, M. (2003). Genetic-dependency of peroxisomal cell functions – emerging aspects. Journal of Cellular and Molecular Medicine 7, 238-248.

Lazarow, P.B. (1978). Rat liver peroxisomes catalyze the beta oxidation of fatty acids. J Biol Chem 253, 1522-1528.

Lazarow, P.B., and De Duve, C. (1976). A fatty acyl-CoA oxidizing system in rat liver peroxisomes; enhancement by clofibrate, a hypolipidemic drug. Proc Natl Acad Sci U S A 73, 2043-2046.

Lazarow, P.B., and Fujiki, Y. (1985). Biogenesis of peroxisomes. Annu Rev Cell Biol 1, 489-530.

Lengeler, K.B., Davidson, R.C., D'Souza, C., Harashima, T., Shen, W.C., Wang, P., Pan, X., Waugh, M., and Heitman, J. (2000). Signal transduction cascades regulating fungal development and virulence. Microbiol Mol Biol Rev 64, 746-785.

Li, X., and Gould, S.J. (2002). PEX11 promotes peroxisome division independently of peroxisome metabolism. J Cell Biol 156, 643-651.

Lindeberg, G., and Lindeberg, M. (1974). Effect of short chain fatty acids on the growth of some mycorrhizal and saprophytic hymenomycetes. Arch Microbiol 101, 109-114.

Lingappa, B.T., and Sussman, A.S. (1959). Endogenous Substrates of Dormant, Activated and Germinating Ascospores of Neurospora Tetrasperma. Plant Physiol 34, 466-472.

Lorenz, M.C., and Fink, G.R. (2001). The glyoxylate cycle is required for fungal virulence. Nature 412, 83-86.

Luo, Y., Karpichev, I.V., Kohanski, R.A., and Small, G.M. (1996). Purification, identification, and properties of a Saccharomyces cerevisiae oleate-activated upstream activating sequence-binding protein that is involved in the activation of POX1. J Biol Chem 271, 12068-12075.

Maassen, J.A., t Hart, L.M., Janssen, G.M., Reiling, E., Romijn, J.A., and Lemkes, H.H. (2006). Mitochondrial diabetes and its lessons for common Type 2 diabetes. Biochem Soc Trans 34, 819-823.

Maggio-Hall, L.A., and Keller, N.P. (2004). Mitochondrial beta-oxidation in Aspergillus nidulans. Mol Microbiol 54, 1173-1185.

Marchler-Bauer, A., Panchenko, A.R., Shoemaker, B.A., Thiessen, P.A., Geer, L.Y., and Bryant, S.H. (2002). CDD: a database of conserved domain alignments with links to domain three-dimensional structure. Nucleic Acids Res 30, 281-283.

Marchler-Bauer, A., Addess, K.J., Chappey, C., Geer, L., Madej, T., Matsuo, Y., Wang, Y., and Bryant, S.H. (1999). MMDB: Entrez's 3D structure database. Nucleic Acids Res 27, 240-243.

Mares, D., Romagnoli, C., Andreotti, E., Forlani, G., Guccione, S., and Vicentini, C.B. (2006). Emerging antifungal azoles and effects on Magnaporthe grisea. Mycol Res 110, 686-696.

Matsumoto, N., Tamura, S., and Fujiki, Y. (2003). The pathogenic peroxin Pex26p recruits the Pex1p-Pex6p AAA ATPase complexes to peroxisomes. Nat Cell Biol 5, 454-460.

Matsuoka, S., Saito, T., Kuwayama, H., Morita, N., Ochiai, H., and Maeda, M. (2003). MFE1, a member of the peroxisomal hydroxyacyl coenzyme A dehydrogenase family, affects fatty acid metabolism necessary for morphogenesis in Dictyostelium spp. Eukaryot Cell 2, 638-645.

McCammon, M.T. (1996). Mutants of Saccharomyces cerevisiae with defects in acetate metabolism: isolation and characterization of Acn- mutants. Genetics 144, 57-69.

McGarry, J.D., and Brown, N.F. (1997). The mitochondrial carnitine palmitoyltransferase system. From concept to molecular analysis. Eur J Biochem 244, 1-14.

Midgley, M. (1993). Carnitine acetyltransferase is absent from acuJ mutants of Aspergillus nidulans. FEMS Microbiol Lett 108, 7-10.

Minami-Ishii, N., Taketani, S., Osumi, T., and Hashimoto, T. (1989). Molecular cloning and sequence analysis of the cDNA for rat mitochondrial enoyl-CoA

hydratase. Structural and evolutionary relationships linked to the bifunctional enzyme of the peroxisomal beta-oxidation system. Eur J Biochem 185, 73-78.

Mishina, M., Kamiryo, T., Tashiro, S., Hagihara, T., Tanaka, A., Fukui, S., Osumi, M., and Numa, S. (1978). Subcellular localization of two long-chain acyl-coenzyme-A synthetases in Candida lipolytica. Eur J Biochem 89, 321-328.

Mitchell, T.K., and Dean, R.A. (1995). The cAMP-dependent protein kinase catalytic subunit is required for appressorium formation and pathogenesis by the rice blast pathogen Magnaporthe grisea. Plant Cell 7, 1869-1878.

Miura, S., Kasuya-Arai, I., Mori, H., Miyazawa, S., Osumi, T., Hashimoto, T., and Fujiki, Y. (1992). Carboxyl-terminal consensus Ser-Lys-Leu-related tripeptide of peroxisomal proteins functions in vitro as a minimal peroxisome-targeting signal. J Biol Chem 267, 14405-14411.

Momany, M., Richardson, E.A., Van Sickle, C., and Jedd, G. (2002). Mapping Woronin body position in Aspergillus nidulans. Mycologia 94, 260-266.

Moreno de la Garza, M., Schultz-Borchard, U., Crabb, J.W., and Kunau, W.H. (1985). Peroxisomal beta-oxidation system of Candida tropicalis. Purification of a multifunctional protein possessing enoyl-CoA hydratase, 3-hydroxyacyl-CoA dehydrogenase and 3-hydroxyacyl-CoA epimerase activities. Eur J Biochem 148, 285-291.

Mourikis, P., Hurlbut, G.D., and Artavanis-Tsakonas, S. (2006). Enigma, a mitochondrial protein affecting lifespan and oxidative stress response in Drosophila. Proc Natl Acad Sci U S A 103, 1307-1312.

Muller-Newen, G., Janssen, U., and Stoffel, W. (1995). Enoyl-CoA hydratase and isomerase form a superfamily with a common active-site glutamate residue. Eur J Biochem 228, 68-73.

Murphy, D.J. (2001). The biogenesis and functions of lipid bodies in animals, plants and microorganisms. Prog Lipid Res 40, 325-438.

Nagase, T., Shimozawa, N., Takemoto, Y., Suzuki, Y., Komori, M., and Kondo, N. (2004). Peroxisomal localization in the developing mouse cerebellum: implications for neuronal abnormalities related to deficiencies in peroxisomes. Biochim Biophys Acta 1671, 26-33.

Nakai, K., and Horton, P. (1999). PSORT: a program for detecting sorting signals in proteins and predicting their subcellular localization. Trends Biochem Sci 24, 34-36.

Naqvi, N.I., Bonman, J.M., Mackill, D.J., Nelson, R.J., and Chattoo, B.B. (1995). Identification of RAPD markers linked to major gene for blast resistance in rice. Molecular Breeding 1, 341-348.

Nishimura, M., Takeuchi, Y., De Bellis, L., and Hara-Nishimura, I. (1993). Leaf peroxisomes are directly transformed to glyoxysomes during senescence of pumpkin cotyledons. Protoplasma 175, 131-137.

Okazaki, K., Takechi, T., Kambara, N., Fukui, S., Kubota, I., and Kamiryo, T. (1986). Two acyl-coenzyme A oxidases in peroxisomes of the yeast Candida tropicalis: primary structures deduced from genomic DNA sequence. Proc Natl Acad Sci U S A 83, 1232-1236.

Osmundsen, H., Hovik, R., Bartlett, K., and Pourfazam, M. (1994). Regulation of flux of acyl-CoA esters through peroxisomal beta-oxidation. Biochem Soc Trans 22, 436-441.

Osumi, T., and Hashimoto, T. (1979). Peroxisomal beta oxidation system of rat liver. Copurification of enoyl-CoA hydratase and 3-hydroxyacyl-CoA dehydrogenase. Biochem Biophys Res Commun 89, 580-584.

Ou, S.H. (1985). Rice Diseases. (United Kingdom: Commonwealth Mycological Institute).

Palosaari, P.M., and Hiltunen, J.K. (1990). Peroxisomal bifunctional protein from rat liver is a trifunctional enzyme possessing 2-enoyl-CoA hydratase, 3-hydroxyacyl-CoA dehydrogenase, and delta 3, delta 2-enoyl-CoA isomerase activities. J Biol Chem 265, 2446-2449.

Park, S.J., and Lee, S.Y. (2003). Identification and characterization of a new enoyl coenzyme A hydratase involved in biosynthesis of medium-chain-length polyhydroxyalkanoates in recombinant Escherichia coli. J Bacteriol 185, 5391-5397.

Pedersen, T.A. (1970). Effect of Fatty Acids and Methyl Octanoate on Resting Mycelium of Boletus variegatus. Physiologia Plantarum 23, 654-666.

Penfield, S., Graham, S., and Graham, I.A. (2005). Storage reserve mobilization in germinating oilseeds: Arabidopsis as a model system. Biochem Soc Trans 33, 380-383.

Petriv, O.I., Tang, L., Titorenko, V.I., and Rachubinski, R.A. (2004). A new definition for the consensus sequence of the peroxisome targeting signal type 2. J Mol Biol 341, 119-134.

Pfanner, N. (2000). Protein sorting: recognizing mitochondrial presequences. Curr Biol 10, R412-415.

Piekarska, K., Mol, E., van den Berg, M., Hardy, G., van den Burg, J., van Roermund, C., Maccallum, D., Odds, F., and Distel, B. (2006). PEROXISOMAL FATTY ACID {beta}-OXIDATION IS NOT ESSENTIAL FOR VIRULENCE OF C. ALBICANS. Eukaryot Cell.

Platta, H.W., Grunau, S., Rosenkranz, K., Girzalsky, W., and Erdmann, R. (2005). Functional role of the AAA peroxins in dislocation of the cycling PTS1 receptor back to the cytosol. Nat Cell Biol 7, 817-822.

Portsteffen, H., Beyer, A., Becker, E., Epplen, C., Pawlak, A., Kunau, W.H., and Dodt, G. (1997). Human PEX1 is mutated in complementation group 1 of the peroxisome biogenesis disorders. Nat Genet 17, 449-452.

Prabhu, A.S., Filippi, M.C., and Zimmermann, F.J.P. (2003). Cultivar response to fungicide application in relatin to rice blast control, productivity and sustainability. Pesquisa Agropecuaria Brasileira 38, 11-17.

Pracharoenwattana, I., Cornah, J.E., and Smith, S.M. (2005). Arabidopsis peroxisomal citrate synthase is required for fatty acid respiration and seed germination. Plant Cell 17, 2037-2048.

Prigneau, O., Porta, A., and Maresca, B. (2004). Candida albicans CTN gene family is induced during macrophage infection: homology, disruption and phenotypic analysis of CTN3 gene. Fungal Genet Biol 41, 783-793.

Prigneau, O., Porta, A., Poudrier, J.A., Colonna-Romano, S., Noel, T., and Maresca, B. (2003). Genes involved in beta-oxidation, energy metabolism and glyoxylate cycle are induced by Candida albicans during macrophage infection. Yeast 20, 723-730.

Prip-Buus, C., Cohen, I., Kohl, C., Esser, V., McGarry, J.D., and Girard, J. (1998). Topological and functional analysis of the rat liver carnitine palmitoyltransferase 1 expressed in Saccharomyces cerevisiae. FEBS Lett 429, 173-178.

Purdue, P.E., and Lazarow, P.B. (2001). Peroxisome biogenesis. Annu Rev Cell Dev Biol 17, 701-752.

Qin, Y.M., Poutanen, M.H., Helander, H.M., Kvist, A.P., Siivari, K.M., Schmitz, W., Conzelmann, E., Hellman, U., and Hiltunen, J.K. (1997). Peroxisomal multifunctional enzyme of beta-oxidation metabolizing D-3-hydroxyacyl-CoA esters in rat liver: molecular cloning, expression and characterization. Biochem J 321 (Pt 1), 21-28.

Ramsay, R.R., Gandour, R.D., and van der Leij, F.R. (2001). Molecular enzymology of carnitine transfer and transport. Biochim Biophys Acta 1546, 21-43.

Reddy, J.K., and Krishnakantha, T.P. (1975). Hepatic peroxisome proliferation: induction by two novel compounds structurally unrelated to clofibrate. Science 190, 787-789.

Rehling, P., Marzioch, M., Niesen, F., Wittke, E., Veenhuis, M., and Kunau, W.H. (1996). The import receptor for the peroxisomal targeting signal 2 (PTS2) in Saccharomyces cerevisiae is encoded by the PAS7 gene. Embo J 15, 2901-2913.

Requena, N., Fuller, P., and Franken, P. (1999). Molecular characterization of GmFOX2, an evolutionarily highly conserved gene from the mycorrhizal fungus

Glomus mosseae, down-regulated during interaction with rhizobacteria. Mol Plant Microbe Interact 12, 934-942.

Richmond, T.A., and Bleecker, A.B. (1999). A defect in beta-oxidation causes abnormal inflorescence development in Arabidopsis. Plant Cell 11, 1911-1924.

Roise, D., and Schatz, G. (1988). Mitochondrial presequences. J Biol Chem 263, 4509-4511.

Rosenkranz, K., Birschmann, I., Grunau, S., Girzalsky, W., Kunau, W.H., and Erdmann, R. (2006). Functional association of the AAA complex and the peroxisomal importomer. Febs J 273, 3804-3815.

Rottensteiner, H., Kal, A.J., Hamilton, B., Ruis, H., and Tabak, H.F. (1997). A heterodimer of the Zn2Cys6 transcription factors Pip2p and Oaf1p controls induction of genes encoding peroxisomal proteins in Saccharomyces cerevisiae. Eur J Biochem 247, 776-783.

Rottensteiner, H., Kal, A.J., Filipits, M., Binder, M., Hamilton, B., Tabak, H.F., and Ruis, H. (1996). Pip2p: a transcriptional regulator of peroxisome proliferation in the yeast Saccharomyces cerevisiae. Embo J 15, 2924-2934.

Rude, T.H., Toffaletti, D.L., Cox, G.M., and Perfect, J.R. (2002). Relationship of the glyoxylate pathway to the pathogenesis of Cryptococcus neoformans. Infect Immun 70, 5684-5694.

Rylott, E.L., Eastmond, P.J., Gilday, A.D., Slocombe, S.P., Larson, T.R., Baker, A., and Graham, I.A. (2006). The Arabidopsis thaliana multifunctional protein gene (MFP2) of peroxisomal beta-oxidation is essential for seedling establishment. Plant J 45, 930-941.

Salon, C., Raymond, P., and Pradet, A. (1988). Quantification of carbon fluxes through the tricarboxylic acid cycle in early germinating lettuce embryos. J Biol Chem 263, 12278-12287.

Sambrook, J., Fritsch, E.F., and Maniatis, T. (1989). Molecular Cloning: A Laboratory Manual. (Cold Spring Harbor, NY: Cold Spring Harbor Laboratory Press).

Sawada, H., Sugihara, M., Takagaki, M., and Nagayama, K. (2004). Monitoring and characterization of Magnaporthe grisea isolates with decreased sensitivity to scytalone dehydratase inhibitors. Pest Manag Sci 60, 777-785.

Schell-Steven, A., Stein, K., Amoros, M., Landgraf, C., Volkmer-Engert, R., Rottensteiner, H., and Erdmann, R. (2005). Identification of a novel, intraperoxisomal pex14-binding site in pex13: association of pex13 with the docking complex is essential for peroxisomal matrix protein import. Mol Cell Biol 25, 3007-3018.

Schliebs, W., and Kunau, W.H. (2004). Peroxisome membrane biogenesis: the stage is set. Curr Biol 14, R397-399.

Schmalix, W., and Bandlow, W. (1993). The ethanol-inducible YAT1 gene from yeast encodes a presumptive mitochondrial outer carnitine acetyltransferase. J Biol Chem 268, 27428-27439.

Schulz, H. (1974). Long chain enoyl coenzyme A hydratase from pig heart. J Biol Chem 249, 2704-2709.

Schulz, H. (1991). Beta oxidation of fatty acids. Biochim Biophys Acta 1081, 109-120.

Schumann, U., Wanner, G., Veenhuis, M., Schmid, M., and Gietl, C. (2003). AthPEX10, a nuclear gene essential for peroxisome and storage organelle formation during Arabidopsis embryogenesis. Proc Natl Acad Sci U S A 100, 9626-9631.

Seifert, G.J. (2004). Nucleotide sugar interconversions and cell wall biosynthesis: how to bring the inside to the outside. Curr Opin Plant Biol 7, 277-284.

Seitz, B., Klos, C., Wurm, M., and Tenhaken, R. (2000). Matrix polysaccharide precursors in Arabidopsis cell walls are synthesized by alternate pathways with organ-specific expression patterns. Plant J 21, 537-546.

Sheridan, R., and Ratledge, C. (1996). Changes in cell morphology and carnitine acetyltransferase activity in Candida albicans following growth on lipids and serum and after in vivo incubation in mice. Microbiology 142 (Pt 11), 3171-3180.

Sisler, H.D., and Cox, C.E. (1954). Effects of tetramethylthiuram disulfide on metabolism of Fusarium roseum. American Journal of Botany 41, 338-345.

Skoneczny, M., Chelstowska, A., and Rytka, J. (1988). Study of the coinduction by fatty acids of catalase A and acyl-CoA oxidase in standard and mutant Saccharomyces cerevisiae strains. Eur J Biochem 174, 297-302.

Skulachev, V.P. (2001). Mitochondrial filaments and clusters as intracellular power-transmitting cables. Trends Biochem Sci 26, 23-29.

Smith, J.D., and Silverman, P.M. (1973). Lipid turnover during morphogenesis in the water mold Blastocladiella emersonii. Biochem Biophys Res Commun 54, 1191-1197.

Smith, J.J., Brown, T.W., Eitzen, G.A., and Rachubinski, R.A. (2000). Regulation of peroxisome size and number by fatty acid beta -oxidation in the yeast yarrowia lipolytica. J Biol Chem 275, 20168-20178.

Solomon, P.S., Lee, R.C., Wilson, T.J., and Oliver, R.P. (2004). Pathogenicity of Stagonospora nodorum requires malate synthase. Mol Microbiol 53, 1065-1073.

Soundararajan, S., Jedd, G., Li, X., Ramos-Pamplona, M., Chua, N.H., and Naqvi, N.I. (2004). Woronin body function in Magnaporthe grisea is essential for efficient

pathogenesis and for survival during nitrogen starvation stress. Plant Cell 16, 1564-1574.

Stemple, C.J., Davis, M.A., and Hynes, M.J. (1998). The facC gene of Aspergillus nidulans encodes an acetate-inducible carnitine acetyltransferase. J Bacteriol 180, 6242-6251.

Subramani, S., Koller, A., and Snyder, W.B. (2000). Import of peroxisomal matrix and membrane proteins. Annu Rev Biochem 69, 399-418.

Susin, S.A., Lorenzo, H.K., Zamzami, N., Marzo, I., Snow, B.E., Brothers, G.M., Mangion, J., Jacotot, E., Costantini, P., Loeffler, M., Larochette, N., Goodlett, D.R., Aebersold, R., Siderovski, D.P., Penninger, J.M., and Kroemer, G. (1999). Molecular characterization of mitochondrial apoptosis-inducing factor. Nature 397, 441-446.

Sweigard, J.A., Carroll, A.M., Farrall, L., Chumley, F.G., and Valent, B. (1998). Magnaporthe grisea pathogenicity genes obtained through insertional mutagenesis. Mol Plant Microbe Interact 11, 404-412.

Swiegers, J.H., Dippenaar, N., Pretorius, I.S., and Bauer, F.F. (2001). Carnitine-dependent metabolic activities in Saccharomyces cerevisiae: three carnitine acetyltransferases are essential in a carnitine-dependent strain. Yeast 18, 585-595.

Talbot, N.J. (2003). On the trail of a cereal killer: Exploring the biology of Magnaporthe grisea. Annu Rev Microbiol 57, 177-202.

Tamura, S., Yasutake, S., Matsumoto, N., and Fujiki, Y. (2006). Dynamic and functional assembly of the AAA peroxins, Pex1p and Pex6p, and their membrane receptor Pex26p. J Biol Chem 281, 27693-27704.

Tenjo, F.A., and Hamer, J.E. (2002). Pathogenic development in Magnaporthe grisea. In Molecular Biology of Fungal Development, H.D. Osiewacz, ed (Frankfurt, Germany: Marcel Decker.

Thieringer, R., and Kunau, W.H. (1991a). The beta-oxidation system in catalase-free microbodies of the filamentous fungus Neurospora crassa. Purification of a multifunctional protein possessing 2-enoyl-CoA hydratase, L-3-hydroxyacyl-CoA dehydrogenase, and 3-hydroxyacyl-CoA epimerase activities. J Biol Chem 266, 13110-13117.

Thieringer, R., and Kunau, W.H. (1991b). Beta-oxidation system of the filamentous fungus Neurospora crassa. Structural characterization of the trifunctional protein. J Biol Chem 266, 13118-13123.

Thines, E., Weber, R.W., and Talbot, N.J. (2000). MAP kinase and protein kinase A-dependent mobilization of triacylglycerol and glycogen during appressorium turgor generation by Magnaporthe grisea. Plant Cell 12, 1703-1718.

Thoms, S., and Erdmann, R. (2005). Dynamin-related proteins and Pex11 proteins in peroxisome division and proliferation. Febs J 272, 5169-5181.

Titorenko, V.I., and Rachubinski, R.A. (2000). Peroxisomal membrane fusion requires two AAA family ATPases, Pex1p and Pex6p. J Cell Biol 150, 881-886.

Titorenko, V.I., and Rachubinski, R.A. (2004). The peroxisome: orchestrating important developmental decisions from inside the cell. J Cell Biol 164, 641-645.

Titorenko, V.I., Chan, H., and Rachubinski, R.A. (2000). Fusion of small peroxisomal vesicles in vitro reconstructs an early step in the in vivo multistep peroxisome assembly pathway of Yarrowia lipolytica. J Cell Biol 148, 29-44.

Torroja, L., Ortuno-Sahagun, D., Ferrus, A., Hammerle, B., and Barbas, J.A. (1998). scully, an essential gene of Drosophila, is homologous to mammalian mitochondrial type II L-3-hydroxyacyl-CoA dehydrogenase/amyloid-beta peptide-binding protein. J Cell Biol 141, 1009-1017.

Tzagoloff, A., and Dieckmann, C.L. (1990). PET genes of Saccharomyces cerevisiae. Microbiol Rev 54, 211-225.

Uchida, Y., Izai, K., Orii, T., and Hashimoto, T. (1992). Novel fatty acid beta-oxidation enzymes in rat liver mitochondria. II. Purification and properties of enoyl-coenzyme A (CoA) hydratase/3-hydroxyacyl-CoA dehydrogenase/3-ketoacyl-CoA thiolase trifunctional protein. J Biol Chem 267, 1034-1041.

Valenciano, S., Lucas, J.R., Pedregosa, A., Monistrol, I.F., and Laborda, F. (1996). Induction of beta-oxidation enzymes and microbody proliferation in Aspergillus nidulans. Arch Microbiol 166, 336-341.

van der Klei, I., and Veenhuis, M. (2002). Peroxisomes: flexible and dynamic organelles. Curr Opin Cell Biol 14, 500-505.

van Roermund, C.W., Elgersma, Y., Singh, N., Wanders, R.J., and Tabak, H.F. (1995). The membrane of peroxisomes in Saccharomyces cerevisiae is impermeable to NAD(H) and acetyl-CoA under in vivo conditions. Embo J 14, 3480-3486.

van Roermund, C.W., Hettema, E.H., van den Berg, M., Tabak, H.F., and Wanders, R.J. (1999). Molecular characterization of carnitine-dependent transport of acetyl-CoA from peroxisomes to mitochondria in Saccharomyces cerevisiae and identification of a plasma membrane carnitine transporter, Agp2p. Embo J 18, 5843-5852.

van Roermund, C.W., Tabak, H.F., van Den Berg, M., Wanders, R.J., and Hettema, E.H. (2000). Pex11p plays a primary role in medium-chain fatty acid oxidation, a process that affects peroxisome number and size in Saccharomyces cerevisiae. J Cell Biol 150, 489-498.

Van Veldhoven, P.P., Vanhove, G., Assselberghs, S., Eyssen, H.J., and Mannaerts, G.P. (1992). Substrate specificities of rat liver peroxisomal acyl-CoA oxidases: palmitoyl-CoA oxidase (inducible acyl-CoA oxidase), pristanoyl-CoA oxidase (non-inducible acyl-CoA oxidase), and trihydroxycoprostanoyl-CoA oxidase. J Biol Chem 267, 20065-20074.

Vanhove, G.F., Van Veldhoven, P.P., Fransen, M., Denis, S., Eyssen, H.J., Wanders, R.J., and Mannaerts, G.P. (1993). The CoA esters of 2-methyl-branched chain fatty acids and of the bile acid intermediates di- and trihydroxycoprostanic acids are oxidized by one single peroxisomal branched chain acyl-CoA oxidase in human liver and kidney. J Biol Chem 268, 10335-10344.

Veenhuis, M., Mateblowski, M., Kunau, W.H., and Harder, W. (1987). Proliferation of microbodies in Saccharomyces cerevisiae. Yeast 3, 77-84.

Vickers, A.E., Bentley, P., and Fisher, R.L. (2006). Consequences of mitochondrial injury induced by pharmaceutical fatty acid oxidation inhibitors is characterized in human and rat liver slices. Toxicol In Vitro 20, 1173-1182.

Vogel, J., and Somerville, S. (2000). Isolation and characterization of powdery mildew-resistant Arabidopsis mutants. Proc Natl Acad Sci U S A 97, 1897-1902.

Wagner, A., and Daum, G. (2005). Formation and mobilization of neutral lipids in the yeast Saccharomyces cerevisiae. Biochem Soc Trans 33, 1174-1177.

Wanders, R.J. (2000). Peroxisomes, lipid metabolism, and human disease. Cell Biochem Biophys 32 Spring, 89-106.

Wanders, R.J., van Grunsven, E.G., and Jansen, G.A. (2000). Lipid metabolism in peroxisomes: enzymology, functions and dysfunctions of the fatty acid alpha- and beta-oxidation systems in humans. Biochem Soc Trans 28, 141-149.

Wanders, R.J., Vreken, P., den Boer, M.E., Wijburg, F.A., van Gennip, A.H., and L, I.J. (1999). Disorders of mitochondrial fatty acyl-CoA beta-oxidation. J Inherit Metab Dis 22, 442-487.

Wang, T., Luo, Y., and Small, G.M. (1994). The POX1 gene encoding peroxisomal acyl-CoA oxidase in Saccharomyces cerevisiae is under the control of multiple regulatory elements. J Biol Chem 269, 24480-24485.

Wang, Z.Y., Thornton, C.R., Kershaw, M.J., Debao, L., and Talbot, N.J. (2003). The glyoxylate cycle is required for temporal regulation of virulence by the plant pathogenic fungus Magnaporthe grisea. Mol Microbiol 47, 1601-1612.

Wang, Z.Y., Jenkinson, J.M., Holcombe, L.J., Soanes, D.M., Veneault-Fourrey, C., Bhambra, G.K., and Talbot, N.J. (2005). The molecular biology of appressorium turgor generation by the rice blast fungus Magnaporthe grisea. Biochem Soc Trans 33, 384-388.

Weber, R.W., Wakley, G.E., Thines, E., and Talbot, N.J. (2001). The vacuole as central element of the lytic system and sink for lipid droplets in maturing appressoria of Magnaporthe grisea. Protoplasma 216, 101-112.

Woeltje, K.F., Esser, V., Weis, B.C., Sen, A., Cox, W.F., McPhaul, M.J., Slaughter, C.A., Foster, D.W., and McGarry, J.D. (1990). Cloning, sequencing, and expression of a cDNA encoding rat liver mitochondrial carnitine palmitoyltransferase II. J Biol Chem 265, 10720-10725.

Wong, D.A., Bassilian, S., Lim, S., and Paul Lee, W.N. (2004). Coordination of peroxisomal beta-oxidation and fatty acid elongation in HepG2 cells. J Biol Chem 279, 41302-41309.

Wu, D., Govindasamy, L., Lian, W., Gu, Y., Kukar, T., Agbandje-McKenna, M., and McKenna, R. (2003). Structure of human carnitine acetyltransferase. Molecular basis for fatty acyl transfer. J Biol Chem 278, 13159-13165.

Wu, W.J., Anderson, V.E., Raleigh, D.P., and Tonge, P.J. (1997). Structure of hexadienoyl-CoA bound to enoyl-CoA hydratase determined by transferred nuclear Overhauser effect measurements: mechanistic predictions based on the X-ray structure of 4-(chlorobenzoyl)-CoA dehalogenase. Biochemistry 36, 2211-2220.

Xu, J.R., and Hamer, J.E. (1996). MAP kinase and cAMP signaling regulate infection structure formation and pathogenic growth in the rice blast fungus Magnaporthe grisea. Genes Dev 10, 2696-2706.

Zolman, B.K., and Bartel, B. (2004). An Arabidopsis indole-3-butyric acid-response mutant defective in PEROXIN6, an apparent ATPase implicated in peroxisomal function. Proc Natl Acad Sci U S A 101, 1786-1791.

APPENDIX

First author publication as listed on page xi.

Host invasion during rice-blast disease requires carnitine-dependent transport of peroxisomal acetyl-CoA

Marilou Ramos-Pamplona[1] and Naweed I. Naqvi[1,2]*

[1]*Fungal Genomics Group, Temasek Life Sciences Laboratory, 1 Research Link, National University of Singapore, Singapore 117604.*

[2]*Department of Biological Sciences, 14 Science Drive, National University of Singapore, Singapore 117543.*

Summary

In lower eukaryotes, beta-oxidation of fatty acids is restricted primarily to the peroxisomes and the resultant acetyl-CoA molecules (and the chain-shortened fatty acids) are transported via the cytosol into the mitochondria for further breakdown and usage. Using a loss-of-function mutation in the *Magnaporthe grisea PEROXIN6* orthologue, we define an essential role for peroxisomal acetyl-CoA during the host invasion step of the rice-blast disease. We show that an *Mgpex6Δ* strain lacks functional peroxisomes and is incapable of β-oxidation of long-chain fatty acids. The *Mgpex6Δ* mutant lacked appressorial melanin and host penetration, and was completely non-pathogenic. We further show that a peroxisome-associated carnitine acetyl-transferase (Crat1) activity is essential for such appressorial function in *Magnaporthe*. *CRAT1*-minus appressoria showed reduced melanization, but were surprisingly incapable of elaborating penetration pegs or infection hyphae. Exogenous addition of excess glucose during infection stage caused partial remediation of the pathogenicity defects in the *crat1Δ* strain. Moreover, *Mgpex6Δ* and *crat1Δ* mycelia showed increased sensitivity to Calcofluor white, suggesting that weakened cell wall biosynthesis in a glucose-deficient environment leads to appressorial dysfunction in these mutants. Interestingly, *CRAT1* was itself essential for growth on acetate and long-chain fatty acids. Thus, carnitine-dependent metabolic activities associated with the peroxisomes, cooperatively facilitate the appressorial function of host invasion during rice-blast infections.

Introduction

In eukaryotes, peroxisomes belong to the microbody class of single-membrane bound organelles and perform distinct functions in lipid metabolism, which includes β-oxidation of fatty acids and synthesis of cholesterol. In addition, peroxisomes serve highly specialized functions (Titorenko and Rachubinski, 2001; 2004) such as: peroxide detoxification, biosynthesis of antibiotics (van Der Bosch *et al.*, 1992), occlusion of septal pores in filamentous fungi (Jedd and Chua, 2000; Soundararajan *et al.*, 2004), methanol utilization in yeasts (Muller *et al.*, 1991), and photorespiration in plants (Tolbert, 1982). Peroxisome biogenesis *per se* has been extensively studied in the yeasts and mutant characterizations therein have revealed a number of Peroxins (products of the PEX genes) that are essential for this process (van der Klei and Veenhuis, 1997; Subramani, 1998). Import of peroxisomal proteins has been shown to be dependent on the consensus peroxisomal targeting signals termed PTS1 or PTS2 (Subramani, 1993; Legakis and Terlecky, 2001).

The β-oxidation of fatty acids is a well-conserved metabolic process that results in the degradation of fatty acids to acetate. In mammalian cells, this process occurs in both mitochondria and peroxisomes (Schulz, 1991; Wanders *et al.*, 1997). Impaired peroxisomal β-oxidation, however, leads to several inherited diseases such as X-linked adrenoleukodystrophy (Wanders *et al.*, 1995) or Zellweger syndrome (Lazarow and Moser, 1989) in humans. In contrast to β-oxidation of fatty acids in mammalian cells, catabolism of fatty acids occurs exclusively in the peroxisomes in yeasts (Kunau *et al.*, 1988; Kurihara *et al.*, 1992; Smith *et al.*, 2000). The resultant acetyl-CoA is then transported from the peroxisomes to the mitochondria for complete oxidation to CO_2 and H_2O. The transfer of activated acyl groups across intracellular membranes depends on L-carnitine. An important pathway for such a transport of acetyl units has been established (van Roermund *et al.*, 1995) and involves an initial conversion of acetyl-CoA into acetyl-carnitine, catalysed by carnitine acetyl-transferase (CrAT; Elgersma *et al.*, 1995), prior to its transportation. As opposed to the wealth of information on the biogenesis of peroxisomes in yeasts (Subramani, 1998) and peroxisomal metabolism detailed above, rather limited insights have been made in the generation and fate of peroxisomal

acetyl-CoA in the filamentous fungi (van Der Bosch *et al.*, 1992; Kimura *et al.*, 2001). Mitochondrial β-oxidation has been recently documented in *Aspergillus* (Maggio-Hall and Keller, 2004).

The rice-blast disease, caused by the ascomycete *Magnaporthe*, offers an excellent system (Valent, 1990) to investigate the relationship between metabolism and virulence-related development in a phytopathogenic fungus. Several virulence-associated events require blast disease propagules (namely the conidia) to respond to changes in the external environments such as the host surface, and to rapidly mobilize lipid and/or carbohydrate reserves and initiate their metabolic breakdown in the appressoria (Wang *et al.*, 2003). An expected consequence of such rapid lipolysis in *Magnaporthe* is the generation of long-chain fatty acids and subsequently, upon β-oxidation, of acetyl-CoA.

In this article, we report the isolation and characterization of two non-pathogenic mutants of *Magnaporthe*, which could be assigned to two distinct complementation and functional groups. The first group (*pex6Δ*) demonstrates that the acetyl-CoA generated by peroxisomal metabolism is essential for *Magnaporthe* pathogenicity. The second category of mutants (*crat1Δ*) showed specific defects in the carnitine-dependent acetyl-unit transport from peroxisomes to cytosol and/or mitochondria. We further demonstrate that the Pex6 and Crat1 proteins are essential for the host invasion step during rice-blast pathogenesis. Crat1 was found to be the major CrAT activity associated with the peroxisomes, and contributed > 95% of the total CrAT activity in *Magnaporthe*. Loss of *PEX6* resulted in the loss of peroxisomal integrity, thus leading to defects in import of matrix proteins, and as a consequence led to a block in β-oxidation of fatty acids. The *pex6Δ* strain lacked appressorial melanin, whereas *crat1Δ* appressoria showed reduced melanization. We further show that Pex6 and Crat1 are essential for elaborating penetration pegs and infection hyphae during pathogenesis. Interestingly, Crat1 function was found to be essential for utilization of various carbon sources such as acetate and long-chain fatty acids. The addition of glucose partially suppressed the pathogenicity defects associated with *crat1Δ* mutant, suggestive of distinct compartmentation of the acetyl-CoA generation, transport and utilization within the unicellular appressorium. Thus, cooperative interaction between the metabolism associated with peroxisomes and the carnitine-mediated transport is essential for appressorium function of host entry during rice-blast infection.

Results

Isolation and characterization of MgPEX6

Random insertional mutagenesis using *Agrobacterium*

Transfer-DNA was carried out in *Magnaporthe grisea* to identify novel pathogenicity factors in a forward genetics approach. TMP6-2 was identified as a mutant strain incapable of causing disease lesions on barley leaf explants. As shown schematically in Fig. 1A, TMP6-2 contained a single-copy insertion of the hygromycin-resistance cassette (*HPH1*) containing T-DNA and disrupted a region on Contig 2.95 (*Magnaporthe* Genome Database, Broad Institute, USA). A 7.25 kb KpnI fragment was identified that corresponded to this region and further annotation of this genomic fragment revealed that the disruption was in the second exon of an open reading frame (ORF) encoding a protein showing extensive homology to Peroxin6 (hereafter Pex6) found in several eukaryotes. We designated this gene *MgPEX6* (hereafter simply referred to as *PEX6*) and further *in silico* analyses of the deduced nucleotide sequence of the gene and the coding sequence suggested that the ORF spans 4.309 kb and is interrupted by two short introns (Fig. 1A). *PEX6* was predicted to encode a protein of 1375 amino acids and depicted a domain organization reminiscent of the members of the AAA ATPase family (Fig. 1A). TMP6-2 failed to undergo sexual development and therefore we created loss-of-function mutants (*pex6::HPH1*; hereafter *pex6Δ*) in the *PEX6* gene by replacing about 44% of the coding sequence, in particular the region encoding the two catalytic domains, with the *HPH1* cassette, using homology-assisted recombination. This exercise was carried out in two separate wild-type (WT) strains B157 and Guy11 and the resultant gene replacement events confirmed by DNA gel blot analysis (Fig. 1B). The KpnI fragment containing the full-length genomic copy of *PEX6* was introduced into the deletion strains to test for complementation of the defects associated with the loss of *PEX6* function. As shown in Fig. 1B, an RFLP associated with the rescued strain was identified between the WT (lane 1) and the rescued strain (lane 3). Genomic DNA digested with EcoRI was probed with the *PEX6* specific probe as described in Fig. 1A. The WT showed a 2.1 kb and a 11.2 kb band, whereas the *pex6Δ* (lane 2) showed the loss of the 2.1 kb band and the appearance of the 12.5 kb fragment. The rescued strain regained the 2.1 kb specific fragment and in addition showed the presence of the 3.5 kb fragment. At least two independent strains in each instance (deletion and complemented) were used for confirmation and further investigations.

Peroxisomal defects of pex6Δ *mutant*

In fungi, metabolism of medium (6–10 Carbon) and long-chain (12–18 Carbon) fatty acids occurs through the process of beta-oxidation which takes place in the peroxisomes (Kunau *et al.*, 1995). To evaluate peroxisomal function in the *pex6Δ* strain, growth utilizing either glucose
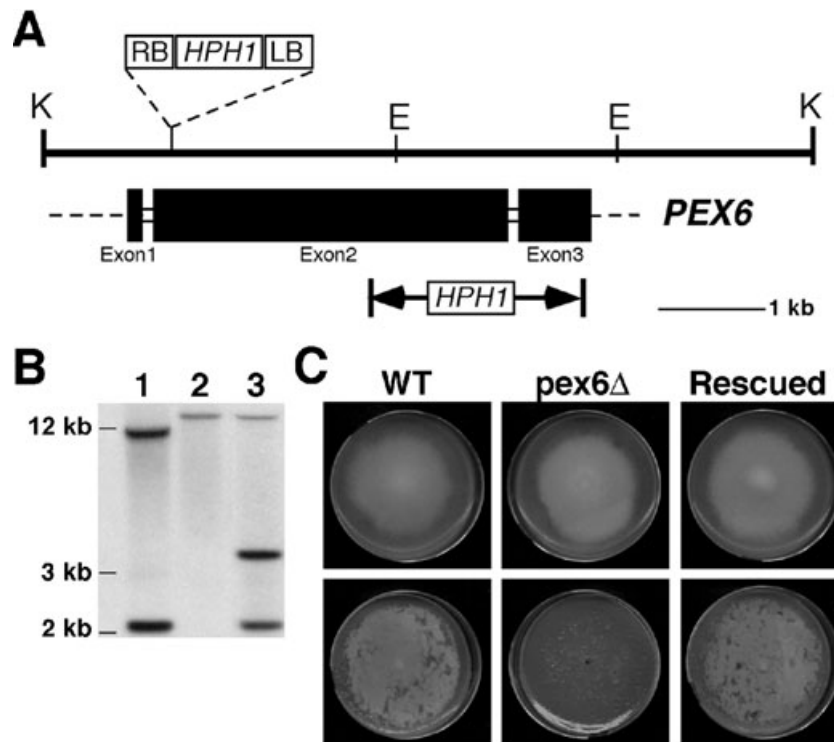
Fig. 1. Identification and characterization of *PEX6* mutant in *Magnaporthe*.
A. Annotation and schematic representation of the *Magnaporthe PEX6* locus spanning a KpnI (denoted as K; E refers to EcoRI sites) fragment on BAC clone 2A14 from *M. grisea*. Solid bars and short open boxes indicate the coding regions and the introns respectively, and are drawn to scale. RB and LB represent the right and left border sequences of T-DNA (open box) integrated in the TMP6-2 mutant strain. Opposing arrows demarcate the genomic region deleted to create the *pex6Δ* strain using the *HPH1* cassette. The *PEX6* region spanning 1 kb either side of the first EcoRI site was used as the probe for the Southern blot analysis shown in (B). Scale bar denotes 1 kb.
B. DNA gel blot analysis of *PEX6* deletion and rescued strains. Genomic DNA from B157 wild type (1), *pex6Δ* (2) and a *pex6* rescued strain (lane 3; carrying an ectopic single copy integration of the KpnI fragment described above) was digested with EcoRI, and processed for DNA gel blot analysis. The appearance of the 12.5 kb band in the *pex6Δ* strain, with the concomitant loss of the wild-type 11.2 kb and 2.1 kb band, was diagnostic of the correct gene replacement event. Ectopic integration of the complementation construct in the rescued strain resulted in the retention of the 12.5 kb band and the restoration of the wild-type 2.1 kb band. The appearance of a 3.5 kb band in the rescued strain is due to an internal EcoRI site in the rescue construct.
C. Loss of fatty acid metabolism in the *pex6Δ* strain. The wild-type, *pex6Δ* and *pex6* rescued strains were grown on basal medium supplemented with either 1% glucose (upper panel) or 1% olive oil (lower panel) for 10 days.

or olive oil as the sole carbon source was assessed. On basal medium with glucose as the carbon source, the *pex6Δ* mutant showed slightly reduced growth compared with the wild type (Fig. 1C). On olive oil containing medium, the wild type grew normally, whereas growth of the *pex6Δ* strain was completely abolished (Fig. 1C).

To evaluate the functional integrity of peroxisomes, we assessed the peroxisomal matrix protein import in the *pex6Δ* strain. Towards this end, green fluorescent protein (GFP) with a C-terminal PTS1 (SRL, Miura *et al.*, 1992) was introduced into both the wild-type and the *pex6Δ* strains. Subcellular localization of GFP-SRL epifluorescence was then investigated during the vegetative (mycelia) and the pathogenic (conidia, germ tubes and appressoria) growth phases of the transformed strains. In the wild-type/GFP-SRL strain, punctate GFP fluorescence, indicative of intact peroxisomes, was observed during all the growth stages (Fig. 2). In contrast, only a

diffused cytoplasmic fluorescence was detected in the different growth stages of the *pex6Δ*/GFP-SRL strain. Taken together, these results helped us to conclude that the *pex6Δ* mutant lacks functional peroxisomes and as a consequence is defective in β-oxidation of long-chain fatty acids and in the import and transport of peroxisomal matrix proteins.

Role of PEX6 during Magnaporthe *pathogenesis*

As *M. grisea* infects several monocot species, the pathogenicity of *pex6Δ* mutant was tested on two different hosts, barley and rice (Fig. 3A). In a barley detached leaf assay, inoculation of wild-type conidia resulted in the formation of visible lesions, starting at 4 days post inoculation, which continued to coalesce and spread over the leaf surface (Fig. 3A, upper panels). However, the *pex6Δ* mutant did not elicit any disease symptoms even when
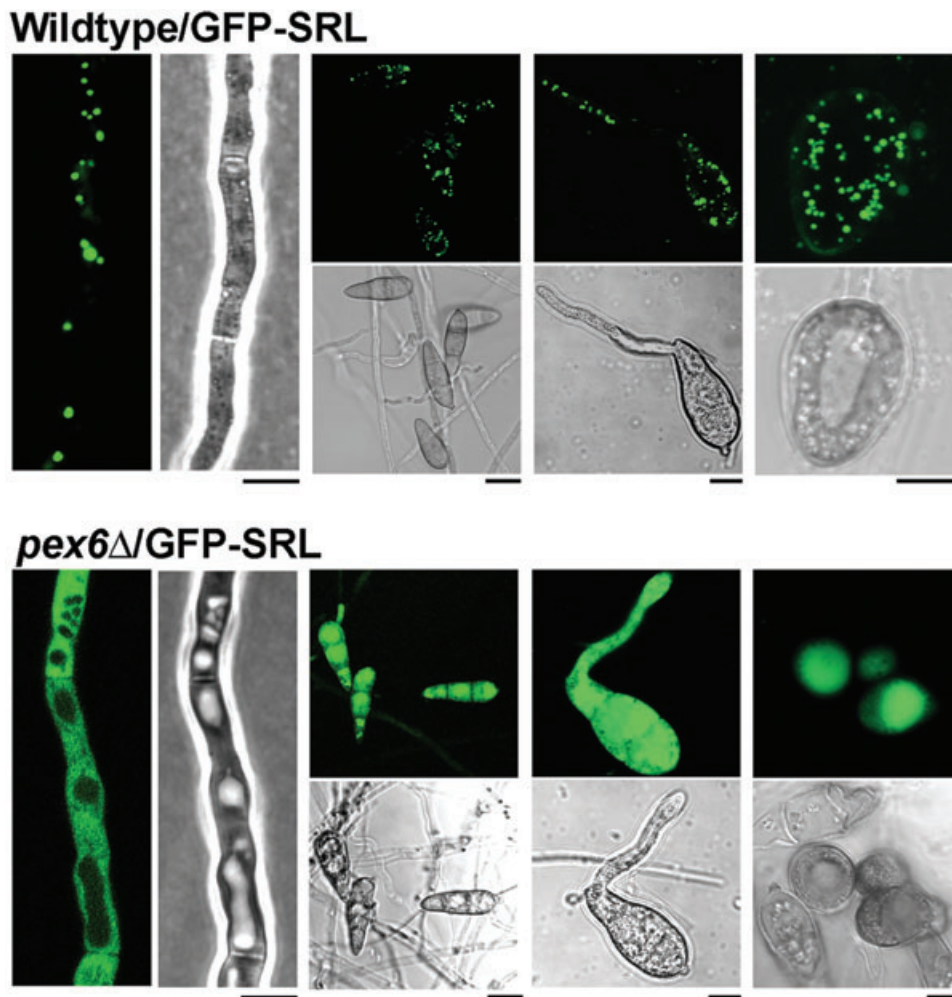
Wildtype/GFP-SRL

pex6Δ/GFP-SRL

Fig. 2. Peroxisomal defects of the *pex6Δ* strain. Impairment of peroxisomal matrix protein import in the *pex6Δ* strain. The wild-type and the *pex6Δ* strains were transformed with a GFP-PTS1 construct and observed using epifluorescence microscopy during the different stages of vegetative and pathogenic development. In the wild-type strain, the GFP-PTS1 fusion protein was observed as punctate fluorescence, whereas in the *pex6Δ* strain, the GFP epifluorescence was predominantly cytoplasmic. Scale bars for panels showing the mycelia, germinating spores or the appressoria = 5 μm. Scale bars sizing conidia represent 10 μm.

inoculated with a fourfold higher conidial load. The *pex6Δ* was likewise completely non-pathogenic on rice cultivar CO39 (Fig. 3A, lower panels). Spray inoculations with even a twofold higher conidial load than the wild type did not enable the *pex6Δ* to cause blast disease on rice seedlings (Fig. 3A, lower panels).

Detailed microscopic observations of the infection process were undertaken to determine which stage of pathogenesis was affected in the *pex6Δ* mutant. The ability to form appressoria (upon conidial germination) was greatly reduced in the *pex6Δ* mutant. Quantitative appressorium formation assays conducted on artificial membranes (Gelbond™, Biowhittaker Molecular Applications, Rockland, ME, USA) and on leaf surfaces demonstrated that the capability to form appressoria in the *pex6Δ* was reduced to ~50% of that observed in the wild-type strain (Fig. 3B).

Moreover, appressoria formed by *pex6Δ* were completely non-functional and unable to elaborate penetration pegs as judged by papillary callose deposition assays using aniline blue (Fig. 3B, appressorium function). The penetration pegs and infection hyphae were never elaborated by *pex6Δ* appressoria during leaf infection assays even after 96 h post inoculation (shown later in Fig. 5B). In wild-type inoculations, ramifying and invasive infectious hyphae, which originate from the appressoria, were clearly seen 48 h after inoculation. These results suggest that the non-pathogenicity defect of *pex6Δ* could be attributed directly to a defect in appressorium-mediated host penetration.

Light microscopic observations revealed that compared with the wild type, the *pex6Δ* mutant showed aberrant appressoria that appeared to lack the dark pigment
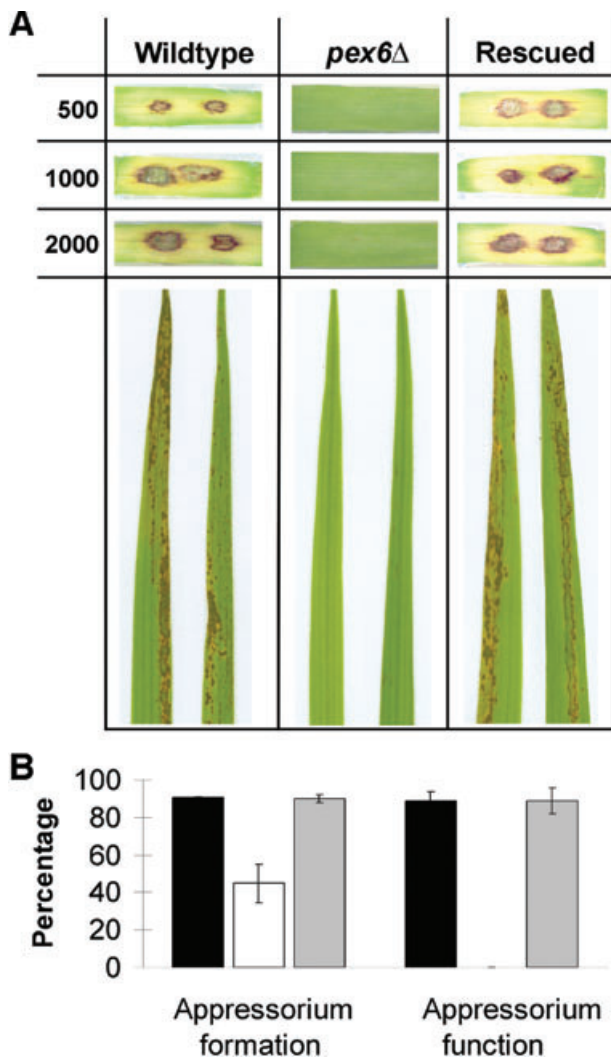
uniformly deposited along the periphery of the entire cell (Fig. 4B, WT). At higher magnifications, a distinct melanin layer was clearly seen between the appressorial cell wall and the plasma membrane (Fig. 4B). In all the sections of

Fig. 3. Pathogenicity of the *pex6Δ* strain.
A. Infection assays on barley and rice. Conidia from the wild-type, *pex6Δ* and rescued strains were used to inoculate leaf explants of barley (upper panel) and seedlings of rice cultivar CO39 (lower panel). The number of conidia inoculated on the detached barley leaf assay is indicated. Disease symptoms for both experiments were assessed 7 days post inoculation.
B. Pathogenesis-related defects of the *pex6Δ* strain. Equal number of conidia of the wild-type (black bar), *pex6Δ* (open bar) and rescued (grey bar) strains were inoculated on both artificial membrane and host surface to evaluate appressorium formation and appressorium function respectively. Appressorium formation was assessed as the number of germinated conidia which formed appressoria after 24 h. Appressorium function was evaluated as the number of appressoria which formed penetration pegs/infectious hyphae after 48 h. Mean values (± SD) presented as percentage points were derived from three independent experiments.

melanin (Fig. 4A). To perform a better analysis of the melanization and to determine why the *pex6Δ* appressoria were non-functional, we performed thin-section electron microscopy (TEM) on 24-h-old appressoria from these strains. In wild-type appressorial sections, an electron dense layer of melanin was distinctly observed and was

Fig. 4. Loss of appressorial melanin and Woronin bodies in the *pex6Δ* strain.
A. Conidia harvested from the wild-type strain or the *pex6Δ* or the rescued strain were incubated on artificial inductive surfaces for 24 h and observed by Hoffman modulation contrast optics based light microscopy.
B. Ultrastructural analysis of the appressorium and mycelium. Twenty-four-hour-old appressoria of the wild-type, *pex6Δ* and rescued strains were processed for TEM. As a control for non-melanized appressoria, wild-type conidia were allowed to form appressoria in the presence of tricylazole. Boxed area in the inset demarcates the magnified region of the outer layers of the appressoria presented in the WT panel. Bar = 200 nm.
C. Ultrastructure of *pex6Δ* mycelia. Mycelia, harvested from 48 h liquid cultures of the wild-type, *pex6Δ* and the rescued strains, were processed for TEM analysis. Bar = 200 nm.

various *pex6Δ* appressoria (*n* = 30) observed, this mela-nin layer was completely absent (Fig. 4B). As a control for non-melanized appressoria, TEM was also conducted on appressoria formed by wild-type conidia in the presence of tricyclazole, a well-known inhibitor of melanin synthesis. As in *pex6Δ* appressoria, the melanin layer was also found to be absent in tricylazole-treated appressoria. Further-more, the melanin layer was restored in the rescued strain carrying the *PEX6* complementing clone (Fig. 4B, res-cued). The aberrant morphology of the *pex6Δ* appressoria was reminiscent of the misshapen appressoria observed in the mutant (*hex1Δ*, Soundararajan *et al.*, 2004) lacking the Woronin bodies. TEM analysis of the *pex6Δ* mutant confirmed that these strains were devoid of Woronin bod-ies (Fig. 4C). We conclude that the *pex6Δ* strains lack Woronin bodies; are incapable of appressorial melaniza-tion and as a major consequence rendered non-functional in the infection cycle.

Carnitine acetyl-transferases in Magnaporthe

It has been proposed that fungal melanin synthesis uti-lizes acetyl-CoA as precursor molecules (Chumley and Valent, 1990) and peroxisomal beta-oxidation of fatty acids could be a potential source for acetyl-CoA biogen-esis (Thines *et al.*, 2000; Kimura *et al.*, 2001). As *pex6Δ* is unable to metabolize long-chain fatty acids, we rea-soned that the transfer of fatty acids and acyl groups from peroxisomes to the cytoplasm and/or to the mitochondria, will either be suboptimal or abolished in this mutant. In eukaryotes, the transfer of acyl groups across intracellular membranes is facilitated by carnitine. Hence, we decided to investigate the role of CrAT (EC number 2.3.1.7), which play a role in the requisite modification and movement of acetyl-CoA between membrane-bound organelles and the cytoplasm. In *Saccharomyces cerevisiae*, there are three CrAT enzymes with specific and overlapping localizations to the peroxisome, mitochondria and cytoplasm. A TBLASTN (Altschul *et al.*, 1997) search of the *S. cerevisiae* CrATs against the *Magnaporthe* genome revealed that there are only two CrATs (designated *CRAT1/*MG01721.4 and *CRAT2/*MG06981.4) encoded within the *M. grisea* genome (Fig. S1).

We re-annotated the MG01721.4 locus and found that the Crat1 protein shows the highest similarity to *S. cerevisiae CAT2* and shared 40% amino acid identity (e = −116). Cat2p localizes to both the mitochondrion and the peroxisome (Swiegers *et al.*, 2001). *In silico* analysis of Crat1 using subcellular localization prediction programs (PSORTII and TARGETP; Nakai and Horton, 1999; Emanuelsson *et al.*, 2000) failed to reveal any canonical mitochondrial localization motif. However, a distinct PTS1 (serine-lysine-leucine; SKL) signature was detected at its C-terminus, thus supporting a peroxisomal localization for

the protein encoded by the *CRAT1/*MG01721 ORF. An as yet uncharacterized mutation termed *Pth2* (Sweigard *et al.*, 1998) has been identified at the MG01721 locus, hereafter we refer to *CRAT1/*MG01721 as *PTH2*. MG06981, the other CrAT that we identified in *Mag-naporthe* showed the highest similarity to *Neurospora crassa FacC* (e = −34, 55% amino acid identity). The *FacC* orthologue in *Aspergillus nidulans* has been studied and is predicted to localize to the cytoplasm (Stemple *et al.*, 1998). MG06981.4 ORF will henceforth be referred to as *CRAT2* and its product as Crat2.

Pathogenesis-related defects in CrAT minus mutants

To determine the role of CrATs in *Magnaporthe* pathogen-esis, deletion strains of the *PTH2, CRAT2* and *PTH2 CRAT2* were generated in the B157 wild-type background. Using single step gene replacement strategy, the com-plete ORF of *PTH2* and *CrAT2* were replaced with the selection markers coding for hygromycin and bialaphos resistance respectively. PCR assisted specific amplifica-tions, and Southern hybridizations confirmed that the cor-rect gene replacement events had taken place in the selected single and double mutant transformants (data not shown). At least two independent deletion strains in each instance were used for all the phenotypic and functional analyses presented here.

The pathogenicity and pathogenesis-related traits of the different CrAT-delete mutants were assessed in detached barley leaf infection assays. Inoculations with increasing conidial loads of *pth2Δ* and *pth2Δ crat2Δ* strains demon-strated that both mutants were completely non-pathogenic (Fig. 5A). In contrast, the *crat2Δ* strain elicited disease symptoms similar to wild-type levels (Fig. 5A). The rate and frequency of appressorium formation was assessed at different time points during infection assays using the CrAT-delete mutants. Both *pth2Δ* and *pth2Δ crat2Δ* mutants exhibited a delay in appressorium formation dur-ing the early period of the process. At 4 h after inoculation, the number of appressoria in these strains was $50 \pm 1.5\%$ of those seen in the wild type. At 6 h post inoculation, appressorium formation had increased to $80 \pm 2.2\%$ of that observed for the wild type. At 24 h, the overall number of appressoria was similar in the wild type and in the *pth2Δ* and *pth2Δ crat2Δ* mutants. Appressorium formation in *crat2Δ* was similar to the wild-type rate throughout the duration of the process. Observations and quantifications for host penetration capability as judged by aniline blue staining for callose deposits and penetration hyphae, revealed that the *pth2Δ* like the *pex6Δ* produced non-functional appressoria that failed to elaborate any pene-tration pegs or infection/penetration hyphae (Fig. 5B). At the 48 h, and even the 96 h time point, these mutant appressoria did not elaborate any host penetration struc-
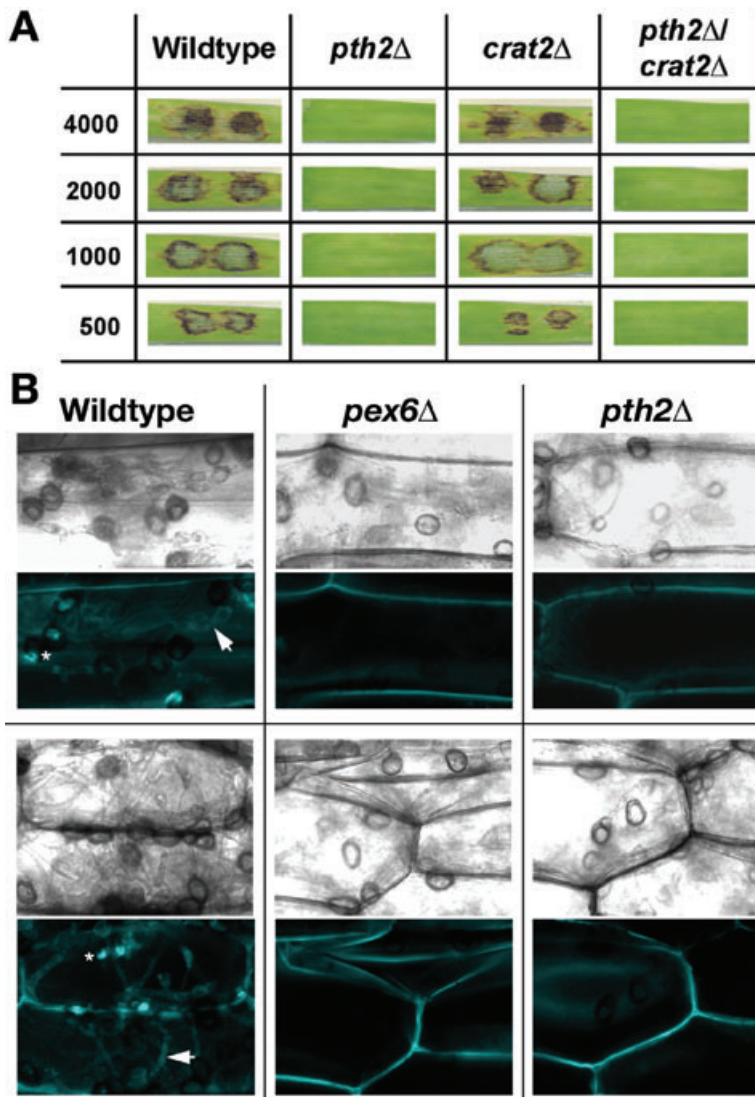
Fig. 5. Pathogenicity related defects in the CrAT-delete mutants.
A. Detached barley leaf infection assay. Leaf explants from barley were inoculated with the indicated number of conidia from the wild type or the indicated CrAT mutants, and disease symptoms were assessed after 7 days.
B. Loss of host penetration in *pth2Δ* and *pex6Δ* mutants. Equal number of conidia from the wild-type, *pex6Δ* or the *pth2Δ* strain were inoculated on barley leaf explants. The number of papillary callose deposits (asterisk) and infection hyphae (arrowhead) were quantified after staining with aniline blue at 48 h (top panel) or 96 h (lower panel) post inoculation. Scale bar represents 10 μm.

tures (Fig. 5B). Thus, we conclude that Pth2 activity plays a major and essential role in the host penetration step of the rice-blast infection cycle.

PTH2 function is required for proper melanization during pathogenic growth

As the host penetration defects observed during appressorium function of *pth2Δ* mutant were remarkably similar to the ones shown by the *pex6Δ* appressoria, we decided to test the appressorial melanization in the *pth2Δ*, *crat2Δ* and *pth2Δ crat2Δ* mutants. As shown in Fig. 6, the *pth2Δ* mutant appressoria showed a significant reduction in the overall melanization of the appressoria. Such reduction in melanin deposition was not seen in the *crat2Δ* mutants, whereas the decrease in the layer was again evident in the appressoria formed by the *pth2Δ crat2Δ* double mutant (Fig. 6, bottom panels). We conclude that the Pth2 activity is involved in efficient melanization of appressoria, and the

defect observed in the appressoria function could be a consequence of this reduction of melanin. It is, however, possible that the loss of pathogenicity in the *pth2Δ* mutant may not be due solely to such a reduction in pigmentation, but could be due to combinatorial defects in the fatty acid utilization pathway, improper melanization in appressoria, or the general defect in acetyl CoA transport as observed in the *pth2Δ* mutant.

Metabolic function of Magnaporthe *CrAT*

Carnitine acetyl-transferase assays utilizing acetyl-CoA as a substrate were conducted to quantify and compare the total levels of CrAT enzyme activity in the wild type, *pth2Δ*, *crat2Δ* and the *pth2Δ crat2Δ* mutant. We found that in the wild-type strain, the total CrAT activity (specific activity 24.5 ± 1.1 nmol min^{-1} mg^{-1} protein) was induced by olive oil and acetate but was not repressed by glucose. In the *pth2Δ* mutant, CrAT activity was found to be
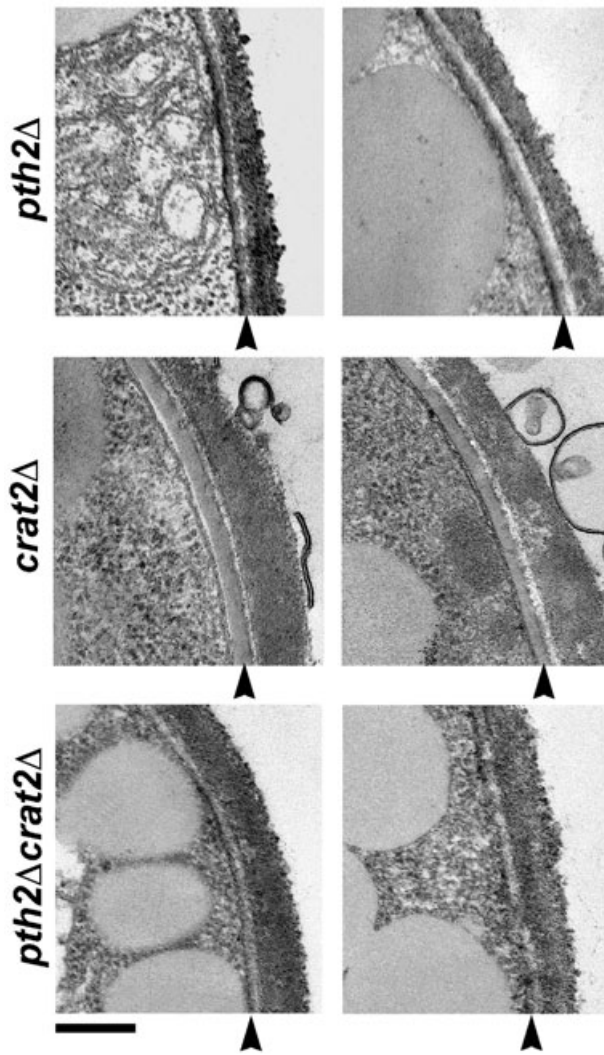
Fig. 6. Reduction of appressorial melanization in the CrAT delete mutants. Conidiospores from the CrAT mutants (*pth2Δ, crat2Δ* and the *pth2Δ crat2Δ*) were spotted onto artificial inductive membranes and allowed to incubate for 24 h and then processed for TEM analysis as described. Bar = 200 nm. Representative images from two independent appressoria from each mutant strain are depicted.

significantly reduced (specific activity 1.6 ± 0.8 nmol min⁻¹ mg⁻¹ protein) and could not be elevated by either olive oil or acetate. In the *crat2Δ*, olive oil and acetate treatment elicited a slight induction in the enzyme activity although not as effectively as in the wild-type strain. CrAT activity was similar in wild-type and *crat2Δ* (specific activity 22.8 ± 1.6 nmol min⁻¹ mg⁻¹ protein) strains during glucose treatment. The *pth2Δ crat2Δ* mutant strain showed negligible amounts (0.09 ± 0.21 nmol min⁻¹ mg⁻¹ protein) of overall CrAT activity.

The ability to metabolize different carbon sources was evaluated for the CrAT-minus mutants (Fig. 7A). Wild-type strain utilized glucose and olive oil equally efficiently, whereas acetate was consumed to a lesser extent. The

pth2Δ and the *pth2Δ crat2Δ* mutant grew normally on glucose containing medium but were unable to utilize olive oil or acetate. There were no discernable differences between the growth of *crat2Δ* strain and the wild type on all the carbon sources tested (Fig. 7A). Based on these results, we conclude that *PTH2* function provides the
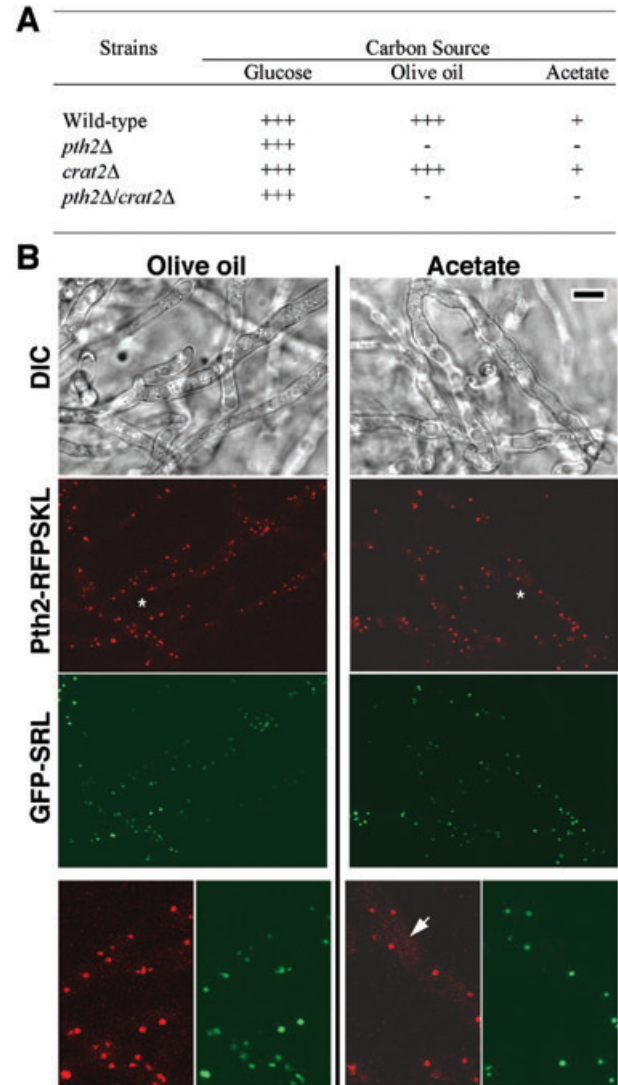
Fig. 7. Utilization of different carbon sources by CrAT-delete mutants and subcellular localization of Pth2.
A. Growth of CrAT minus mutants on different carbon sources. *Magnaporthe* wild-type and the indicated CrAT mutant strains were cultured on basal medium containing either 1% glucose or 1% olive oil or 50 mM acetate as carbon source. Growth was assessed after 10 days.
B. Subcellular localization of Pth2–RFPSKL. *Magnaporthe* strain B1163 (relevant genotype *PTH2:RFP-SKL*; *GFP-PTS1*) was cultured in medium containing either olive oil or acetate as the sole source of carbon. Laser scanning confocal microscopy using appropriate filters (or DIC, differential interference contrast) was then performed on such mycelia to image GFP and RFP epifluorescence. Scale bar depicts 5 μm. The lower panels represent 4× magnifications of the regions denoted by the asterisk in each instance together with their respective GFP counterparts.

major CrAT activity in *Magnaporthe* and it also regulates the utilization of fatty acids and acetate as carbon source. The contribution of Crat2 to cellular CrAT levels and its role in fatty acid or acetate utilization were inferred to be insignificant.

Our semiquantitative reverse transcriptase polymerase chain reaction (RT-PCR) based analyses revealed that the transcription of *PTH2* (and to some extent *CRAT2*) was induced by olive oil and acetate in the wild-type strain (Fig. S2; also please refer to Bhambra *et al.*, 2006 for detailed analysis of *PTH2* transcript levels). *In silico* predictions suggested a peroxisomal location for Pth2p, but our findings that Pth2 was essential for acetate utilization raised the possibility that Pth2 might also be present in a non-peroxisomal pool. We therefore proceeded to carry out a detailed analysis of the subcellular localization of a Pth2–RFPSKL fusion protein (using strain B1163 and laser scanning confocal microscopy) during growth in olive oil or acetate containing medium. As shown in Fig. 7B, the subcellular location of the Pth2–RFPSKL protein was the same as that observed for the GFP-PTS1 signal, with both the fusion proteins colocalizing predominantly within the peroxisomes. Such colocalization pattern of the Pth2–RFPSKL and the GFP-PTS1 did not differ significantly when compared between growth on olive oil or acetate. However, under both the conditions, a separate albeit limited subcellular localization (inferred to be cytosolic) of Pth2–RFPSKL was evident which was distinct from the GFP-PTS1 containing compartments (Fig. 7B, magnified insets). This cytoplasmic pool appeared to be more prominent under acetate replete conditions (Fig. 7B, arrowhead). We conclude that *PTH2* transcription is induced by fatty acids and acetate and that Pth2 is predominantly peroxisomal but could also be present in the cytosol although in very limited amounts.

Role of peroxisomal acetyl-CoA in Magnaporthe pathogenesis

Our findings showed that the *pex6Δ* mutant has a strong defect in fatty acid β-oxidation in peroxisomes and further suggested that the peroxisome-associated Pth2 activity could be required to fulfil some of the β-oxidation pathway requirements during pathogenesis. Further support for this hypothesis came from the observation that the loss of *CRAT2* function did not influence *Magnaporthe* virulence (Fig. 5A) and that *CRAT2* was not expressed during the pathogenic phase (Fig. S2).

Studies in some lower eukaryotes have shown that acetyl-CoA produced by β-oxidation in the peroxisomes is transported to the mitochondrion to replenish the intermediates of the citric acid cycle. However, the transport of the products of β-oxidation out of the peroxisomes and into the mitochondria is not well understood (Hooks,

2002). Products of the peroxisomal β-oxidation are also routed into gluconeogenesis via the glyoxylate cycle, through which two carbon compounds are assimilated into the tricarboxylic acid (TCA) cycle. We reasoned that the *pex6Δ* mutant might be unable to supply such products and/or their precursors. Additionally, glucose metabolism supplies some of the intermediates of the citric acid cycle in a peroxisome-independent manner. We therefore investigated appressorial function in the *pex6Δ* and the *pth2Δ* mutant in the presence of excess metabolic intermediates such as glucose, citrate, malate or succinate. As shown in Fig. 8A, appressorium-mediated host penetration and blast disease elaboration was normal in the WT strain in the presence (or absence) of glucose or citrate. On the other hand and rather interestingly, the presence of glucose (but not citrate or malate or succinate) caused a slight remediation of the host penetration defect in the *pth2Δ* mutant (Fig. 8A). Upon quantification, such limited restoration of appressorium function in the *pth2Δ* was found to be about $18.8 \pm 0.4\%$ (Fig. 8B). However, the resultant penetration hyphae in the glucose-treated *pth2Δ* samples were found to be incapable of proper proliferation within the host tissue (Fig. 8C and A). Rather surprisingly, treatment with either glucose or citrate did not restore the appressorial function (of host penetration) in the *pex6Δ* mutant (Fig. 8A), thus maintaining the *pex6Δ* mutant's inability to gain entry into (and to elicit disease symptoms) on host leaf surfaces (Fig. 8A and B).

Our earlier results (Fig. 6) hinted at a significant reduction in overall thickness of the appressorial cell walls in the *pth2Δ* mutant. We therefore tested whether cell wall integrity was compromised in these mutants. To this end, we decided to analyse the sensitivity of the wild type, the *pex6Δ* and the *pth2Δ* to cell wall-perturbing agents such as Calcofluor white and Congo red. Compared with the WT strain, the *pth2Δ* and the *pex6Δ* mutant were found to be significantly sensitive to Calcofluor white (Fig. 8D) whereas the *pex6Δ* showed increased sensitivity to cell wall perturbations with Congo red (Fig. 8D). Based on these results, we conclude that the *pth2Δ* and the *pex6Δ* mutant show weakened cell walls, and speculate that such reduced cell wall integrity (or biosynthesis) in a glucose-deficient environment is the likely cause of the loss of appressorial function in the *pth2Δ* and the *pex6Δ* mutant. We also construe that acetyl-CoA generated by peroxisomal activity likely feeds into the glyoxylate cycle and gluconeogenic pathway for cell wall synthesis during penetration-peg formation.

Discussion

In recent years, it has become clear that fatty acid metabolism plays a crucial role during fungal pathogenesis (Kimura *et al.*, 2001; Both *et al.*, 2005). In *Magnaporthe*,
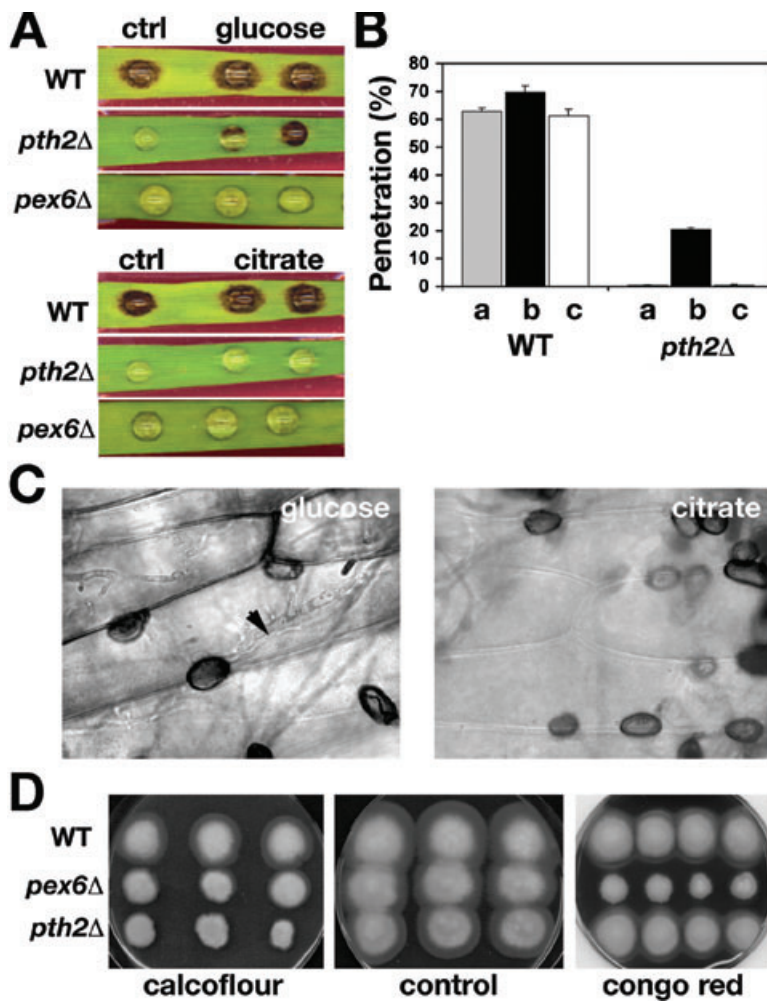
Fig. 8. Chemical supplementation partially rescues the pathogenicity defects in *pth2Δ* strain.
A. Appressorium formation and function. Conidia from wild-type (WT), *pth2Δ* or *pex6Δ* strains were inoculated on barley leaf explants and allowed to form appressoria in water (Ctrl) or 2.5% glucose or 1% sodium citrate. The number of appressoria was assessed 24 h after inoculation and penetration efficiency after a 36 h incubation. Disease symptoms were evaluated 7 days post inoculation.
B. Quantification of appressorium function. Conidia of wild-type, or *pth2Δ* strains were inoculated on barley leaf explants in the presence of water (a), 2.5% glucose (b) or citrate (c). Penetration peg formation and infectious hyphae development were evaluated 3 days post inoculation.
C. Light microscopic analysis of acid fuchsin stained fungal structures in the chemical remediation experiments described in panels A and B above.
D. Weakening of fungal cell walls due to loss of *PEX6* or *PTH2* function. Conidia from the wild-type, *pex6Δ* or the *pth2Δ* strains were grown in the presence (100 μg ml^{-1}) or absence (control) of Calcofluor white or Congo red.

the degradation of lipid reserves contributes to turgor generation in the developing appressorium (Thines *et al.*, 2000). The loss or reduction in the pathogenicity of mutants in different glyoxylate cycle enzymes, such as isocitrate lyase (Lorenz and Fink, 2001; Idnurm and Howlett, 2002; Wang *et al.*, 2003) and malate synthase (Solomon *et al.*, 2004), likewise indicates that fatty acid β-oxidation is the predominant catabolic process during early pathogenesis in fungi. Across different organisms, fatty acid β-oxidation has been shown to occur primarily within the peroxisomes. However, very little is known about the mechanisms that transport the products of the peroxisomal fatty acid metabolism. In this study, we initially identified a *PEX6* orthologue in *Magnaporthe* that is required for growth on fatty acids and is essential for pathogenicity. Loss of *PEX6* function led to completely non-melanized appressoria, which were unable to elaborate penetration pegs and infection hyphae. Based on its inability to utilize long-chain fatty acids, and the failure to import PTS1-containing peroxisomal matrix proteins, we showed that the *pex6Δ* mutant lacked functional peroxi-

somes. Through genetic complementation analysis using a WT *PEX6* allele, we confirmed that the phenotypic and metabolic defects in the *pex6Δ* strain resulted solely from the disruption of the *PEX6* function in this mutant.

Previously characterized *Magnaporthe* mutants, which harbour lesions that downregulate enzymes of the melanin biosynthesis pathway, have been shown to be similarly blocked in the initial host penetration stage (Chumley and Valent, 1990). Fungal melanin is synthesized through a polyketide pathway, which presumably utilizes acetyl-CoA as precursor (Kimura *et al.*, 2001). This raised the possibility that acetyl-CoA derived from fatty acid catabolism in peroxisomes is an important pool of such precursors for appressorial melanin biosynthesis in *Magnaporthe*. The acetyl-CoA molecule is membrane-impermeable and its transport between intracellular compartments for energy production and biosynthesis functions is mediated through the formation of carnitine intermediates. CrAT catalyse the reversible reaction, which transfers the acetate moiety between coenzyme-A and carnitine (Ramsay and Naismith, 2003). To further investigate the functional

importance of the peroxisomal acetyl-CoA pool and its transport, we created loss-of-function mutants in the two genes, *PTH2* (MG01721) and *CRAT2* (MG06981), encoding CrAT in *Magnaporthe*. A double mutant that disrupted both these CrATs was also analysed. Characterization of these CrAT-delete mutants revealed that *PTH2* was indispensable for the appressorial function of host penetration and that *CRAT2* did not play any significant role during the pathogenic growth phase in *Magnaporthe*.

In *Aspergillus*, CrAT activity is contributed by two genes: *ACUJ* which encodes a putative peroxisomal and/or mitochondrial CrAT, and *FacC* which produces a putative cytosolic CrAT (Stemple *et al.*, 1998). Using subcellular localization studies, we confirmed that the Pth2–RFPSKL fusion protein is predominantly peroxisomal, with a minor pool confined to the cytoplasm. The intrinsic PTS1 signal in Pth2 protein is thus fully functional as has been confirmed in a parallel study too (Bhambra *et al.*, 2006). On the other hand, Crat2 is expected to be exclusively cytoplasmic based simply on *in silico* predictions (European Bioinformatics Institute, http://www.ebi.ac.uk; and PSORT, http://psort.ims.u-tokyo.ac.jp).

Rather surprisingly, *PTH2* was found to be essential for utilization of long-chain fatty acids and of acetate. In contrast, *CRAT2* function was dispensable under these growth conditions. In *Aspergillus* and in yeast, the major source of CrAT activity depends on the growth substrate and each CrAT is individually required for the metabolism of a specific class of substrates, for example *ACUJ* for fatty acids, *FACC* for acetate and *YAT2* for ethanol (Elgersma *et al.*, 1995; Stemple *et al.*, 1998; Swiegers *et al.*, 2001). Our quantifications of total CrAT specific activity in non-induced (glucose) and induced (olive oil or acetate) cultures of *Magnaporthe* WT and CrAT-delete strains revealed that Pth2 provides the major CrAT activity (> 95% of total) in the rice-blast fungus. Interestingly, *PTH2* was also found to be essential for mobilization of lipid bodies during early appressorium development in *Magnaporthe* (data not shown; Bhambra *et al.*, 2006). It is thus possible that the dual localization (peroxisomal and cytoplasmic) of Pth2 allows it to function as a unique and the major CrAT (and likely a fatty-acid acyl carrier too) in *Magnaporthe*.

Our results proved that carnitine-based transport of acetyl-CoA is essential for *Magnaporthe* infectivity. The pathogenicity defects in the *pth2Δ* related particularly to the delay in appressoria formation and to the lack of penetration pegs were identical to those shown by the *pex6Δ* further confirming that Pth2 is the major CrAT that transports peroxisomal acetyl-CoA (and/or other related products of fatty acid β-oxidation therein) in the appressoria. Our observations that *pth2Δ* (and the *pth2Δ crat2Δ*) appressoria show reduced melanization, rather than a complete loss of melanin deposition observed in *pex6Δ*,

indicated that melanin biosynthesis in the appressoria does not depend exclusively on the peroxisome-derived acetyl-CoA pool. Thus, it is possible that there are other distinct source(s) of acetyl-CoA available for melanin synthesis in the appressorium, although these alternate pools of acetyl-CoA are unable to compensate for the loss of the peroxisomal pool. Alternatively, peroxisomes might provide chain-shortened fatty acids to the mitochondrial β-oxidation machinery in *Magnaporthe* and that the proposed auxiliary fatty acid metabolism pathway (Maggio-Hall and Keller, 2004) within the mitochondria contributes some acetyl-CoA for melanin synthesis in the appressoria. It is also possible that the peroxisomal acetyl-CoA takes an alternate exit route, such as the glyoxylate shunt to be assimilated in the TCA cycle and subsequently the gluconeogenesis pathway (Gainey *et al.*, 1992; Lorenz and Fink, 2001). The glyoxylate shunt has been shown at least in part to be peroxisomal in plants and fungi, although it does share some of the mitochondrial enzymes as well (Gainey *et al.*, 1992; Pracharoenwattana *et al.*, 2005).

Our data from the chemical supplementation experiments revealed that excess (2.5%) glucose could partially suppress the pathogenicity defects associated with the *pth2Δ* mutant. We did not find any remediation of these mutant defects neither with lower concentrations of glucose nor with the products of the glyoxylate pathway such as citrate, malate or succinate. It is likely that such exogenous glyoxylate intermediates are not assimilated by the mitochondria or that the overall reduction of cytoplasmic acetyl-CoA (due to the loss of peroxisomal acetyl-CoA pool) inactivates the pyruvate carboxylase.

Based on our observations that the cell walls in the *pex6Δ* and the *pth2Δ* are weakened (as judged by sensitivity to Calcofluor white and Congo red, and by direct TEM analysis), and that glucose can partially remediate the pathogenicity related defects in *pth2Δ*, we tend to believe that peroxisome-derived acetyl-CoA feeds into the glyoxylate and gluconeogenic pathways for glucan and chitin synthesis during the penetration peg formation. Glucose-based remediation partially reinstated the formation of penetration pegs and infectious hyphae in the *pth2Δ* mutant, thus supporting our working hypothesis that cell wall biosynthesis in a nutrient-limiting environment is the likely cause for the lack of appressorium function at least in the *pth2Δ* mutant background. Although the *pex6Δ* and *pth2Δ* mycelia were equally sensitive to Calcofluor white, the perturbations with Congo red revealed a major difference between *pex6Δ* and *pth2Δ*. The fungal cell wall consists of mannosylated proteins and three kinds of polysaccharide chains (reviewed in Klis *et al.*, 2002) and this apparently rigid and dynamic structure maintains a high degree of flexibility for adaptation to different developmental programmes (Duran and Nombela, 2004). The exact mechanism of action of Congo red remains elusive,

although it is known to interfere with proper cell wall assembly and to associate with mannosylated proteins (Kopecka and Gabriel, 1992). In budding yeast, treatment with cell wall-perturbing agents elicits a cell survival response called 'the compensatory mechanism' that is characterized by an increase of chitin content, an over-production of mannoproteins, changes in the association between cell wall polymers, and redistribution of β-1, 3 glucan synthase and activation of stress signalling (Smits *et al.*, 2001; and references therein). Our data on sensitivity of mutants towards Congo red suggest that intact/functional peroxisomes are necessary for the elaboration of such compensatory cell survival mechanism(s), which perhaps does not rely as much on the transfer of acetyl-CoA or fatty acids across the requisite organellar/subcellular compartments.

Additionally, we have shown here that the *pex6Δ* lacks Woronin bodies, and shows similar defects in the appressorial morphology as seen in the *hex1Δ* mutant (Soundararajan *et al.*, 2004). The lack of even a partial restoration with glucose in the *pex6Δ* could be due to the harmful effects either of excess fatty acid accumulation in this mutant, or retention of some toxic intermediates, or of defects in other peroxisomal activities related to either Woronin body function in *Magnaporthe* (Soundararajan *et al.*, 2004) or those involved in the downregulation of hydrogen peroxide. Future research will address some of these issues and will aim to gain insight into the products of the peroxisomal and mitochondrial β-oxidation machineries, and examine the overall generation, transport and specific utilization of acetyl-CoA within the unicellular appressorium in *Magnaporthe*.

Experimental procedures

Fungal strains and culture conditions

The *M. grisea* wild-type strains B157 was obtained from the Directorate of Rice Research (Hyderabad, India), and WT strains Guy11 and TH3 were a kind gift from CIRAD (France). For culture maintenance and conidiation, wild-type and mutant strains were grown on prune agar medium (PA; per litre: 40 ml of prune juice, 5 g of lactose, 1 g of yeast extract and 20 g of agar, pH 6.0). For assessment of growth on different carbon sources, basal medium (0.67% yeast nitrogen base without amino acids, 0.1% yeast extract, pH 6.0 with Na$_2$HPO$_4$) was supplemented with either 1% glucose or 1% olive oil or 50 mM sodium acetate. Mycelia used for genomic DNA, total RNA, and total protein extractions was harvested from cultures grown in liquid complete medium (CM) or minimal medium (MM), as described previously (Soundararajan *et al.*, 2004).

Molecular methods

The potassium acetate method was used for extraction of fungal DNA (Naqvi *et al.*, 1995). DNA gel blot analysis was performed using standard protocols (Sambrook *et al.*, 1989). Probe-labelling and DNA blot detections were done using the ECL direct nucleic acid labelling and detection system (Amersham Biosciences, UK).

Magnaporthe deletion mutants were generated using the standard one-step gene replacement strategy. For each gene, about 1 kb of 5′ and 3′ regions were PCR amplified and ligated into pFGL59 or pFGL97 vector which contained the hygromycin phosphotransferase gene or ammonium glufosinate-resistance gene, respectively, under the TrpC promoter. The gene-replacement constructs were introduced into *M. grisea* and transformants were selected either on CM containing 250 μg ml^{-1} hygromycin or defined complex medium (DCM; 0.16% yeast nitrogen base without amino acids, 0.2% asparagine, 0.1% ammonium nitrate and 1% glucose, pH 6.0 with Na$_2$HPO$_4$) containing 40 μg ml^{-1} ammonium glufosinate (Cluzeau Info Labo, France). Correct gene replacement events were confirmed by PCR and DNA gel blot analyses. A 7.2 kb KpnI fragment from BAC clone 2A14, which contained the entire *Magnaporthe PEX6* locus, was used to rescue the *pex6Δ* strain.

For RT-PCR analyses, total RNA was extracted from cultures grown 24 h in glucose MM and then transferred to the medium containing either glucose, olive oil or acetate for 8 h. RNA was extracted using sodium acetate buffer (50 mM sodium acetate, 10 mM EDTA, 1% SDS) and acidic phenol and precipitated with isopropanol. AMV reverse transcriptase (Roche Diagnostics, Penzberg, Germany) was used to synthesize cDNA from 2 μg of total RNA. RT-PCR products were amplified using primers designed for the following *Magnaporthe* genes: *PTH2* (MG01721.4), *CRAT2* (MG06981.4), MG00803.4 (β-tubulin) and *MPG1*. Additionally, ethidium bromide-stained rRNA (not shown) served as a loading control too. To assess the specificity and to serve as a negative control (not shown), the RNA sample in each instance was also processed without a reverse transcriptase step prior to the PCR amplification.

For expression of GFP-PTS1, GFP-SRL was cloned under the control of the *MPG1* promoter and TrpC terminator from plasmid pFC2-ORF-GFP (a kind gift from Heidi Bohnert and Marc-Henri Lebrun). This construct was transformed into the wild-type and the *pex6Δ* strains. For subcellular localization of Pth2 protein, an RFP-SKL tag was introduced at the C-terminus immediately before the SKL coding region of the genomic copy of *PTH2*. The fusion construct pFGL421 was created by cloning 1 kb of the *PTH2* 3′UTR into the PstI/HindIII sites of pFGL347. The gene encoding red fluorescent protein (RFP) was amplified from the plasmid pDsRed-Monomer-N1 (Clontech, CA, USA) with a reverse primer that incorporated the tripeptide SKL before the stop codon. The RFP-SKL was cloned in frame with the last 377 bp of the *PTH2* C-terminus (just proximal to the codons encoding SKL, which were excluded) in the XhoI/BamHI sites of pFGL421. The fusion construct was verified by nucleotide sequencing and transformed into a *Magnaporthe* strain expressing GFP-PTS1 (see above). Transformants were selected on hygromycin and bialaphos-supplemented medium and correct gene replacement events confirmed by PCR and nucleotide sequence analyses. Selected transformants (including the strain B1163 that was finally used) were also tested for

growth on olive oil medium to further confirm that the RFP-SKL tag did not compromise the *PTH2* function.

Appressorial assays and pathogenicity tests

Conidia were harvested from 10-day-old PA-medium grown cultures and inoculated at equivalent concentrations on artificial membranes (Gelbond™, Biowhittaker Molecular Applications, Rockland, ME, USA) and/or detached barley leaves. The total number of appressoria formed was quantified after an incubation of 24 h. Appressorial function was assessed by counting the number of penetration pegs and penetration hyphae on barley leaves at 24, 48, 72 and 96 h after inoculation with the requisite conidial suspension. We assessed penetration peg formation by staining papillary callose deposits with aniline blue (Adam and Somerville, 1996; Vogel and Somerville, 2000; Jacobs *et al.*, 2003). Penetration/infection hyphae were detected by autofluorescence under ultraviolet light or by aniline blue stainings (Jacobs *et al.*, 2003). For lesion formation on detached barley leaves, inoculated samples were incubated for 9 days in a growth chamber (22°C, 16 h light/8 h dark). Spray inoculations on rice cultivar CO39 were conducted as previously described (Naqvi *et al.*, 1995). For chemical supplementation experiments, equal number of conidia were inoculated on barley leaf explants in the presence of 0.1% or 2.5% glucose, or 1% sodium citrate, or 1% sodium malate or 1% succinate.

Carnitine acetyl-transferase assays

Magnaporthe grisea strains were grown for 3 days (28°C, 120 rpm) in MM + glucose, after which they were transferred to MM containing either 1% glucose or 1% olive oil or 50 mM sodium acetate and incubated for another 4 h. Protein extracts were prepared by grinding filtered mycelia in liquid nitrogen and resuspending in extraction buffer (50 mM Tris-Cl pH 7.5, 50 mM NaCl, 0.2% Triton X-100, proteinase inhibitors). Cell debris was removed by centrifugation and total protein concentrations were determined using the Bio-Rad protein assay reagent (Bio-Rad Laboratories, Hercules, CA, USA). Equal protein concentrations were used for the assays. CrAT assays and quantifications of the specific activity therein were performed as described (Stemple *et al.*, 1998).

Fluorescence and electron microscopy

GFP epifluorescence was observed using a Zeiss LSM510 inverted confocal microscope (Carl Zeiss, Thornwood, NY, USA) equipped with a 30 mW argon laser. The objectives used were either a 63× Plan-Apochromat (numerical aperture, 1.4) or a 100× Achromat (n.a. 1.25) oil immersion lens. EGFP was imaged with 488 nm wavelength laser excitation, using a 505–530 nm band pass emission filter, while RFP imaging used 543 nm laser and a 560 nm long-pass emission filter.

Twenty-four-hour-old appressoria formed on inductive membranes (Gelbond™) were processed for TEM. For tricyclazole (Cluzeau Info Labo, France) treatment, wild-type conidia were allowed to germinate and form appressoria in the presence of 8 μg ml⁻¹ tricyclazole. Processing and imaging of TEM samples were done as described previously (Soundararajan *et al.*, 2004).

References

Adam, L., and Somerville, S.C. (1996) Genetic characterization of five powdery mildew disease resistance loci in *Arabidopsis thaliana*. *Plant J* **9:** 341–356.

Altschul, S.F., Madden, T.L., Schaffer, A.A., Zhang, J., Zhang, Z., Miller, W., and Lipman, D.J. (1997) Gapped BLAST and PSI-BLAST: a new generation of protein database search programs. *Nucleic Acids Res* **25:** 3389–3402.

Bhambra, G.K., Wang, Z.Y., Soanes, D.M., Wakley, G.E., and Talbot, N.J. (2006) Peroxisomal carnitine acetyl-transferase is required for elaboration of penetration hyphae during plant infection by *Magnaporthe grisea*. *Mol Microbiol* doi:10.1111/j.1365-2958.2006.05209.x.

Both, M., Csukai, M., Stumpf, M.P., and Spanu, P.D. (2005) Gene expression profiles of *Blumeria graminis* indicate dynamic changes to primary metabolism during development of an obligate biotrophic pathogen. *Plant Cell* **17:** 2107–2122.

Chumley, F.G., and Valent, B. (1990) Genetic analysis of melanin-deficient, non-pathogenic mutants of *Magnaporthe grisea*. *Mol Plant Microbe Interact* **3:** 135–143.

van Der Bosch, H., Schutgens, R.B.H., Wanders, R.A., and Tager, J.M. (1992) Biochemistry of peroxisomes. *Annu Rev Biochem* **61:** 157–197.

Duran, A., and Nombela, C. (2004) Fungal cell wall biogenesis: building a dynamic interface with the environment. *Microbiology* **150:** 3099–3103.

Elgersma, Y., van Roermund, C.W., Wanders, R.J., and Tabak, H.F. (1995) Peroxisomal and mitochondrial carnitine acetyl-transferases of *Saccharomyces cerevisiae* are encoded by a single gene. *EMBO J* **14:** 3472–3479.

Emanuelsson, O., Nielsen, H., Brunak, S., and von Heijne, G. (2000) Predicting subcellular localization of proteins based on their N-terminal amino acid sequence. *J Mol Biol* **300:** 1005–1016.

Gainey, L.D., Connerton, I.F., Lewis, E.H., Turner, G., and Ballance, D.J. (1992) Characterization of the glyoxysomal isocitrate lyase genes of *Aspergillus nidulans* (acuD) and *Neurospora crassa* (acu-3). *Curr Genet* **21:** 43–47.

Hooks, M.A. (2002) Molecular biology, enzymology, and the physiology of β-oxidation. In *Plant Peroxisomes*. Baker, A.,

and Graham, I.A. (eds). London: Kluwer Academic Publishers, pp. 19–55.

Idnurm, A., and Howlett, B.J. (2002) Isocitrate lyase is essential for pathogenicity of the fungus *Leptosphaeria maculans* to canola (*Brassica napus*). *Eukaryot Cell* **1:** 719–724.

Jacobs, A.K., Lipka, V., Burton, R.A., Panstruga, R., Strizhov, N., Schulze-Lefert, P., and Fincher, G.B. (2003) An *Arabidopsis* callose synthase, GSL5, is required for wound and papillary callose formation. *Plant Cell* **15:** 2503–2513.

Jedd, G., and Chua, N.H. (2000) A new self-assembled peroxisomal vesicle required for efficient resealing of the plasma membrane. *Nat Cell Biol* **2:** 226–231.

Kimura, A., Takano, Y., Furusawa, I., and Okuno, T. (2001) Peroxisomal metabolic function is required for appressorium-mediated plant infection by *Colletotrichum lagenarium*. *Plant Cell* **13:** 1945–1957.

van der Klei, I.J., and Veenhuis, M. (1997) Yeast peroxisomes: function and biogenesis of a versatile cell organelle. *Trends Microbiol* **5:** 502–509.

Klis, F.M., Mol, P., Hellingwerf, K., and Brul, S. (2002) Dynamics of cell wall structure in *Saccharomyces cerevisiae*. *FEMS Microbiol Rev* **26:** 239–256.

Kopecka, M., and Gabriel, M. (1992) The influence of Congo red on the cell wall and (1,3)-β-D-glucan microfibril biogenesis in *Saccharomyces cerevisiae*. *Arch Microbiol* **158:** 115–126.

Kunau, W.H., Buhne, S., de la Garza, M., Kionka, C., Mateblowski, M., Schultz-Borchard, U., and Thieringer, R. (1988) Comparative enzymology of beta-oxidation. *Biochem Soc Trans* **16:** 418–420.

Kunau, W.H., Dommes, V., and Schulz, H. (1995) Beta-oxidation of fatty acids in mitochondria, peroxisomes, and bacteria: a century of continued progress. *Prog Lipid Res* **34:** 267–342.

Kurihara, T., Ueda, M., Kanayama, N., Kondo, J., Teranishi, Y., and Tanaka, A. (1992) Peroxisomal acetoacetyl-CoA thiolase of an n-alkane-utilizing yeast, *Candida tropicalis*. *Eur J Biochem* **210:** 999–1005.

Lazarow, P.B., and Moser, H.W. (1989) Disorders in peroxisome biogenesis. In *The Metabolic Basis of Inherited Disease*. Schriver, C.R., Beaudet, A.L., Sly, W.S., and Vallee, D. (eds). New York: McGraw-Hill, pp. 1479–1509.

Legakis, J.E., and Terlecky, S.R. (2001) PTS2 protein import into mammalian peroxisomes. *Traffic* **2:** 252–260.

Lorenz, M.C., and Fink, G.R. (2001) The glyoxylate cycle is required for fungal virulence. *Nature* **412:** 83–86.

Maggio-Hall, L.A., and Keller, N.P. (2004) Mitochondrial beta-oxidation in *Aspergillus nidulans*. *Mol Microbiol* **54:** 1173–1185.

Miura, S., Kasuya-Arai, I., Mori, H., Miyazawa, S., Osumi, T., Hashimoto, T., and Fujiki, Y. (1992) Carboxyl-terminal consensus Ser-Lys-Leu-related tripeptide of peroxisomal proteins functions *in vitro* as a minimal peroxisome-targeting signal. *J Biol Chem* **267:** 14405–14411.

Muller, W.H., van der Krift, T.P., Krouwer, A.J., Wosten, H.A., van der Voort, L.H., Smaal, E.B., and Verkleij, A.J. (1991) Localization of the pathway of the penicillin biosynthesis in *Penicillium chrysogenum*. *EMBO J* **10:** 489–495.

Nakai, K., and Horton, P. (1999) PSORT: a program for detecting sorting signals in proteins and predicting their subcellular localization. *Trends Biochem Sci* **24:** 34–36.

Naqvi, N.I., Bonman, J.M., Mackill, D.J., Nelson, R.J., and Chattoo, B.B. (1995) Identification of RAPD markers linked to a major gene for blast resistance in rice. *Mol Breed* **1:** 341–348.

Pracharoenwattana, I., Cornah, J.E., and Smith, S.M. (2005) Arabidopsis peroxisomal citrate synthase is required for fatty acid respiration and seed germination. *Plant Cell* **17:** 2037–2048.

Ramsay, R.R., and Naismith, J.H. (2003) A snapshot of a carnitine acetyl-transferase. *Trends Biochem Sci* **28:** 343–346.

van Roermund, C.W., Elgersma, Y., Singh, N., Wanders, R.J., and Tabak, H.F. (1995) The membrane of peroxisomes in *Saccharomyces cerevisiae* is impermeable to NAD(H) and acetyl-CoA under *in vivo* conditions. *EMBO J* **14:** 3480–3486.

Sambrook, J., Fritsch, E.F., and Maniatis, T. (1989) *Molecular Cloning: A Laboratory Manual*. Cold Spring Harbor, NY: Cold Spring Harbor Laboratory Press.

Schulz, H. (1991) Beta oxidation of fatty acids. *Biochim Biophys Acta* **1081:** 109–120.

Smith, J.J., Brown, T.W., Eitzen, G.A., and Rachubinski, R.A. (2000) Regulation of peroxisome size and number by fatty acid beta-oxidation in the yeast *Yarrowia lipolytica*. *J Biol Chem* **275:** 20168–20178.

Smits, G.J., Van Den, E.H., and Klis, F.M. (2001) Differential regulation of cell wall biogenesis during growth and development in yeast. *Microbiology* **147:** 781–794.

Solomon, P.S., Lee, R.C., Wilson, T.J., and Oliver, R.P. (2004) Pathogenicity of *Stagonospora nodorum* requires malate synthase. *Mol Microbiol* **53:** 1065–1073.

Soundararajan, S., Jedd, G., Li, X., Ramos-Pamplona, M., Chua, N.H., and Naqvi, N.I. (2004) Woronin body function in *Magnaporthe grisea* is essential for efficient pathogenesis and for survival during nitrogen starvation stress. *Plant Cell* **16:** 1564–1574.

Stemple, C.J., Davis, M.A., and Hynes, M.J. (1998) The *facC* gene of *Aspergillus nidulans* encodes an acetate-inducible carnitine acetyltransferase. *J Bacteriol* **180:** 6242–6251.

Subramani, S. (1993) Protein import into peroxisomes and biogenesis of the organelle. *Annu Rev Cell Biol* **9:** 445–478.

Subramani, S. (1998) Components involved in peroxisome import, biogenesis, proliferation, turnover, and movement. *Physiol Rev* **78:** 171–188.

Sweigard, J.A., Carroll, A.M., Farrall, L., Chumley, F.G., and Valent, B. (1998) *Magnaporthe grisea* pathogenicity genes obtained through insertional mutagenesis. *Mol Plant Microbe Interact* **11:** 404–412.

Swiegers, J.H., Dippenaar, N., Pretorius, I.S., and Bauer, F.F. (2001) Carnitine-dependent metabolic activities in *Saccharomyces cerevisiae*: three carnitine acetyl-transferases are essential in a carnitine-dependent strain. *Yeast* **18:** 585–595.

Thines, E., Weber, R.W., and Talbot, N.J. (2000) MAP kinase and protein kinase A-dependent mobilization of triacylglycerol and glycogen during appressorium turgor generation by *Magnaporthe grisea*. *Plant Cell* **12:** 1703–1718.

Titorenko, V.I., and Rachubinski, R.A. (2001) Dynamics of peroxisome assembly and function. *Trends Cell Biol* **11:** 22–29.

Titorenko, V.I., and Rachubinski, R.A. (2004) The peroxisome: orchestrating important developmental decisions from inside the cell. *J Cell Biol* **164:** 641–645.

Tolbert, N.E. (1982) Leaf peroxisomes. *Ann N Y Acad Sci* **386:** 254–268.

Valent, B. (1990) Rice blast as a model system for plant pathology. *Phytopathology* **80:** 33–36.

Vogel, J., and Somerville, S. (2000) Isolation and characterization of powdery mildew-resistant *Arabidopsis* mutants. *Proc Natl Acad Sci USA* **97:** 1897–1902.

Wanders, R.J., Schutgens, R.B., and Barth, P.G. (1995) Peroxisomal disorders: a review. *J Neuropathol Exp Neurol* **54:** 726–739.

Wanders, R.J., Denis, S., Wouters, F., Wirtz, K.W., and Seedorf, U. (1997) Sterol carrier protein X (SCPx) is a peroxisomal branched-chain beta-ketothiolase specifically reacting with 3-oxo-pristanoyl-CoA: a new, unique role for SCPx in branched-chain fatty acid metabolism in peroxisomes. *Biochem Biophys Res Commun* **236:** 565–569.

Wang, Z.Y., Thornton, C.R., Kershaw, M.J., Debao, L., and Talbot, N.J. (2003) The glyoxylate cycle is required for temporal regulation of virulence by the plant pathogenic fungus *Magnaporthe grisea*. *Mol Microbiol* **47:** 1601–1612.

Supplementary material

The following supplementary material is available for this article online:

Fig. S1. CLUSTAL alignment of *Magnaporthe* CrAT.

Fig. S2. Expression analysis of *PTH2* and *CRAT2* transcripts.

This material is available as part of the online article from http://www.blackwell-synergy.com